Harnessing the potential of zebrafish model system towards therapeutic programming of T lymphocytes in melanoma

A thesis submitted to The University of Manchester

for the degree of

DOCTOR OF PHILOSOPHY

in the Faculty of Biology Medicine and Health

School of Medical sciences

2016

Raghavendar Thyagaraja Nagaraju

Table of Contents

Word count: 29,496

List of tables

List of Figures

Abbreviations

BAC: Bacterial artificial chromosome

bp: Base pair

dH2O: Distilled water

DNA: Deoxyribonucleic acid

dpf: Day post fertilization

hpf: Hour post fertilization

PBS: Phosphate buffered saline

PCR: Polymerase chain reaction

PFA: Paraformaldehyde

RNase: Ribonuclease

RT-PCR: Reverse transcription polymerase chain reaction

WT: Wild type

MS222: tricaine methane sulphonate

FACS: fluorescence activated cell sorting

CT: cycle threshold

BSU: Biological Services Unit

Kb: Kilobase

LB: Luria-Bertani

mRNA: messenger RNA

rpm: Rotation per minute

RNA: Ribo Nucleic Acid

TE: Tris-EDTA

TAE: Tris acetic EDTA

wpf: weeks post fertilisation

w/v: Weight/volume

Abstract

Malignant melanoma is one of the most aggressive types of malignancies in humans resulting in 50,000 deaths worldwide annually. Malignant melanoma is highly immunogenic and it is now well established that the host immune system can detect and kill melanoma. In this thesis, our work has focused on establishing zebrafish as a viable model system to study $CD4^+$ T cell mediated immune responses against melanoma as well as an *in-vivo* model system compatible for testing multiple immunotherapy strategies. We have created BAC transgenic zebrafish with vibrantly labeled $CD4^+$ cells allowing us to scrutinize the development and specialization of zebrafish $CD4^+$ leukocytes *in-vivo*. We demonstrate the utility of this zebrafish resource for interrogating the complex behavior of immune cells at cellular resolution by the imaging of intimate contacts between $CD4^+$ T cells and mononuclear phagocytes. We reveal that sub-specialization of $CD4^+$ T cells in to T_H1, T_H2 and T_{reg} cells is conserved in zebrafish and most importantly, as in mammals, we show that zebrafish $CD4^+$ T cells will infiltrate melanoma tumours and obtain a phenotype consistent with a type 2 immune microenvironment. We have built a Tamoxifen inducible $CreER^{T2}$ system, which can be used to specifically induce the expression of selected immune-regulatory molecules by the zebrafish melanocytes. We report that forced expression of IFNγ in the tumour microenvironment using this system has resulted in enhanced tumour regressing in our autochthonous zebrafish melanoma model. However, new tumour nodules were also observed to develop in the vicinity of regressing nodules which are unpigmented and potentially hypo-immunogenic. In parallel, we have observed that forced secretion of the ectopic domain of zebrafish PDL1 homologue suppresses tumour formation but again late escapee tumours were unpigmented. RNA sequencing of the resistant tumours (IFNγ or PDL1 expressing) could reveal unique but also shared signatures for progressing tumours, which can be used to predict immunotherapy responses in human patients.

Declaration

I hereby declare that no portion of the work referred to in the thesis has been submitted in support of an application for another degree or qualification of this or any other university or other institute of learning.

Copyright statement

i. The author of this thesis (including any appendices and/or schedules to this thesis) owns certain copyright or related rights in it (the "Copyright") and s/he has given The University of Manchester certain rights to use such Copyright, including for administrative purposes.

ii. Copies of this thesis, either in full or in extracts and whether in hard or electronic copy, may be made only in accordance with the Copyright, Designs and Patents Act 1988 (as amended) and regulations issued under it or, where appropriate, in accordance with licensing agreements which the University has from time to time. This page must form part of any such copies made.

iii. The ownership of certain Copyright, patents, designs, trademarks and other intellectual property (the "Intellectual Property") and any reproductions of copyright works in the thesis, for example graphs and tables ("Reproductions"), which may be described in this thesis, may not be owned by the author and may be owned by third parties. Such Intellectual Property and Reproductions cannot and must not be made available for use without the prior written permission of the owner(s) of the relevant Intellectual Property and/or Reproductions.

iv. Further information on the conditions under which disclosure, publication and commercialisation of this thesis, the Copyright and any Intellectual Property University IP Policy (see http://documents.manchester.ac.uk/display.aspx?DocID=24420), in any relevant Thesis restriction declarations deposited in the University Library, The University Library's regulations (see http://www.library.manchester.ac.uk/about/regulations/) and in The University's policy on Presentation of Theses

Contributions to the work

The majority of the data presented in this thesis is from my own work. Some complete experiments were performed by fellow colleagues in the lab and some experiments were performed with collaboration, which are outlined below.

Chapter 4 within the thesis is a paper I have published in the 'Journal of immunology' as a joint first author along with Christopher Dee. My contribution includes figure 4.1, figure 4.2, figure 4.3 (A-C, F), figure 4.4, figure 4.5 (I), figure 4.6, and the contribution of the co-authors includes figure 4.3 (D, E, G, H), figure 4.5 (A-H), figure 4.7 and figure 4.8. This article was published with open access under a creative commons agreement and I have obtained the permission from the co-authors to include it in my thesis.

The sectioning and staining of adult zebrafish tissue used for Figure 5.7 (C, D) was performed by Mai Abdulmouti.

Reagents (TYR guide RNA and cas9 mRNA) used for CRISPR/CAS9 knock down of *tyr* gene were generated by Jorge Barriuso.

Abigail Elliott helped with the injection of minicoopR constructs resulting in Figure 5.9 C.

Acknowledgements

Thank you Adam for giving me this wonderful opportunity, I will be ever so grateful for your confidence in my ability and your perseverance in securing the fellowship to support my work in the lab. Your enthusiasm and passion for science are immensely inspirational and I am fortunate enough to benefit from it for a longer period of time. From zebrafish transgenics to project development, I will cherish many valuable skills I have gained under your tutelage. I am forever a privileged 'Hurlstonian'.

I would like to thank my advisor Prof. Werner Muller, for his guidance throughout my PhD. I would also like to specially thank Prof. Claudia Wellbrock for her ever so insightful feedback during the lab meetings, which immensely helped in shaping most part of my PhD.

These last 4 years would not have been so enlightening and enjoyable without your association Jorge, a true friend and a mentor. I would like to thank you for all those educational and at times re-assuring chats.

I would like to thank all the present and past members of the Hurlstone and Wellbrock labs, especially Hannah, Helen, Jen, Imanol and Laura, for all their help and support over the past 6 years. Thank you very much Michel and Andy for your help in getting me 'viva ready', much appreciated. A special thanks to Chris Dee, with whom I share my first ever lead author publication, for his support in developing and publishing that CD4 project.

Thank you mum and dad for all your care, affection and at times for that much needed counselling which enabled me to stay disciplined and motivated towards achieving my professional goals. I am blessed to have such a passionate, devoted and yet practical parents whose able guidance in my tender days shaped a bright future for me.

Finally, it was the appeal from a pure and divine sole in its final moments that has motivated me to take up his fight against the cancer, towards which this PhD is one tiny step. I dedicate this thesis to Jack, the shepherd of my intellectual prowess.

Chapter 1. Introduction

Cancer in simple terms can be defined as 'uncontrolled growth of cells'. Multiple factors contribute to the transformation of a healthy cell to a cancerous cell including aberration of very fundamental mechanisms like cellular division and DNA replication (Vesely *et al*. 2011). Research from the past fifty years has revealed that cancer is a genetic disease which is the result of somatic cells gradually acquiring multiple mutations that overpower the cellular regulation and drive the cells towards cancerous state (Vesely *et al*. 2011). Melanoma, a form of skin cancer, represents a well-studied example to illustrate various steps involved in cancer initiation and progression.

1.2 Genetic changes leading to melanoma development and progression.

Melanoma arises from uncontrolled proliferation of transformed melanocytes. Melanocytes are highly specialized melanin producing cells of the skin that originate in the neural crest before migrating to the epidermal basement membrane (Yaar & Park. 2012). The development of melanoma is a multi-staged process, from a benign nevus through a radial growth phase (RGP) and vertical growth phase (VGP) to the metastatic stage, involving various genetic alterations such as deletions in tumour suppressor genes and mutations in oncogenes (Figure 1.1, Wellbrock & Hurlstone. 2010). Activating mutations in BRAF, a MAP kinase kinase kinase, that drive hyper-activation of MAP kinase pathway (MAPK pathway) can lead to transformation of melanocytes (Gray-Schopfer et al. 2006). BRAF mutations are one of the earliest genetic alterations

to occur in melanoma and are detected in ~50% of melanomas. The most common activating BRAF mutation, representing over 95% of all BRAF mutations, is a substitution of valine for glutamic acid at codon 600 (V600E) in exon 15 (Davies et al. 2002, Wellbrock et al. 2004). Activating mutations in NRAS, a homologue of RAS GTPase, have also been identified in ~15% of benign nevi, however mutations in NRAS and BRAF are mutually exclusive (Pollock et al. 2003, Poynter et al. 2002).

Melanoma development begins with the clonal expansion of the transformed melanocytes which then aberrantly proliferate to form benign nevi (Figure 1.1, Miller & Mihm. 2006). These nevi rarely develop in to malignant tumours as cellular senescence is triggered possibly due to increased expression of cell cycle inhibitor CDKN2/p16 (Gray-Schopfer et al. 2006, Figure 1.1). Overcoming this cellular senescence is essential for melanoma progression to RGP, a dysplastic growth of melanocytes usually confined to the epidermis (Miller and Mihm. 2006). One of the ways oncogenic BRAF expressing melanoma cells overcome this senescence is by up-regulating cell cycle progression genes such as CCND1 and CDK2 (Bhatt et al. 2005, Wellbrock et al. 2008).

In the VGP stage of melanoma progression, further oncogenic aberrations such as activation of PI3-kinase/AKT pathway are acquired by the melanoma cells leading to their proliferation into the dermis (Wellbrock & Hurlstone. 2010, Figure 1.1). The activation of the PI3-kinase (PI3K) pathway is usually seen when melanoma has reached the vertical growth phase and has been reported to be part of the changes required to abolish the mutant BRAF induced senesence

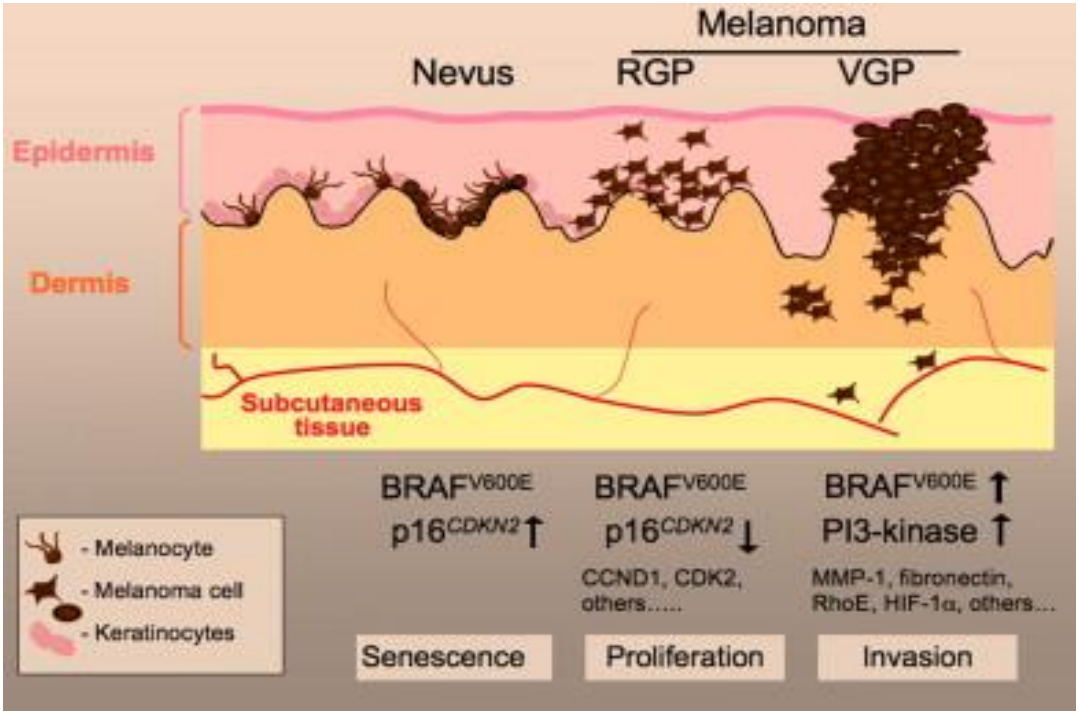

Figure 1.1 Melanoma progression. Diagram showing the different stages of melanoma progression including Radial Growth Phase (RGP) and Vertical Growth Phase (VGP). Also shown are common changes in melanoma that drive progression, such as acquisition of activating mutation in the kinase BRAF, cell cycle machinery changes and increased signalling through additional pathways such as PI3-kinase/AKT signalling. (Figure taken from Wellbrock & Hurlstone, 2010)

(Vredeveld et al 2012). Correspondingly, increased AKT expression, an important regulator of cell proliferation and anti-apoptotic signaling, is found in ~77% of metastatic melanomas compared to only ~14% in benign nevi (Dia et al 2005). Active PI3K produces phosphatidylinositol (3,4,5)-trisphosphate (PI3P), which in-turn activates AKT through mTOR (Meier et al 2005). PI3K activation of AKT is regulated by PTEN phosphatase through de-phosphorylation of PI3P to yield phosphatidylinositol (3,4)-bisphosphate (PI2P) that is inactive and does not signal through AKT (Maehama et al 1999). While activating mutations in PI3K are not common in melanoma, the loss of function mutations in PTEN are freqeuntly observed (Omholt et al 2006). The functional loss of PTEN results in inceased AKT signalling promoting growth and progression in melanoma (Vredeveld et al 2012, Dia et al 2005).

1.3 Cell intrinsic and extrinsic tumour suppressor mechanisms

Although cellular mechanisms are error prone, a variety of intrinsic tumour suppressor mechanisms are in place to repair genetic mutations and in-case they fail to do so, senescence or apoptosis is triggered to arrest the proliferation of genetically damaged cells (Xue *et al*. 2007). Numerous cellular proteins, such as p53, induce senescence (permanent cell cycle arrest) after sensing genomic disturbances caused by mutagenic insults (Xue *et al*. 2007). In addition, cellular senescence is also triggered when oncogenes are activated and such a cell has to first overcome this oncogene-induced senescence by acquiring a second cooperating mutation/defect that can override senescence (Serrano *et al*. 1997). Furthermore, in-case of any other abnormalities

such as cellular stress, injury, lack of survival signals, alterations in mitochondrial integrity, executioner caspases (caspase 3, caspase 6 and caspase 7) are terminally activated via pro-apoptotic effectors to trigger cell death (Danial *et al*. 2004). In contrast, a tumour necrosis factor (TNF) related apoptosis mechanism can also be activated by apical caspase 8 to limit the growth of damaged and abnormal cells (Peter *et al*. 2003).

Apart from the above discussed intrinsic tumour suppressor mechanisms, at least three general extrinsic tumour suppressor mechanisms have been identified by which the presence of a cancerous cell is sensed by its adjacent healthy cells and tissues (Janes *et al*. 2006). The first one is based on cell's obligatory dependency on specific signals from its microenvironment. The moment the cell stops responding to its microenvironment, it is forced to die. Just like in the scenario where the disassociation of the epithelial cell from the cell-extracellular matrix results in its death (Janes *et al*. 2006). The second one appears to be the cross talk between genes that control cell polarity (especially that regulate inter-cellular junctions) and cell proliferation. In the event of dysregulated expression of junctional complexes (a trademark event in cancer proliferation), the cell proliferation is halted thereby restricting the potential outgrowth of cancer (Humbert *et al*. 2003). The third extrinsic tumour suppressor mechanism is facilitated by effector leukocytes of the immune system which play a critical role in limiting both transformation in to the cancerous state and also the tumour cell growth (Vesely *et al*. 2011).

The immune system can protect the host from cancers by 3 ways: a) By eliminating or suppressing viral infections, the immune system can protect the host from virus-induced tumours; b) Preventing the establishment of an inflammatory environment that is favorable to tumorigenesis by timely elimination of the pathogens and prompt resolution of inflammation; c) The immune system, in certain tissues, can identify and eliminate tumour cells based on the antigens specifically expressed by tumour cells (tumour-specific antigens, TSA), this process is referred to as cancer immunosurveillance (Zitvogel *et al*. 2006). A transformed cell that escaped the cell-intrinsic tumour suppressor mechanisms, if identified by the immune system, will be eliminated (via induced cell death by mitochondrial and cell death receptors) before they can establish malignancy (Dunn *et al*. 2002, Zitvogel *et al*. 2006).

1.4 Basics of Innate immunity

In mammals, the first line of host defense during infection is provided by the innate immune system. It plays a vital role in early recognition of invading pathogens and mounts a pro-inflammatory response against the same. On the contrary, the adaptive immune system is responsible for elimination of pathogens in the later stages of infection along with generation of immunological memory (Medzhitov et al. 2000). By the virtue of a broad repertoire of antigen-specific receptors on lymphocytes, the adaptive immune response is targeted towards the infected cells and the pathogen. On the other hand, the innate immune responses are regarded as relatively nonspecific and are primarily mediated primarily phagocytic cells and antigen-presenting cells

(APCs), such as granulocytes, macrophages, and dendritic cells (DCs) (Iwasaki et al. 2004).

The innate immune response relies on recognition of evolutionarily conserved pathogen-associated molecular patterns (PAMPs) on pathogens, through pattern recognition receptors (PRRs). PRRs, such as Toll-like receptors (TLRs), are germ line-encoded and limited in number (Akira et al. 2006 and Medzhitov et al. 2000). PAMPs are essential for the survival of the pathogen and are characterised by being invariant among the entire classes of pathogens and distinguishable from "self" (Janeway et al. 1989). However, in certain circumstances, host factors are also recognised by PRRs as "danger" signals, when they are present in uncharacteristic locations or abnormal molecular complexes formed as a consequence of infection, inflammation, or other types of cellular stress such as cancer (Beg et al. 2002 and Matzinger et al. 2002). In the event of an infection/detection of transformed cells, PRRs present intracellularly or at the cell surface induce signaling to trigger proinflammatory and antimicrobial responses by activating a series of intracellular signaling pathways, including transcription factors, kinases and adaptor molecules (Akira et al. 2004). PRR-induced signal transduction subsequently initiates synthesis of a spectrum of molecules, including immune-receptors, cell adhesion molecules, cytokines and chemokines (Akira et al. 2006). Together, these molecules orchestrate the early host response to infection (also cancer), while simultaneously representing an important link to the activation of adaptive immune responses.

Phagocytic cells and antigen presenting cells (APCs) are essential effector cells of innate immunity. While resident macrophages acting as the first responder phagocytes eliminate invading pathogens before they can spread, following antigen uptake activated DCs initiate adaptive immune responses through pathogen-antigen presentation to naïve T cells (Branger et al. 2004). The link between innate and adaptive immunity facilitated by PRRs, in particular the TLR mediated maturation of DCs and subsequent activation of antigen specific T lymphocytes, is well established (Iwasaki et al. 2004) and Reddy et al. 2004). Activated DCs migrate to the regional lymph nodes where they present antigenic peptides on MHC molecules. Recognition of pathogens by TLRs triggers maturation of DCs leading to upregulation of costimulatory molecules (CD86, CD80, and CD40 along with antigen-presenting MHC molecules), switch in chemokine receptor expression and cytokine secretion (Hoebe et al. 2003, Honda et al. 2003, Hoshino et al. 2002 and Iwasaki et al. 2004). Mature DCs acquire the ability to stimulate naïve $CD4^+$ T lymphocytes differentiation in to various T helper (T_H) subsets (T_H1, T_H2 or T_H17) under the control of various factors including TLR-induced cytokines.

1.5 Basics of Adaptive immunity

Activation of naive T helper (T_H) cells is facilitated through the interaction of the T-cell receptor (TCR) with a peptide antigen–class II major histocompatibility complex (MHC II) presented on antigen-presenting cells (APCs). Activated T_H cells then begin to divide and/or give rise to a clone of $CD4^+$ effector cells that are specific for the same MHC II

complex (Goldsby et al. 2003). Based on their distinct cytokine secretion profiles, these $CD4^+$ effector T_H cells can be divided into three main types, T_H type-1 (T_H1), T_H type-2 (T_H2) or T_H type-17 (T_H17) cells, each with unique functional characteristics. In this thesis, we will not be focusing on T_H17 cells.

1.5.1 T_H1 polarizing cytokine signals

Upon activated by the intracellular pathogens, macrophages and dendritic cells (DC) release cytokines such as IL-12, IFN-α and IFN-β in to the micro-environment initiating T_H1 cell development (Farrar et al. 2002). IL-12 induces the production of IFN-γ by these differentiated T_H1 cells, which in turn by acting in an autocrine manner, further stimulates the production of IL-12 by the T_H1 cells (Murphy et al. 2000). In another amplifying positive feedback loop, IL-12 can also activate natural killer (NK) cells to produce IFN-γ, which then enhances IL-12 expression by the macrophages and DCs (Lafaille et al. 1989). While the differentiation of T cells in to T_H1 cells is directly induced by IFN-γ, IL-12 and type 1 IFNs, it is only the IFN-γ that can also inhibit the T_H2 differentiation pathway by inhibiting proliferation of T_H2 cells (Murphy et al. 2000 and Lafaille et al. 1989). On the other hand, IFN-γ attachment to its receptor complex (IFNGR) on naive T_H cells leads to the activation of transcription factor STAT1 trough JAK1 and JAK2, which then induces the expression of T-bet (Gerard et al. 2008). T-bet is a member of the TATAAA-box family of transcription factors and is regarded as the master regulator for commitment to the T_H1 cell lineage (Mullen et al. 2001). Expression of T-bet initiates the remodeling of the IFN-γ gene locus, the production of

IFN-γ and expression of the IL-12 receptor (Mullen et al. 2001). Expression of IL-12 receptor enables IL-12 mediated signaling by activating transcription factors STAT3, STAT4 and nuclear factor-κB which promotes the production cytokines associated with the T_H1 phenotype, thereby further reinforcing the differentiation of T_H1 cells (Afkarian et al. 2002). These newly developing T_H1 cells, by secreting IFN-γ, stimulate polarization of surrounding naïve T_H cells in to T_H1 cells in a self-renewing paracrine loop (Kidd et al. 2003).

1.5.2 TH2 POLARIZING CYTOKINE SIGNALS

The differentiation of naïve T cells in to T_H2 effector cells is primarily facilitated by cytokines IL−4, IL−6, and IL−11. Interestingly, the source of the IL-4 that leads to T_H2 phenotype has not been identified, but it is believed to arise from natural killer T cells, eosinophils or mast cells (Kidd et al. 2003, Lafaille et al. 1989 and Wang et al. 2006).Naïve T cells exposed to IL-4 start producing STAT6, which in turn activates the expression of GATA-3, a zinc finger transcription factor (Kaplan et al. 1996 and Ouyang et al. 1998). GATA-3 and T-bet are mutually antagonistic, while IFN-γ, IL-12 and T-bet expression in T_H1 cells inhibits the production of GATA-3, in T_H2 cells, IL-4 and GATA-3 expression suppresses T-bet and IL-12 receptor production (Mullen et al. 2001, Ouyang et al. 1998 and Farrar et al. 2002). Combined signaling from IL-4 and T cell receptor (TCR) is required to up-regulate GATA-3 transcription. GATA-3 then in-turn can induce expression of a cluster of cytokine genes (IL-4, IL−5, IL−9, IL−10 and IL−13) that are characteristic of the T_H2 phenotype through epigenetic remodeling of regions that

control their expression (Zheng et al. 1997). Once GATA-3 expression increases to a certain threshold, its own gene expression is activated through an intrinsic positive-feedback loop, thereby stabilizing the T_H2 phenotype (Farrar et al. 2002).

Apart from GATA-3, c-MAF is another transcription factor that is specific to T_H2 cells. In T_H2 committed cells, c-MAF along with NFAT regulates IL-4 production by activating its promoter (Ho et al. 2002). These maturing T_H2 cells will start producing increasing levels of IL-4 thereby generating a paracrine loop that induces T_H2 differentiation of neighboring naïve T cells (Kidd et al. 2003). Furthermore, IL-6 produced by macrophages, mast cells and pulmonary DCs in the early stages of TH2 immune response, upregulates IL-4 while inhibiting the phosphorylation of STAT1, thereby preventing IFN-γ gene expression (Detournay et al. 2005 and Dodge et al. 2005). In humans, myeloid cells derived IL-11 acts directly on T cells to inhibit IFN-γ production while simultaneously stimulating IL-4 and IL-5 synthesis. Furthermore, by suppressing IL-12 secretion from macrophages, IL-11 also indirectly contributes to T_H2 differentiation through this mechanism (Curti et al. 2001).

1.6 The concept of cancer immunoediting

The idea that the host immune system can identify and kill cancer cells is well established (Vesely *et al*. 2011). Moreover, in past two decades, data from mouse models and cancer patients has provided key evidence that the immune system not only has a tumour suppressive role but it also promotes tumour growth (Teng *et al.*

2015). This complex role of immune system where it both suppresses and facilitates tumour growth is termed cancer immunoediting (Dunn *et al*. 2002).

The concept of immunoediting was first proposed by the Schreiber laboratory after making an interesting observation that tumours developing in hosts with intact immune system were less immunogenic compared to those developing in immunodeficient hosts (Dunn *et al*. 2002). Firstly, they observed that methylcholanthrene (MCA) treatment induced tumours in significantly higher number of $Rag2^{-/-}$ mice (lacking T, B and NKT cells) compared to control immunocompetent mice. More interestingly, they observed that tumours developing in control immunocompetent mice ('edited' tumours) were less immunogenic compared to those developing in immunodeficient $Rag2^{-/-}$ mice ('un-edited' tumours) (Dunn *et al*. 2002). Subsequently, they have identified and validated a point mutation in Spectrin-b2 gene that resulted in appearance of neo-epitope on 'un-edited' tumours of $Rag2^{-/-}$ mice. When the sarcoma cell line derived from MCA treated $Rag2^{-/-}$mice was injected in to immunocompetent (MHC matched) mice, this neo-epitope functioned as a major immunodominant rejection antigen leading to T cell mediated elimination of cancer (Matsushita *et al.* 2012). Based on data from various genetic mouse models and human cancer patients, other groups have also reached to similar conclusions thus strengthening the concept of cancer immunoediting (Mittal *et al.* 2014). Together, these studies have provided unequivocal evidence in support of cancer immunoediting being the consequence of a T cell dependent immune-selection process.

Cancer immunoediting is a dynamic process composed of three distinct reversible phases: elimination, equilibrium and escape (Dunn *et al*. 2002) (Figure 1.2).

1.6.1 Elimination

The process of eliminating cancer by the immune system can be divided in to 4 stages. In the first phase of elimination, as the solid tumours increase in size and grow invasively, they require more blood supply as the tumour cells start producing stromagenic and angiogenic proteins (Hanahan *et al.* 2000). This invasive growth results in minor disruptions within the surrounding tissue which induce inflammatory signals facilitating the recruitment of NKT, NK, γδ T cells, macrophages and dendritic cells (cells of the innate immune system) to the tumour site (Girardi *et al.* 2001, Smyth *et al.* 2001, Matzinger *et al.* 1994). Once in the tumour site, these cells by identifying the structures (such as NKG2D ligands) on the transformed cells get stimulated to produce IFN-γ (Yokoyama *et al.* 2000, Diefenbach *et al.* 2001). In the second phase, initially produced IFN-γ may trigger anti-proliferative (Bromberg *et al.* 1996) and apoptotic (Kumar *et al.* 1996) mechanisms (though in limited number of tumour cells) to induce tumour death.

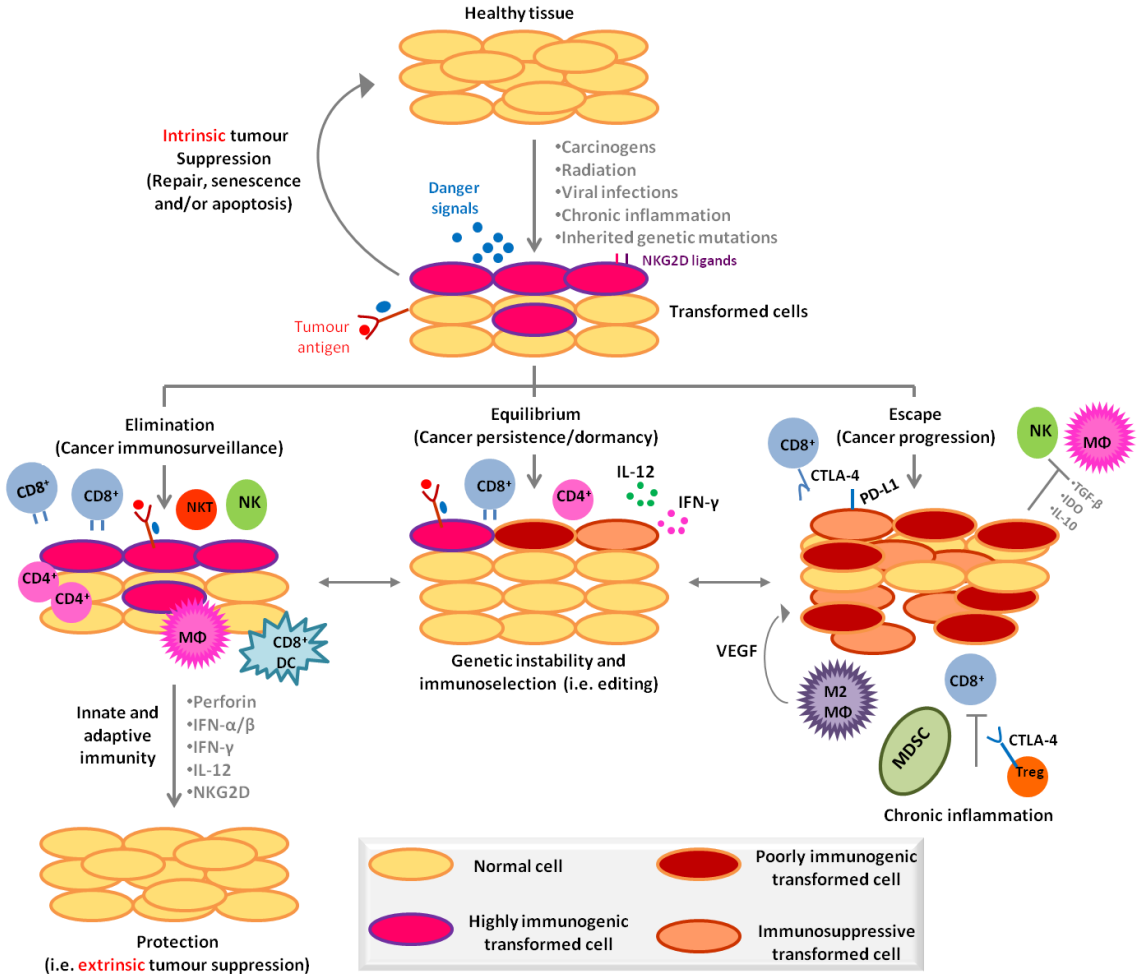

Figure 1.2: The three phases of cancer immunoediting. Cancer immunoediting is the result of three processes, elimination, equilibrium and escape, that function either independently or in sequence to control and shape cancer. (Abbreviations: CTLA-4, cytotoxic T lymphocyte associated protein-4; IDO, indoleamine 2,3-deoxygenase; IFN, interferon; IL, interleukin; MΦ, macrophage; MDSC, myeloid-derived suppressor cells; NK, natural killer; NKG2D, NK group 2, member D; PD-L1, programmed cell death 1 ligand 1; TGF-β, transforming growth factor-β; TRAIL, tumour necrosis factor-related apoptosis-inducing ligand; Treg, regulatory T cell; VEGF, vascular endothelial growth factor) (Concept adapted from Vesely *et al*. 2011).

Apart from this, IFN-γ also induces the production of the chemokines CXCL10 (interferon inducible protein-10, IP-10), CXCL9 (monokine induced by IFN-γ, MIG) and CXCL11 (interferon-inducible T cell α chemoattractant, ITAC) from the tumour cells and as well as from adjacent normal host tissues (Luster *et al.* 1993; Liao *et al.* 1995; Cole *et al.* 1998). Some of the above chemokines have potential angiostatic capacities and thus block the formation of new blood vessels within the tumour leading to more tumour cell death (Sgadari *et al.* 1996, Coughlin *et al.* 1998, Qin Z *et al.* 2000). While the elevated levels of chemokines recruit more NK cells and macrophages to the tumour site, the cell debris formed as a result of IFN-γ induced cell death are ingested by locally present dendritic cells, which then home to draining lymph nodes (Luster *et al.* 1987).

In the third phase, the dendritic cells immigrated to the draining lymph node induce production of tumour-specific $CD4^+$ T helper cells expressing IFN-γ (T_H1 cells), in turn, facilitating the development of tumour-specific $CD8^+$ T cells (Pardoll *et al.* 2002, Gerosa F *et al.* 2002, Ferlazzo *et al.* 2002, Piccioli *et al.* 2002). In the meantime at the tumour site, the NK cells and macrophages transactivate one another by mutual production of IFN-γ and IL-12, and kill more tumour cells by involving tumour necrosis factor–related apoptosis-inducing ligand, perforin and reactive oxygen and nitrogen intermediates related mechanisms (Bancroft *et al.* 1991, Trinchieri *et al.* 1995, Ikeda *et al.* 2002, Takeda *et al.* 2002). In the fourth phase, tumour specific $CD4^+$ and $CD8^+$ T cells home to the tumour site to destroy the remaining antigen-bearing tumour cells which were already immunogenically modified due to their exposure to locally produced IFN-γ (Shankaran *et al.* 2001).

Direct evidence for elimination of cancer cells *in-vivo* is hard to obtain as the read out for elimination is absence of tumours, a negative result (Mittal *et.al* 2014). This makes it challenging to distinguish between the scenarios where in established tumours were eliminated and where tumours originally failed to initiate (Mittal *et.al* 2014). However, with new *in-vivo* models becoming available, we are starting to obtain more positive evidence for cancer elimination process. A recent study, using myc driven B cell lymphoma mouse model, has shown that B cells in early stages are tumourigenic and undergo sharp regression (Croxford *et al.* 2013). In this model, DNA damage was induced through sustained expression of myc and the resulting DNA damage response can induce new ligands enhancing immune recognition. Regression of the transformed B cells was impaired by blockade of DNAM-1, a lymphocyte receptor for one such new ligand (CD155), or deletion of T cells and $NK1.1^{+}$ cells (Croxford *et al.* 2013). Other studies have also been published recently indicating the role of innate immune cells in cancer elimination, but we are not discussing them in this thesis.

1.6.2 Equilibrium

In the equilibrium process (Figure 1), the host immune system and any tumour cells that have survived the elimination process enter into a dynamic equilibrium. At this stage the lymphocytes and IFN-γ selectively exert pressure on the tumour cells to contain them, but cannot fully remove the genetically unstable and rapidly mutating tumour cells from the system.

During this period, Darwinian selection can be observed where many of the original variants of the tumour cells are destroyed and new variants are generated which carry different mutations that can provide the tumour cells with increased resistance to immune attack (Dunn GP *et al*. 2002). Most likely, equilibrium is the longest of the three processes and may prolong for many years (Dunn GP *et al*. 2002).

1.6.3 Escape

A selective pressure is excreted on tumours by the immune system through a variety of processes like elimination of antigen-positive tumour cells by $CD8^+$ T cells (Dunn *et al*. 2002). As a consequence, immunogenic tumour cells are eliminated from the system, leaving behind tumour cell variants that are more capable at evading immune-mediated destruction (Dunn *et al*. 2002). Over time, these tumours evolve to acquire some intrinsic and extrinsic immune suppressive mechanisms by which they can elude or inhibit immunity (Smyth *et al*. 2001). Tumour cells evade immunity by making the following Intrinsic alterations: a) down regulating antigen presentation (MHC); b) up regulating inhibitors of apoptosis (B cell lymphoma extra-long (Bcl-XL), apoptosis-stimulating fragment-associated protein with death domain-like interleukin-1 converting enzyme-like inhibitory protein (FLIP)); c) expressing inhibitory cell surface molecules like programmed cell death 1 ligand (PD-L1) and Fas ligand (FasL) that directly kill cytotoxic T cells (Dunn *et al*. 2002). Additionally, tumour cells secrete factors like TGF-β, IL-10, VEGF, LXR-L, IDO, gangliosides, or soluble MICA inhibiting the functions of effector immune cells or they can also recruit regulatory cells to the

tumour site which then release compounds (IL-4, IL-13, GM-CSF, IL-1β, VEGF, or PGE2) which generates an immunosuppressive microenvironment also altering the nutrient content of the microenvironment (Smyth *et al*. 2001). In particular, secreted IL-4 and IL-13 facilitate recruitment and polarization of M2 macrophages from myeloid precursors, which in-turn express TGF-β, IL-10, and PDGF to inhibit T cells (Zitvogel *et al*. 2006). IL-1β, VEGF, or PGE2 (colony-stimulating factors) released by tumour cells enhances the accumulation of myeloid-derived suppressor cells (MDSCs) that in-turn express TGF-β, ARG1, and iNOS blocking the T cell function (Zitvogel *et al*. 2006). Also, regulatory T cells (Tregs), through multiple mechanisms including expression of cytotoxic T lymphocyte associated protein-4 (CTLA-4), can inhibit effector T cell functions (Dunn *et al*. 2002, Zitvogel *et al*. 2006, and Smyth *et al*. 2001).

1.7 T cells and their role in cancer

Precursors of lymphocytes arise in the hematopoietic tissue (like bone marrow) while their maturation occurs in thymus, a dedicated primary lymphoid organ for lymphocyte maturation in vertebrates (Boehm *et al*. 2011). The thymic epithelial cells facilitate the MHC class differentiation of CD4/CD8 double positive progenitor T cells in to either $CD4^+$ or $CD8^+$ T-cells (Vanaudenaerde *et al*. 2011). Upon activation by antigen presenting cell (APC), $CD4^+$ helper T cells specialize to become distinct subsets that produce restricted patterns of cytokines. Besides the well-known T_H1 and T_H2 cells, four new subsets have been identified, including T_H17), T_H9, follicular helper T (Tf_H), and T_H22 cells (Vanaudenaerde *et al*. 2011).

Helper T cells in tumour biopsies have been studied for decades to understand their potential impact on prognosis (Hadrup *et al*. 2013). Mainly using immune histochemistry (IHC), early studies have reported a correlation between 'brisk' (dense) infiltration of T cells in primary melanoma lesions and improved prognosis in patients (Clark *et al*. 1991). Subsequent studies in the later years have resulted in a standardized histological classification of melanoma lesions in to 'Brisk' (densely infiltrated), 'non-Brisk' (sparsely infiltrated) and 'Absent' (no infiltration), reflecting the heterogeneity in T cell responses against melanoma in humans (Busam *et al*. 2001). Overall, lesions with 'Brisk' tumour infiltrating lymphocytes (TILs) show better prognosis, compared to lesions with 'non-Brisk' or no T cell infiltrate (Busam *et al*. 2001). Recently, similar observations have been made in other cancers including renal cell carcinoma (RCC) (Nakano *et al*. 2001), ovarian cancer (Sato *et al*. 2005) and bladder cancer (Sharma *at al*. 2007).

Lymphocytes are regarded as workhorses of the adaptive immune systems in vertebrates (Boehm *et al.* 2011). As detailed above, now T cells have been established to play a vital role in shaping tumour progression. In particular, tumour-specific $CD4^+$ T cells play a key role in orchestrating the immune responses towards cancer. While $CD4^+$ T_H1 cells can help in tumour suppression, through cytokine-mediated activation of tumour-specific cytotoxic $CD8^+$ T cells (DeNardo *et al*, 2009), T_H2 $CD4^+$ T cells stimulate cancer progression and metastasis by educating tumour associate macrophages (TAMs) to produce pro-angiogenic and pro-metastatic factors (DeNardo *et al*, 2009). Induced T regulatory cells ($iT_{regs)}$ can contribute to cancer progressing by suppressing

anti-tumour immune responses (Gallimore *et al.* 2008), while they can also inhibit cancer progression by suppressing the cancer promoting inflammation (Erdman *et al*. 2005).

It has been observed that higher number of tumour specific T_H1 cells in the tumour micro-environment leads to better prognosis in solid tumours (Haabeth *et al*. 2011). As illustrated in figure 1.3, tumour specific T_H1 cells together with TAMs can induce tumour suppression by synergizing a variety of cytokines and chemokines. In the absence of sufficient numbers of tumour-specific T_H1 cells in the microenvironment, the cytokines secreted by TAMs may promote tumour progression by stimulating angiogenesis, vascular permeability and tumour invasiveness (Haabeth *et al*. 2011).

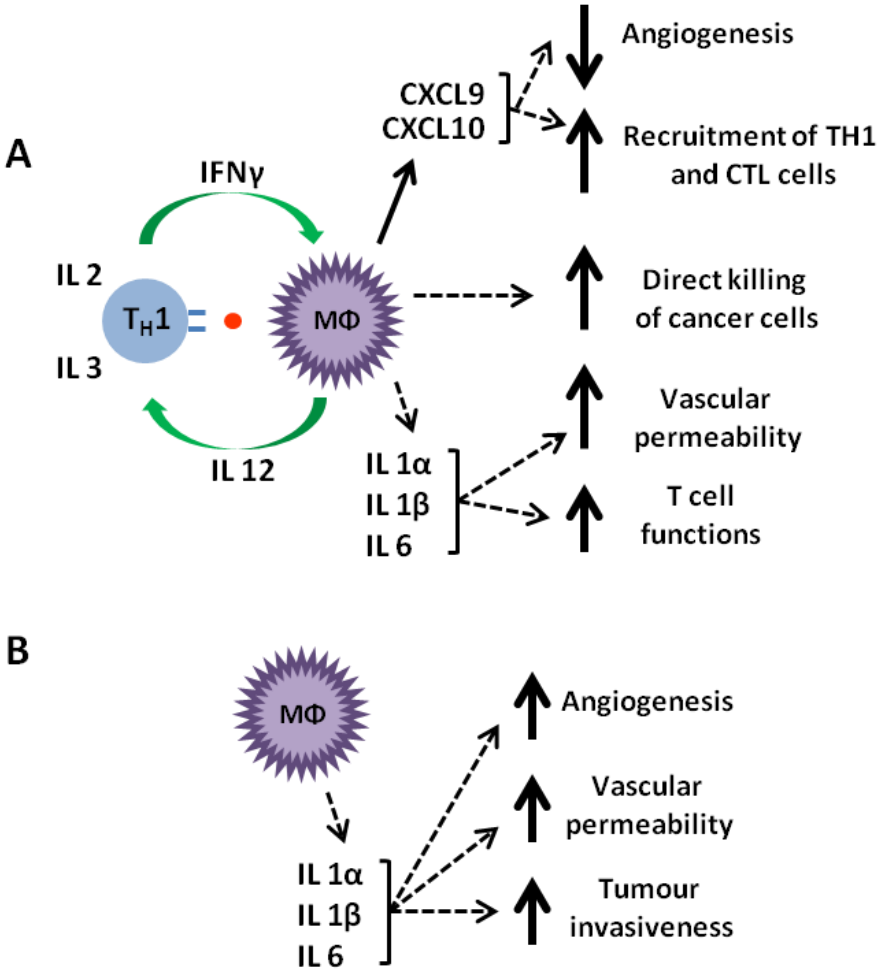

Figure 1.3: Higher number of T_H1 cells in tumour micro-environment leads to better prognosis. (A) Tumour-suppressive inflammation. Successful cancer immunosurveillance is mediated by a tumour-specific T_H1-driven inflammation. (B) Tumour-promoting inflammation. In the absence of sufficient numbers of tumour-specific T_H1 cells, IL-1α, IL-1β and IL-6 may participate in tumour progression by stimulating angiogenesis, vascular permeability and tumour invasiveness. MΦ, macrophage; CTL, cytotoxic $CD8^+$ T cells. (Concept adapted from Haabeth *et al*. 2011)

1.8 $CD4^+$ T cells in zebrafish

$CD4^+$ T cells are pivotal for mounting an effective immune response, but also in the maintenance of peripheral tolerance, the prevention of immunopathology and increasing evidence suggests a central involvement in tumour progression (Bilate and Lafaille 2012, Kara, Comerford et al. 2014, Whiteside 2014, Schmitt and Ueno 2015). Such a crucial function might intuitively imply an ancient and conserved role for these cells in the history of adaptive immunity. However, our knowledge of the evolution of these cells is remarkably limited. Teleost fish represent one of the most ancient and diverse taxa to possess a system of adaptive immunity driven by B- and T-lymphocytes, and have therefore been the focus of considerable attention in recent years (Sunyer 2013, Wang and Secombes 2013, Yamaguchi, Takizawa et al. 2015). However, despite significant progress, basic questions remain as to the development and function of zebrafish $CD4^+$ cells.

In mammals, naïve $CD4^+$ T cells are activated by antigen stimulation and differentiate into specialised T-helper (T_H) effector subsets under the direction of the cytokine microenvironment and the induction of lineage determining transcription factors (TFs). Two major T_H subsets, T_H1 and T_H2, elicit cell mediated immunity to intracellular pathogens and humoral immunity to extracellular pathogens respectively. Differentiation of T_H1 cells is promoted by IL-12 inducing the expression of T-bet and STAT4; T_H1 cells elaborate IFNγ that stimulates macrophages and CTLs (Schmitt *et al.* 2015). Differentiation of T_H2 cells is promoted by IL-4 induction of GATA3 and STAT6; T_H2 cells produce IL-4, -5,-6, -9, -10 and -13 that stimulate B-cells, eosinophils and mast

cells (Schmitt *et al.* 2015). Since the discovery of T_H1 and T_H2 cells, the complexity and plasticity of the T-helper system has become increasingly clear and additional subpopulations have subsequently been identified. These include T_H3, T_H9, T_H17, T_H22, Tr1 and T follicular helper (T_{fh}) cells with distinct transcription factor and cytokine expression profiles which specialise in mounting an immune response to neutralise particular pathogens (for example helminths or fungi) and that are enriched at certain anatomical sites (Comerford *et al*. 2014). Another important class of $CD4^+$ T cells, regulatory T cells (T_{reg}), typically characterised by expression of the TF FoxP3 and expression of the anti-inflammatory cytokines IL-10 and TGFβ, are essential for resolution of an immune response and for maintaining peripheral tolerance (Bilate and Lafaille 2012). Cytotoxic $CD4^+$ T cells have also been described (Husain et al. 2013). In addition, the CD4 protein, which acts as a critical co-receptor molecule in T cells, is also known to be expressed in certain populations of mononuclear phagocytes (MNPs) in the mouse, including a specialised population within the thymus (Sekiguchi et al. 2003, Ito et al. 2004). Moreover, CD4 expression is widespread among human MNPs (Jefferies et al. 1987), and whilst the function of CD4 receptor in MNPs is not well understood, recent evidence has indicated a critical role in driving differentiation of human monocytes into inflammatory macrophages (Gibbings and Befus 2009, Krutzik et al. 2014).

There is currently no definitive evidence that T_H subsets truly exist in fish and little is known about the evolutionary origin of these cells. Fish genomes usually contain multiple *cd4*-like paralogues designated *cd4-1* and *cd4-2,* and while the

function of the latter gene is currently unknown, we and others have reported evidence that *cd4-1* encodes a canonical CD4 molecule (Yoon et al. 2015, Montero et al. 2016, Magadan et al. 2016). Notably, the CD4-1 and CD4-2 proteins of various fish species differ in terms of immunoglobulin (Ig) domain structure, with CD4-1 exhibiting a four Ig domain structure comparable to that of mammalian CD4 (Bernard et al. 2011, Hansen 2011). In contrast, CD4-2 proteins contain fewer (2-3) Ig domains and the functional significance of this is currently unclear. Interestingly, a recent study of the rainbow trout (*Oncorhynchus mykiss*) identified a minor population of T cells which express only CD4-2, and this side population were found to be less proliferative and restricted in TCR repertoire (Magadan et al. 2016). However, evidence suggests that these proteins are widely co-expressed in the T cells of both rainbow trout and zebrafish (Yoon et al. 2015, Magadan et al. 2016).

While $CD4^+$ cells have not yet been extensively characterised in bony fish, T-bet, GATA, and STAT family TFs (as well as FoxP3) (Alnabulsi et al. 2010) are represented in most teleost genomes as are many interleukins (Wang and Secombes 2013). Moreover, $CD4^+$ cells isolated from zebrafish, Japanese pufferfish (*Takifugu rubripes*), sea bass (Dicentrarchus labrax) and the common carp (*Cyprinus carpio*) treated with non-specific immunostimulants express signature T_H1, T_H2 and T_H17 cytokines (Alnabulsi et al. 2010, Kono and Korenaga 2013, Katakura et al. 2013, Gerdol et al. 2014). In addition, adoptive transfer experiments using the ginbuna crucian carp (*Carassius auratus lansdorfii*) have provided some evidence that $CD4^+$ T cells provide helper function (Kondo et al. 2014, Araki et al. 2014). Recent studies employing antisera to

zebrafish and rainbow trout CD4-1 proteins have indicated that fish CD4-1^+ T cells primed and boosted with antigen, or infected with pathogenic bacteria, will express T_H1, T_H2 and T_H17 associated TFs and cytokines (Yoon et al. 2015, Montero et al. 2016, Magadan et al. 2016). Thus, in broad terms, it appears likely that T cell function as understood in mammals had already evolved in bony fish. However, the immune responses described in these experiments were heterogeneous, and were therefore unable to identify $CD4^+$ T cells biased towards a particular T_H-phenotype. Exploring both the conservation and distinctiveness of teleost T cells is of profound interest not just for the evolution of these versatile cells, but also the application of zebrafish as a model for biomedical research as well as to research into health management of valuable fish species in commercial aquaculture.

1.9 Zebrafish melanoma model systems

The choice of a good model organism in research depends on the requirement and the conditions of the research. The zebrafish (*Danio rerio*) is an established model organism for development and disease research as they are vertebrates and have genes that are similar to the human genes (Nathan et al. 2008). Zebrafish is also conducive for imaging owing to its transparency at early stages of development which makes it an optimum model to visualize different dynamic interactions of immune cells with peripheral tumours. Moreover, compared to mice, they are inexpensive to maintain and have short generation time laying up to 400 eggs/pair a week. They are easy to manipulate genetically as the egg fertilization occurs externally in the water,

allowing for manipulation at early developmental stages, less than 1 hour post fertilization.

Using the zebrafish model to study melanoma is increasingly getting popular and many groups including ours' have developed zebrafish models for studying different aspects of melanoma. One of the first animal models of a $BRAF^{V600E}$-driven cancer was developed in zebrafish by expressing oncogenic human $BRAF^{V600E}$ gene under the control of the melanocyte-specific 'mitfa' promoter (Patton et al. 2005). Our laboratory has generated the zebrafish model of a $HRAS^{G12V}$ driven melanoma by expressing oncogenic human $HRAS^{G12V}$ in their melanocytes, Tg(*mitfa:V12RAS; mitfa:GFP*) (Michailidou et al. 2009). As illustrated in figure 1.4, expression of $HRAS^{G12V}$ in melanocytes produced superficial spreading (also termed radial growth phase [RGP]) melanoma. Occasionally, the progression is intensified and result in formation of visible tumor nodules which is accompanied by more invasive growth, this is comparable to vertical growth phase (VGP) melanoma (figure 1.4, Michailidou et al. 2009).

Zebrafish is emerging as an excellent model for studying different immunological aspects ranging from developmental to disease specific (including cancer). Over the last decade, a few groups have developed different transgenic fish to study immune cells particularly T cells and macrophages (David M. L et al., 2004; Felix E et al., 2011). An LCK promoter driven GFP transgenic zebrafish line (Tg(lck:gfp)) generated by David M.L *et al.* demonstrating the presence of T cells in zebrafish (David M. L et al., 2004). Later, Isabell H *et al.* demonstrated that in zebrafish T-cell

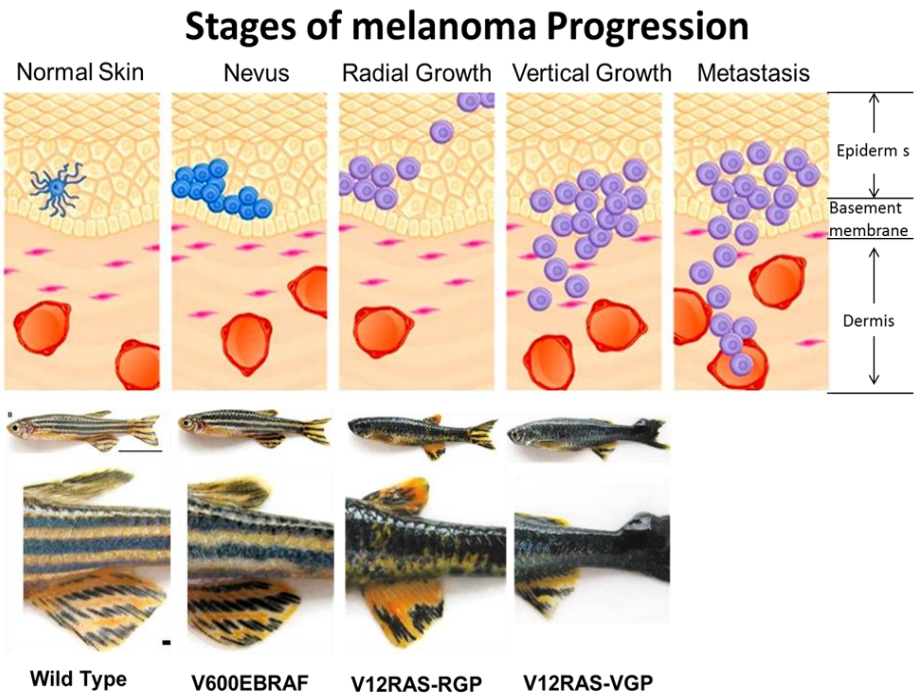

Figure 1.4: Stages of cutaneous melanoma progression and our respective zebrafish models. At the stage of the benign nevus, *BRAF, NRAS or cKIT* mutation and activation of the ERK MAPK pathway occur. Further progression of melanoma is associated with decreased differentiation and the decreased expression of melanocyte markers regulated by microphthalmia-associated transcription factor (MITF) such as TRPM1, and increased expression of proliferation factors such as cyclin D1 (CD1). Vertical-growth phase and metastatic melanomaare notable for striking changes in the control of cell adhesion, including the loss of E-cadherin and increased expression of N-cadherin, αVβ3integrin, and matrix metalloproteinase 2 (MMP2).(*Adapted from Journal of Investigative Dermatology,* 2008)

maturation occurs in the thymus (Isabell H *et al.,* 2012). Although it was established that zebrafish had T cells but it was unclear whether they can differentiate in mammalian equivalent of CD4, CD8, T_H1, T_H2 and T_{reg} cells.

1.9 Aims

The key aims of this project are:

- To generate a transgenic zebrafish CD4-1 reporter line.
- To explore if zebrafish have $CD4^+$ T cells that can differentiate in T_H1, T_H2 and T_{reg} like cells?
- To determine whether CD4-1^+ T cells in zebrafish respond to tumour development?
- To develop an in-vivo model system to facilitate induction of immunoregulatory molecules in the tumour microenvironment.

Chapter 2. Materials and Methods

2.1 Reagents and material

Table 1: Buffers and solutions used in this study

Solution	Procedure	Components
Chorion water + Methylene blue (optional)	Embryo Culture	60 mg Instant Ocean Salts (Tropic Marin ®) 10-5% Methylene Blue 1L dH2O
MS222	Anestheting/ Killing fish	7.7 mM MS222, 1 mM tris, pH 8.5 in dH2O
Alkaline Lysis Solution I	Plasmid miniprep	100 mM Tris pH 8.0, 50 mg/ml RNase A
Alkaline Lysis Solution II	Plasmid miniprep	0.2 N NaOH in 1% SDS
Alkaline Lysis Solution III	Plasmid miniprep	4 M KAc, 11.5% glacial acetic acid
TAE buffer	DNA electrophoresis	40 mM tris base, 1mM EDTA, 0.1% glacial acetic acid
10x TBE	Pulse field gel electrophoresis	108g Tris Base, 55g Boric acid (or orthoboric acid), 9.3g EDTA and adjust to 1liter with dH_2O
DNA Lysis Buffer	DNA Extraction	50 mM Tris (pH 8), 100 mM EDTA, 0.5% SDS (w/v), pH 7.2
TE Buffer	Re-constituting DNA	10 mM Tris (pH 7.5, 1 mM EDTA
1x TBS	Histology	25 mM Tris-Base pH7.5 (Thermo Scientific), 136 mM NaCl (Thermo Scientific), 2.7 mM KCl (Thermo Scientific)
TBST	Histology	1x TBS, 0.1% Tween-20 (Sigma)
1x PBS	Histology	137 mM NaCl, 2.7 mM KCl, 10 mM Na2HPO4, 2 mM KH2PO4,pH7.

Table 2: List of primers used in this study for cloning**.**

Name of the primer	**Sequence of the primer**
CD4-1_Harm1	**F:(attB1)** GGGGACAAGTTTGTACAAAAAAGCAGGCTGGGAGGAAGAGAGGGGGTGTTC **R: (attB5r)** GGGGACAACTTTTGTATACAAAGTTGTCTTTCGGTCCTCAGATCAGA
CD4-1_Harm2	**F:(attB3)** GGGGACAACTTTGTATAATAAAGTTGGGTTTGATTCTAATACCGCTGTTCA **R: (attB2)** GGGGACCACTTTGTACAAGAAAGCTGGGTACTTTAGGCTGTATAGAAGTGTCTTGA
mCherry	**F: (attB5)** GGGGACAACTTTGTATACAAAAGTTGGGGGATCCACCATGGTGAGCAA **R: (attB4)** GGGGACAACTTTGTATAGAAAAGTTGGGTGGGGGTACCGGGCCCAATT
Gal4vp16	**F: (attB5)** GGGGACAACTTTGTATACAAAAGTTGGGATGAAGCTACTGTCTTCTATCG **R: (attB4)** GGGGACAACTTTGTATAGAAAAGTTGGGTGAACCTCCCACATCTCCCCCT
SpecR	**F: (attB4r)** GGGGACAACTTTTCTATACAAAGTTGGGCCAGCCAGGACAGAAATGCCT **R: (attB3r)** GGGGACAACTTTATTATACAAAGTTGTTTATTTGCCGACTACCTTGGT
iTol2 Kan	**F:** TGGGATAGTGTTCACCCTTGTTACACCGTTTTCCATGAGCAAACTGAAACCCCTGCTCGAGCC GGGCCAAGTG **R:** GTAGAAACTGCCGGAAATCGTCGTGGTATTCACTCCAGAGCGATGAAAACATTATGATCC TCTAGATCAGATCT
CD4-1_Harm1	**F:** AACCGCACTCCCGTCTCAGCACCA

_seq	
CD4-1 _Harm2 _seq	**R:** GCGCTACGCCACTGTGCCTT
XhoI_IFNγcds	**F:** GGGCCCCTCGAGATGATTGCGCAACACATGATG
AvrII_IFNγcds	**R:** GGGCCCCCTAGGACCTCTATTTAGACTTTTGCTTCTTGAT
PDL1-T	**F: (attB1)** GGGGACAAGTTTGTACAAAAAAGCAGGCTGGATGTGCAGTATTC ATCAGGGGTCA **R:(HA_attB2)** GGGGACCACTTTGTACAAGAAAGCTGGGTGTCAAGCGTAATCTG GAACATCGTATGGGTAAGCAGAACCGTGAAGAGGGA

Table 3: List of primers used in this study for qPCR.

Gene	Primer Sequences
lck	F: CAAACTAGAGCGCAGACTGG R: GGGTGCTGTAGGGACTTCAT
tcra	F: CTTAAAACGTCGGCTGTCCG R: TGAACAAACGCCTGTCTCCT
mpeg1	F: ATGTGGATTCCCCAAACTTCAACT R: TGGTAAATGCCACCAAAGCTAAGA
c-fms	F: GGCCAAAATCTGTGACTTCGGA R: ACCAGACGTCACTCTGAACCG
cd4-1	F: GTGTTTGGACATGCCAGTTG R: AAGCACAGGGAATGCTGACT
cd8a	F: AGGTTGTGGACTTTTCCTCGT R: GGAGCTAGAAGTGGCTGGTG
ThPok	F: CGCCCTTTATTAATGACCCGCG R: AGGCAGCTTGACCTTTCACATG
cd4-2.1	F: GCCTGGACTTGCTGGAGAAATTTT R: AGAACCACAGAAAAGGCTCCTACA
cd4-2.2	F: GGGAAGTTTGTGTGTGAAGTGGAG R: AAACGCACAGTGCGTGTAGATCTG
runx3	F: CAAACTTTCTCTGCTCGGTCCTG R: AATTCTCATCATTTCCCGCCATCA
eomesb	F: AATAACAAGGGCGCGAACATCAA R: AAGATCTGAGTGTTTGAGTCTCGC
tbet	F: GCAGCTCCAACAACGTAGCA R: ATCCTCCTTCACCTCCACGATG
gata3	F: GGTGAGATGTAGGGAGAGGAAACC R: TGCCCAAGACCTATAACACATCCA
il-4/13b	F: CTGTTGGTACTTACATTGGTCCCC R: AGTGTCCTGTCTCATATATGTCAGGT
il-4/13a	F: GCACTGTATTCGTCTCGGGTTTTA R: TTTTCCCCAGATCTACAAGGAAGA
IFNγ1-2	F: CCTGGGGAGTATGTTTGCTGTTTT R: GGGTGTGCATTATGTAGCTGAGAA
foxp3a	F: CCGTCACAACACTGCTACATGG R: ACCTTTCCTTCCTTCAACACGC
il-10	F: CTTTAAAGCACTCCACAACCCCAA R: CTTGCATTTCACCATATCCCGCTT
Beta actin	F: CGAGCTGTCTTCCCATCCA R: TCACCAACGTAGCTGTCTTTCTG

2.2 Zebrafish husbandry

Zebrafish were housed at the biological services unit (BSU) in the University of Manchester and maintained according to standard conditions as described in the zebrafish handbook (Westerfield, 2000). Embryos and larvae up to 5 dpf were maintained at 28.5 ^{0}C in chorion water (Table 1) and later transferred to the main aquarium system. Animals which developed a tumour were sacrificed using Schedule I methods. Fish were overdosed with 20% Ethyl 3-aminobenzoate methanesulfonate (MS222, Table 1) for around 5 minutes and soon after imaging were preserved in PFA (Table 1).

2.2.1 Breeding and embryo collection

On the day before the injection of constructs (BACs), adult male and female zebrafish were transferred in to thoron crossing boxes (Thoren Aquatics, Inc.) and were separated by a plastic divider overnight. Next morning, soon after the lights were switched on, dividers were removed to initiating spawning. After around 20 minutes, fertilized embryos were collected from the outer thoron box.

2.2.2 Microinjection of constructs

Constructs were injected in to one-cell zebrafish embryos at the yolk-sac margin. An injection volume of around 1/10th of the embryo diameter was injected using a PLI-90 Pico-Injector micro-injection station (WPI instruments). Following injections, embryos were incubated at 28.5 ^{0}C and were later transferred to the main aquarium system at 5

dpf. At 23 dpf juvenile zebrafish were screened for positive reporter transgenic fish and were later separated in to a fresh tank.

2.2.3 Injection solutions

Injection solution was prepared by mixing equal volumes of 50ng/l construct to be injected (CD4-1 BAC etc.) and 50ng/l *Tol2* transposase mRNA solutions. A 0.05% (w/v) phenol red was added to the final volume to enhance the visibility of the injected solution.

2.2.4 Preparation of injection plates

Agarose gel solution (1.5 %) was prepared using chorion water (Table 1). To create grooves, a plastic mould (eppendorf Inc.) was placed at the centre of 94mm Petri dish and the above gel was poured up to the height of mould.

2.2.5 Screening of transgenic zebrafish

Embryos were monitored and maintained daily up to 5 dpf in the incubator at 28.5 ^{0}C. At 23 dpf, injected fish were screened for the red thymus using a fluorescent microscope (Leica M205FA stereo microscope). Any positive reporter transgenic fish observed were separated into a fresh tank.

2.3 Maxi Prep

Large scale Plasmid isolation of different constructs was carried out using QIAfilter^{TM} Plasmid Maxi kit (Qiagen) according to the manufacturer's instructions.

2.4 Construction of clones

LR clones containing mcherry and gal4vp16 BAC targeting cassette was made using Multisite Gateway® four-fragment vector construction kit (invitrogen). Please refer (Figure 2.1) for a schematic representation of complete process.

2.4.1 Flanking of cDNA with '*att*' sites

'att' sequences were included in the 5' and 3' gene specific primers (Table 2) and using these primers cDNA/DNA was amplified in a thermal cycler (PTC-100, MJ Research).

PCR reaction:

10X Buffer (Novagen)	5 µl
dNTPs (final concentration 0.2 mM)	5 µl
KOD XL DNA polymerase (Novagen)	1 µl
5' primer (10 µm)	2 µl
3' primer (10 µm)	2 µl
dH_2O	34 µl
DNA (up to 50ng)	1 µl
TOTAL VOLUME	50 µl

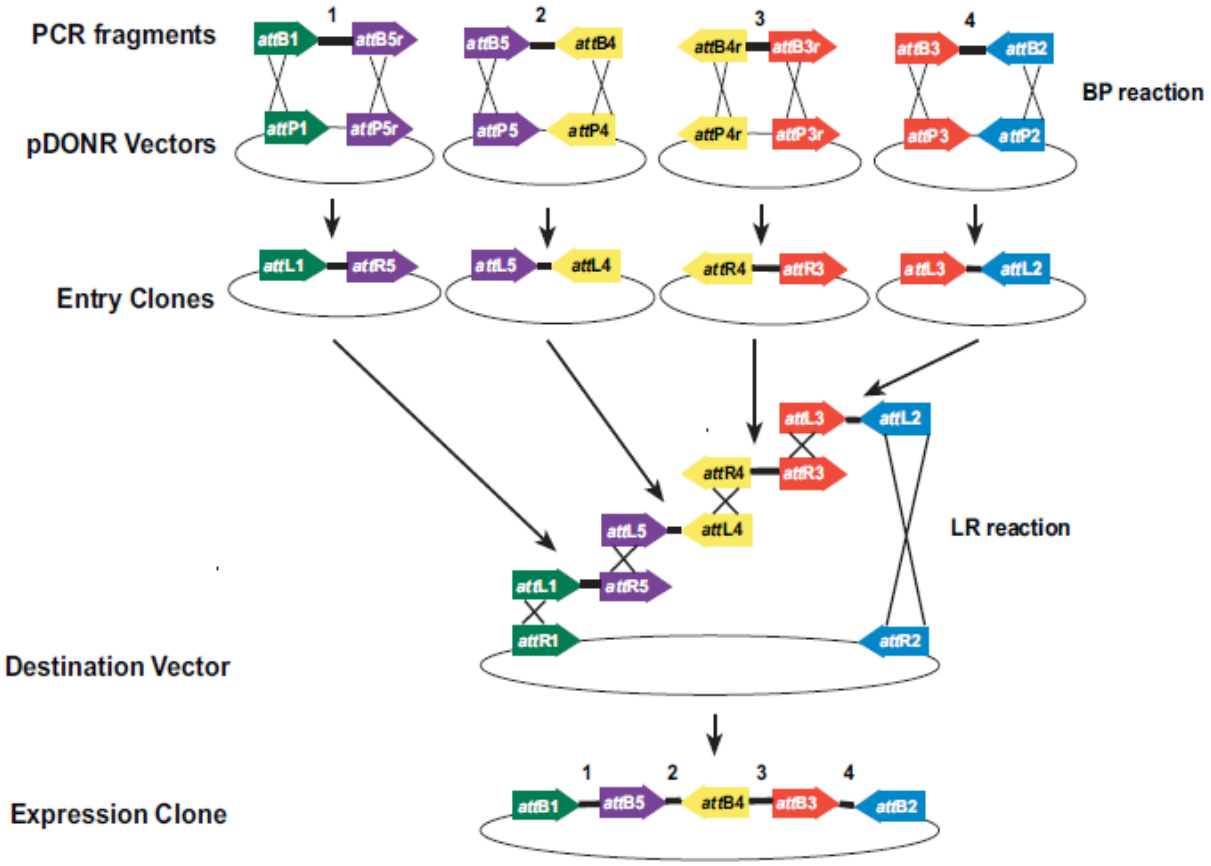

Figure 2.1: Flow chart illustrating construction of LR clones (Figure taken from Gateway® cloning manual).

PCR programme:

Hot lid 110^{o}C

Denature 94^{o}C for 5 minutes

Denature 94^{o}C for 30 seconds

Anneal 55^{o}C for 5 seconds

Extend 74^{o}C for 60 seconds

28 cycles

Final extension 74^{o}C for 10 minutes

Store at 4^{o}C

2.4.2 BP reaction and transformation

Flanked cDNA was inserted in to the entry clones, pDONR™ vectors (invitrogen), using BP Clonase™ II enzyme mix (invitrogen).

BP reaction mix:

att PCR product (50 fmoles)	1-7 µl
pDONR™ 221 (150 ng/µl)	1 µl
TE buffer, pH 8.0	up to 8 µl
BP Clonase™ II enzyme mix	2 µl

This reaction was incubated at 25^{o}C for 1 hour and was later terminated by adding 1 µl of proteinase K solution (invitrogen) at 37^{o}C. After 10 minutes of incubation, 1 µl of this BP reaction mix was transformed in to DH5α cells as per the specified protocol. Following transformation, cells were spread on LB plates containing 50 µg/ml kanamycin.

2.4.3 LR reaction

As illustrated in the (Figure 2.1), the LR reaction was performed with LR Clonase™ II enzyme mix (invitrogen) using four entry clones (homology arm-1, homology arm-2, mcherry/gal4vp16 and spectinomycin) and pcs2 R1-R2 destination vector.

LR reaction mix:

Entry clone containing homology arm-1	(20 fmoles)	1 µl
Entry clone containing homology arm-2	(20 fmoles)	1 µl
Entry clone containing mcherry	(20 fmoles)	1 µl
Entry clone containing spectinomycin	(20 fmoles)	1 µl
Pcs2 destination vector	(40 fmoles)	1 µl
TE buffer, pH 8.0		3 µl
LR Clonase™ II enzyme mix (invitrogen)		2 µl

The reaction was incubated at 25^{o}C for overnight and was later terminated by adding 1 µl of proteinase K solution (invitrogen) and incubation the reaction at 37^{o}C for 1 hour. Following transformation, DH5α cells were spread on LB plates containing 50µg/ml ampicillin and 50µg/ml spectinomycin for the screening of transforments. Positive clones, once confirmed with sequencing, were maxi prepped and injected in to the embryos of zebrafish as mentioned in section 2.2.2.

2.5 Agarose gel electrophoresis

1% agarose gels were prepared by dissolving agarose (w/v) in to 1x TAE buffer (Table 1) and the mixture was heated for 2-3 minutes in microwave. After it was cooled down to about 50^{o}C ethidium bromide (Fluka) was added at 0.5µg/ml concentration and the gel was casted. Along with hyperladder I, DNA samples mixed with 5x loading dye (Bioline) were loaded in to the wells. Gels were run in the gel tank (Power pack Consort E132, gel tank jencons, HUI3) immersed in 1x TAE buffer at 90 V. DNA bands were visualised using UV light.

2.6 DNA extraction and purification from agarose gel

DNA extraction and purification from agarose gel was done using GFX purification kit (GE health care) according to manufacturer's instructions.

2.7 Quantification of DNA

DNA was quantified using Nanodrop™ (Thermo Scientific) machine. The DNA sample of 1µl was used to measure the concentration.

2.8 Sequencing

Sequencing was carried out to check the presence of our desired gene (mCherry or Gal4vp16) in BP clones, final LR clones and in the final BAC constructs. Using the ABI BigDye Terminator Cycle Sequencing Ready-reaction kit (Applied Biosystems) the following PCR reaction and programme were performed in a thermal cycler (PTC-100, MJ Research). The *att* cDNA primers were used for sequencing various LR clones whereas the following M13 primers were used for BP clone:

M13 forward: 5'-GTAAAACGACGGCCAG-3'

M13 reverse: 3'-CAGGAAACAGCTATGAC-5'

Reaction:

Big Dye Terminator enzyme	2µl
Big Dye Buffer	3 µl
Primer (3.3µM)	1 µl (for BAC 10µM was added)
Plasmid/ BAC DNA	300ng/ 1ug
dH_2O	...
TOTAL VOLUME	20 µl

Program:

Hot lid 110^{o}C

Denature 94^{o}C for 30 minutes

Denature 94^{o}C for 10 seconds
Anneal 55^{o}C for 5 seconds
Extend 60^{o}C for 4 minutes
} 30 cycles

Store at 4^{o}C

The PCR products were mixed with 2µl of 3 M sodium acetate and 50µl of 95% ethanol. 1µl of Glycoblue (Ambion) was added to enhance the visualisation of DNA pellet. After mixing, the samples were centrifuged at 13,000 rpm for 20 minutes to precipitate the DNA and the supernatant was discarded. The DNA pellets were washed with 100µl of 70% ethanol and centrifuged at 13,000 rpm for 15 minutes. The supernatant was discarded, leaving the DNA pellets which were dried at room temperature. The pellets

were sent to the University of Manchester sequencing service for further processing. The resulting sequences were analysed using the BioEdit software.

2.9 Restriction digestion

Various clones (BP, LR, and BAC) were subjected to digestion using a variety of enzymes. The following reaction was incubated at 37^{o}C for 3 hours.

Plasmid DNA	5µg
Enzyme buffer	2µl
Restriction enzyme	0.5µl (5 units)
dH_2O	....
TOTAL VOLUME	20µl

2.10 BAC recombineering

The *cd4-1* BAC clone CH73-296E2 was supplied by BACPAC resources center (BPRC), USA as agarose stabs which were streaked on LB agarose plates (chloramphenicol). Single clones were cultured and stored as glycerol stocks at -80^{o}C. BACs were recombined using Red/ET BAC recombineering kit (GeneBridges, Germany). Please refer to figure 8 for the schematic process of BAC recombineering.

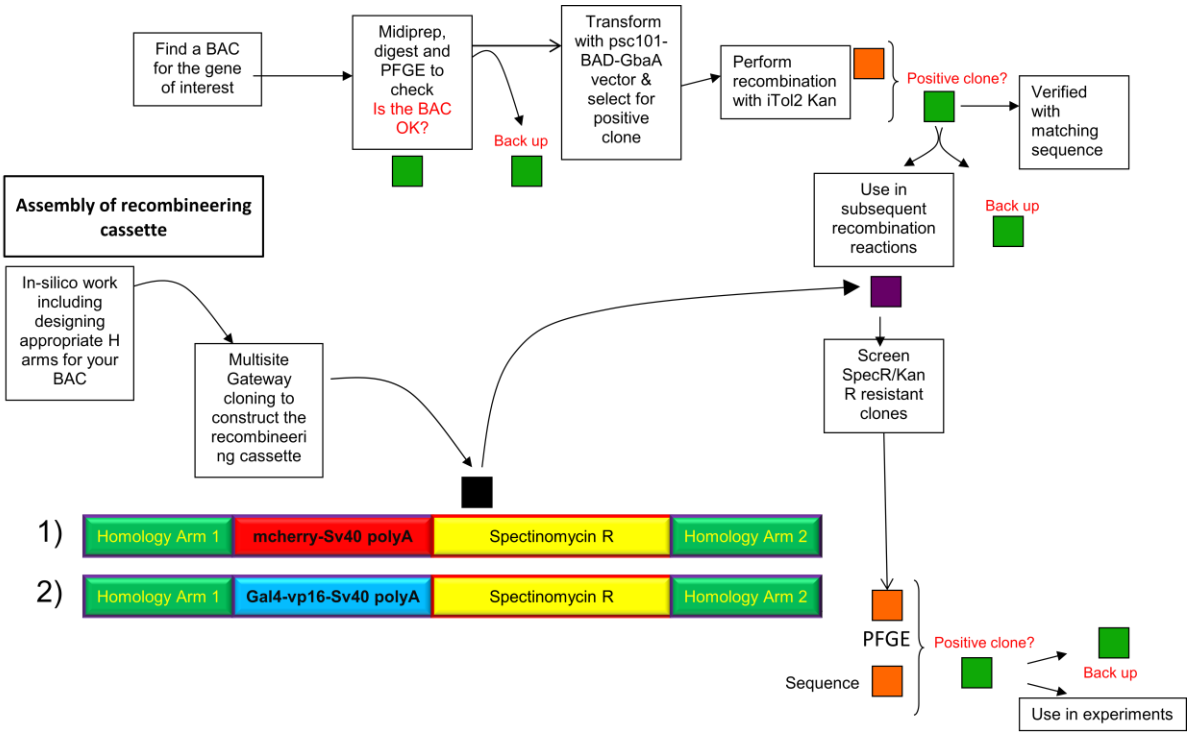

Figure 2.2: Schematic for homologous BAC recombineering process.

2.10.1 Preparing electro-competent, recombination efficient bacteria

Bacteria containing the BAC of interest were grown overnight (@ 32^{o}C, 180 rpm) in 5 ml LB culture with respective antibiotic selection. The subsequent morning, 1ml of overnight culture was diluted into 50ml fresh LB media with the same antibiotic selection and allowed to grow in a 250ml conical flask until it reached an OD_{600} of 0.6. When the culture reached the desired density, it was divided to 2 flasks each of 25ml bacterial culture. To activate the recombineering vector (pCS101-BAD-gbaA-tet) we added 350ul of 10% L- Arabinose to one of the flasks (induced) while in the rest of 25ml, 350ul of sterile water was added (un-induced, control) and both the flasks were incubated at 37^{o} C, 180 rpm for 40 minutes followed by cooling on ice for 2 minutes. Subsequently, we used the following protocol to make the bacteria electro-competent:

1) Spin in pre-chilled centrifuge at 4000 rpm for 5 minutes and remove the supernatant
2) Resuspend in 10ml ice cold sterile water.
3) Repeat step 1 and 2 for 2 more times
4) Spin in pre-chilled centrifuge at 4000 rpm for 5 minutes and remove the supernatant
5) Resuspend in 1ml ice cold sterile water.
6) Spin in pre-chilled table top centrifuge at 13000 rpm for 2 minutes and remove the supernatant
7) Repeat step 5 and 6 for 2 more times

8) Add 40 ul of ice cold sterile water and store the vials on ice.

The cells are now electro-competent.

2.10.2 BAC recombineering by electroporation of targeting cassette

The above prepared electro-competent cells were mixed with 150 ng of the targeting cassette (iTol2KAN cassette/ CD4mcherry/ CD4gal4vp16) and left on ice for 5 minutes without pipetting up and down (iTol2KAN cassette was a kind gift from Prof. Stephen Renshaw, University of Sheffield). The bacteria-DNA mixture was transferred in to a pre-chilled electroporation cuvette (0.1cm) and was subjected to electroporation using the following settings:

- Voltage: 1.8kV
- Capacitance: 25uF
- Resistance: 200ohms

The bacteria were immediately rescued by adding 250ul of SOC medium and transferred to a 1.5ml eppendorf tube. The tube was incubated at 32^{o}C, 180 rpm for 90 minutes and subsequently plated on either kanamycin (after Tol2 recombineering, 50 ng/ul) or kanamycin (50 ng/ul)+spectinomycin (50 ng/ul) (after mcherry and gal4vp16) plates. All the plates were incubated at 32^{o}C overnight and later the bacterial colonies (5-7 colonies) were expanded in a 5ml LB broth with respective antibiotic. Following the extraction of BAC DNA, positive clones identified by PCR and restriction digestion analysis.

2.10.3 Pulse Field Gel Electrophoresis (PFGE)

PFGE is used to resolve large fragments of DNA which fail to separate on a conventional agarose gel. DNA fragments (>20, 000bp) tend to migrate at the same speed and these fragments cannot be resolved. The pulse field unit regularly changes the direction of the electric field, and thus introduces another variable in DNA migration, namely the ability of the DNA to turn, or change direction, within the gel, and much greater size resolution can be obtained.

PFGE Protocol using CHEF DRII BIORAD apparatus:

Gel:	1% agarose gel in 0.1X TBE with 15/20 lane comb
Running Buffer:	0.1X TBE (about 3 litres needed)
Markers:	Mid-Range PFG marker I and Mid-Range PFG Marker II (NEB catalogue number N3551S and N3552S respectively). They are in a gel syringe dispenser from which a small circle of gel was sliced, enough to fit into well.

The buffer was cooled to 14^{o}C in the unit using the chiller while the gel was loaded with samples on the bench. Both the chiller and the pump were turned off and the loaded gel was carefully immersed into its position within the unit. The gel was run for about 10 minutes with the pump off allowing the samples to enter the gel thus minimizing the risk of sample loss by exiting the well.

Run parameters:

Duration of run: 15-18 hours

Power: 6V/cm

Switching time: 1-6 seconds

Temperature: 14^{o}C

2.11 Flow cytometry and cytology

Single cell suspensions were prepared from zebrafish organs essentially as described previously (Yoon, 2015). Briefly, organs were dissected in to 1.5ml eppendof tube containing L-15 medium (Gibco) with 10% FCS (Sigma). The tissues were pooled from 5-6 fish and cells dissociated manually by pushing through a 40µm pore size cell strainer (BD Falcon) and then further passed through a 50µm pore size filter (BD Biosciences) to ensure removal of aggregated cells. Cells were centrifuged at 400xg for 5 min at 4^{o}C and resuspended in L-15 media (without phenol red, Gibco) with 2% FCS. Dissected intestine and tumour samples were first treated for 1 hour at 37^{o}C with Liberase enzyme cocktail to facilitate dissociation of cells (Roche, 0.2unit/ml in PBS). Flow cytometry was performed using a FACSAria Fusion flow cytometer (BD Biosciences) and data was analysed using Diva 8.0.1 software (BD Biosciences). For flow cytometry of cells from 20 dpf *Tg(cd4-1:mCherry)* zebrafish, single cell suspensions were prepared from individual larvae by manual dissociation in trypsin (Sigma) for 1 hour at 37^{o}C. Flow cytometry was performed using an Attune NXT (Applied Biosystems) and data was analysed using Attune NXT software v2.1. Cytospin and Wright/Giemsa staining was

carried out as previously described (Stachura, 2011) and cells were imaged using a Zeiss AxioVision microscope.

2.12 Real-time quantitative polymerase chain reaction (Q-PCR)

RNA was isolated from cells or homogenised tissues using the RNeasy micro kit (Qiagen), including on column DNase digestion, and stored at $^{-}80^{O}$C. Reverse transcription was carried out using the ProtoScript II First Strand cDNA synthesis kit (New England Biolabs) with oligo-dT (deoxy-thymine) primers. Depending on the number of samples Q-PCR was performed either using SYBR Green JumpStart *Taq* ReadyMix (Sigma) and the MX300P system (Stratagene), or using the Biomark HD microfluidic platform (Fluidigm) according to the manufacturer's instructions, with the majority of data replicated using both methods. Briefly, for Fluidigm Biomark, high throughput Q-PCR is performed in two steps. Firstly, target genes are preamplified in a single 14 cycle reaction by combining 25ng cDNA with a pooled target primer mix and TaqMan PreAmp Master mix (Applied Biosystems) following conditions recommended by the manufacturer (Fluidigm), and then treated with *ExoI* (New England Biolabs) to remove unincorporated primers. Secondly, 48 x 48 (samples x primers) Q-PCR reactions are performed on the Biomark HD dynamic array using EvaGreen for detection and following the manufacturer's instructions. Ct values were calculated using the system software (Fluidigm Real Time PCR Analysis Version 3). Data was analysed by the ΔCt method using *bactin* (or *ef1a* where indicated) for normalisation ($2^{-[Ct,gene\ -\ Ct,bactin]}$), or

the ΔΔCt method using *bactin* and a control sample for normalisation. For primer sequences see Table 3.

2.13 Tissue preparation, cryosectioning, immunohistochemistry

Dissected gills were fixed in Bouin's fixative and mounted in 1% low melting temperature agarose (Flowgen). For sectioning, the gut was fixed in 4% paraformaldehyde, embedded in 25% fish gelatine/ 15% sucrose and sectioned at 20µm thickness on a Leica 3050S cryostat. Immunohistochemistry was performed for EGFP or mCherry according to standard protocols using rabbit polyclonal anti-GFP (1/500, Ab290, AbCam), mouse monoclonal anti-mCherry (1/500, Living Colours, Clontech), anti-rabbit Alexa 488 (1/500, Molecular Probes) and anti-mouse Alexa 594 (1/500, Molecular Probes).

2.14 4-OHT treatment

Adult zebrafish were treated with 5µm 4- Hydroxytamoxifen (4-OHT) overnight (in dark cycle) and were returned to their respective tanks the next morning. No treatment was given the following night. This cycle was repeated 3 more times to ensure a robust induction of cre/lox recombineering of the target construct (mitfa:lox-mCherry-lox:IFNγ-P2A-venus). Fish were then allowed to recover for a couple of days before they were screened for expression of green fluorescence. The follow up imaging was done once every week.

2.15 Live imaging and microscopy

Zebrafish larvae were anaesthetised using 4% MS-222 (Sigma) and immobilised in 1% low melting temperature agarose (Flowgen). Time lapse imaging (one image every 1-2 min) was performed using a Leica SP5 confocal microscope. Z-stacks of approximately 40µm (2-3µm/ Z-slice) were projected onto a single plane. Videos were generated using NIH Image J. Sections and fixed preparations were imaged using either a Leica SP5 or a Nikon A1R confocal microscope. Fluorescence microscopy was performed using a Leica M205FA stereo microscope. For imaging of 20 dpf *Tg(fms:GFP)SH377;Tg(cd4-1:mCherry)* compound transgenics, larvae were fixed in 4% paraformaldehyde for 24 hours at 4^{o}C, washed in 0.1% Tween-20 PBS and imaged using a Nikon Ti fluorescence microscope.

2.16 Statistical Analysis

Data was analysed as appropriate using a non-parametric Mann-Whitney *U* test, a one-way ANOVA test, or a Kruskal-Wallis test with Dunn's multiple comparison post-hoc test (Prism 6.0, Graphpad). In all cases the significance threshold was set at $p \leq 0.05$.

Chapter 3. BAC recombineering

Results

3.1 CD4-1 BAC selection

As mentioned earlier, zebrafish, like other teleosts, express two full length *cd4* paralogues, termed *cd4-1* and *cd4-2.1* (*cd4-2.2*, a third paralogue unique to zebrafish is predicted to lack a cytoplasmic tail or LCK CXC docking motif, and may perform a novel regulatory function) (Yoon *et al*. 2015). CD4-1 is likely to represent a functional orthologue of mammalian CD4 as it has a closer genomic organisation, Ig domain structure and conserved regulatory regions. So, we decided to make CD4-1 transgenic reporter zebrafish and chose to use a BAC mediated approach. Bacterial Artificial Chromosomes (BACs) are widely used for generating various transgenic model vertebrates, including zebrafish, (Suster et al., 2009) mainly because they provide a unique opportunity to express target cDNA under the control of native regulatory mechanisms of the target gene. Using ZFIN database, we selected a BAC (CH73-296E2) that contains exons 1-3 of CD4-1 gene along with more than 50 kb of upstream sequence which potentially include the entire gene promoter and enhancer elements (figure 3.1).

Using the ensemble database, the transcription initiation site for CD4-1 gene (in the 2nd exon) was identified and around 400bp sequence upstream and downstream to the transcription initiation site was selected as homology arms 1 and 2 respectively (Table 2.1).

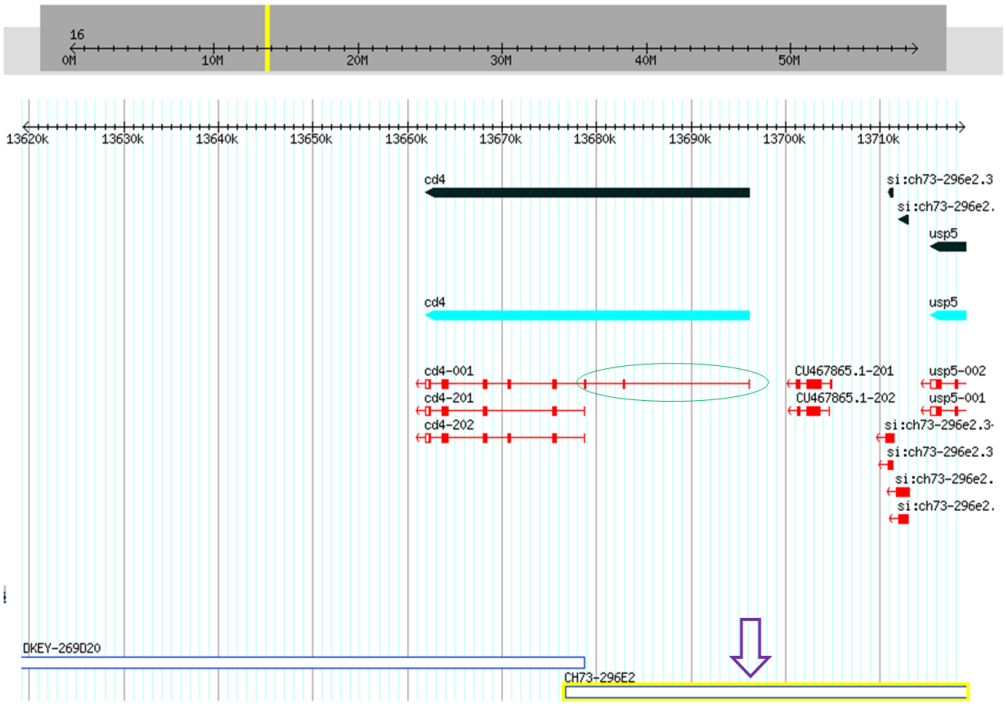

Figure 3.1: **CD4-1 BAC selection.** Location of *cd4-1* gene on chromosome 16 with the position of the selected BAC (CH73-296E2) indicated with an arrow. Length of the *cd4-1* gene transcript included in the BAC is circled in green.

3.2 Tol2 cassette was successfully integrated in to CD4-1 BAC

With the CD4-1 BAC selected, our next objective was to clone the Tol2 transposon 'arms' in to the BAC backbone thus facilitating the generation of stable transgenic fish lines. In the presence of Tol2 transposase, the region of the BAC flanked by tol2 transposons is efficiently integrated at random in to the zebrafish genome (Kawakami et al. 2007). Using a template plasmid for 'iTol2' kindly provided by Dr. Stephen Renshaw (University of Sheffield), we PCR amplified the Tol2 transposon arms along with kanamycin resistance gene using template specific primers flanked with 50bp of sequence homologous to the chloramphenicol resistance gene (Table2.2). The PCR product (from now on referred to as 'iTol2Kan cassette') was resolved on an agarose gel and we observed a band around 1500 bp, corresponding to the expected length of the amplicon (1568 bp) (figure 3.2 A).

After purification, using the above iTol2Kan cassette as a targeting construct against the chloramphenicol resistance gene in CD4-1 BAC vector, we performed BAC homologous recombineering to clone the Tol2 transposon arms in to the CD4-1 BAC. Subsequently, the purified BAC DNA was analyzed for integration of the iTol2Kan cassette by PCR (using a set of primers that are specific to vector backbone and the iTol2Kan cassette, table 2.2) and the products were resolved on an agarose gel. As expected, we observed bands at around 400 bp (expected length 396 bp), 500 bp (expected length 507 bp) and 1700 bp (expected length 1748 bp) (figure 3.2 B) confirming the appropriate integration of the iTol2Kan cassette, replacing the

chloramphenicol resistance gene with the kanamycin resistance gene. The positive clone was partially sequenced to check for any possible mutations around the integration site. The resultant sequence was mutation free showing close to 100% similarity with the expected sequence.

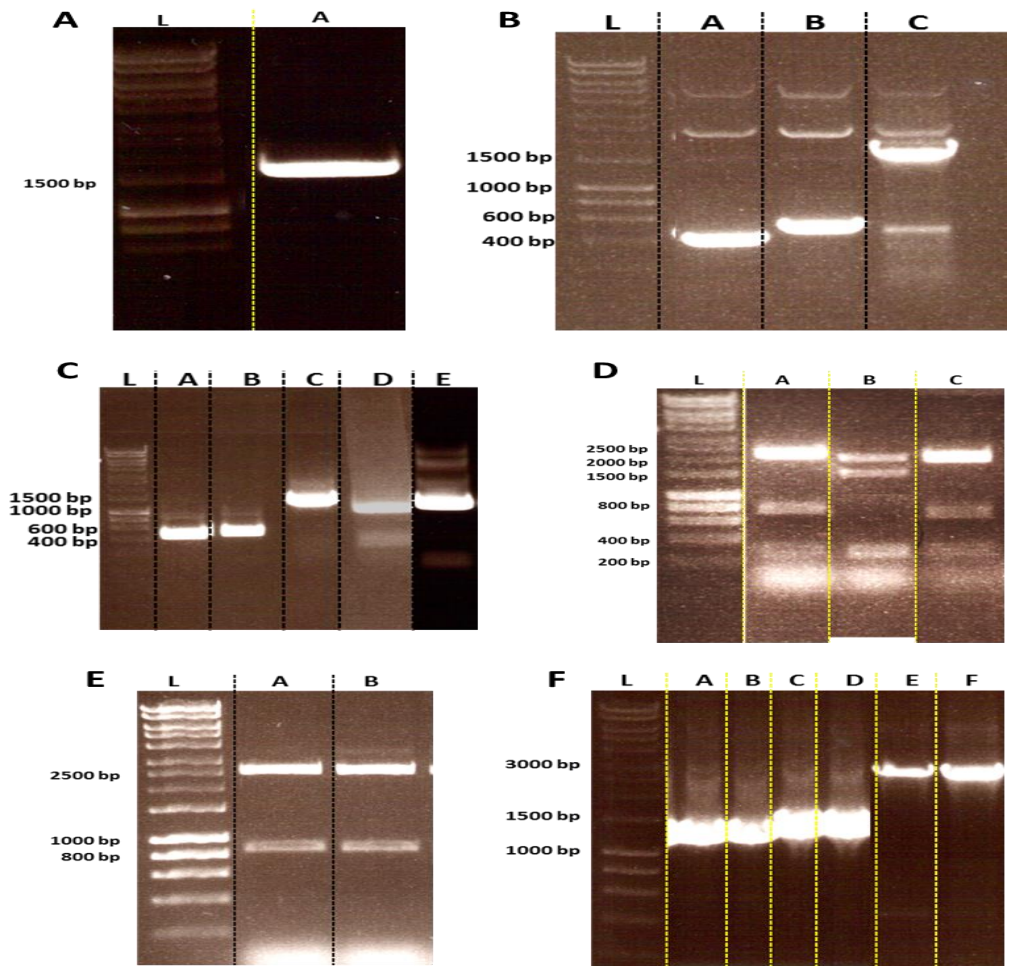

Figure 3.2: Gateway cloning to generate CD4-1 BAC targeting constructs (A) PCR amplification of iTol2Kan cassette from template DNA (actual length is 1548 bp). **(B)** PCR verification of a positive clone of BAC recombined with iTol2Kan cassette. Prominent bands in lane A and lane B correspond to the Tol2 left and right transposon arms respectively, while the prominent band in lane C indicates the integration of the entire iTol2Kan cassette in to the CD4-1 BAC. **(C)** 'att' products for BP reaction; Lanes A-E for CD4 homology arm-1, CD4 homology arm-2, spectinomycin resistance gene, gal4vp16 and mCherry. **(D)** Verification of BP entry clones using Restriction enzymes**;** Entry clones corresponding to CD4 homology arm-1 (lane A), CD4 homology arm-2 (lane B), and spectinomycin resistance gene (lane C) were digested with NheI and EcoRV enzymes whereas **(E)** entry clones corresponding to gal4vp16 (lane A) and mcherry (lane B) were digested with PsiI enzyme. **(F)** Validation of LR clones using PCR amplification; Lanes A (homology arm-1+gal4vp16, 1367 bp), C (spectinomycin+homology arm-2, 1564 bp) and E (from homology arm-1 until homology arm-2, 2963 bp) corresponds to gal4vp16 LR clone whereas lanes B (homology arm-1+mcherry, 1360 bp), D (Spectinomycin+homology arm-2, 1564 bp) and F (from homology arm-1 until homology arm-2, 2957 bp) corresponds to mcherry LR clone. All bands were of expected sizes thus validating the LR clones. Lane 'L' corresponds to hyper ladder-I, all products were resolved on in 1 % agarose gel.

3.3 Cloning of mCherry and gal4vp16 targeting constructs

With the Tol2 transposon arms cloned in to the CD4-1 BAC, we initiated the next step of the project, namely to assemble our mCherry and gal4vp16 targeting cassettes (refer to section 2.5). To achieve this, we used Multisite Gateway® cloning technology. The following sections deal with the construction of mCherry and gal4vp16 targeting cassettes.

3.3.1 Step 1: Flanking of DNA with 'att' sites

cDNA of mCherry, gal4vp16 and spectinomycin genes along with the DNA segments of homology arm-1 and homology arm-2 were PCR amplified, from their corresponding template plasmids, in a form compatible with BP clonase reaction using respective sequence specific 'att' primers. PCR products were resolved on an agarose gel and we observed bands around 1000 bp (mCherry, length of cDNA is 1095 bp), 1000 bp (Gal4vp16, length of cDNA is 1056 bp), 1200 bp (Spectinomycin, length of cDNA is 1245 bp), 400 bp (Homology arm-1, length of DNA is 408 bp) and 500 bp (Homology arm-2, length of DNA is 455 bp) corresponding to the lengths of the respective genes (Figure 3.2 C).

3.3.2 Step 2: BP clonase reaction

Independent entry clones for mCherry, gal4vp16, spectinomycin, homology arm-1 and homology arm-2 were prepared by cloning their above flanked cDNA/DNA in to their

respective ‘pDONR’ vectors using BP Clonase™ II enzyme (refer to section 2.5). Following transformation in to E. coli, plasmids were purified and subjected to restriction digestion. The entry clones of homology arm-1, homology arm-2 and spectinomycin were digested with NheI and EcoRV restriction endonuclease enzymes, whereas mcherry and gal4vp16 were digested with PsiI enzyme. All the digested products were analysed on an agarose gel (Figure 3.2 D, figure 3.2 E) and positive clones were sequenced to confirm the presence of the target DNA.

3.3.3 Step 3: LR clonase reaction

Vectors for both targeting cassettes (mCherry and gal4vp16) were generated by an ‘LR reaction’ assembling the four entry clones (homology arm-1, mCherry/ gal4vp16, spectinomycin, and homology arm-2) in to pcs2 destination vector catalysed by LR Clonase™ II enzyme (refer to section 2.5). Subsequently, the purified LR clones were analyzed for integration of the respective target genes by PCR (using a set of primers that are specific to different elements of targeting cassette, table 2.2) and the products were resolved on agarose gel. As expected, we observed bands at around 1300 bp (contains homology arm-1 and mcherry, 1360 bp), 1300 bp (contains homology arm-1 and gal4vp16, 1367 bp), 1500 bp (contains spectinomycin and homology arm-2 of CD4-1:mcherry BAC, 1546 bp), 1500 bp (contains spectinomycin and homology arm-2 of CD4-1:gal4vp16 BAC, 1546 bp), 3000 bp (entire mCherry targeting cassette, 2957 bp) and 3000 bp (entire gal4vp16 targeting cassette, 2963 bp) (figure 3.2 F) confirming appropriate integration of the entry clones. Positive clones were sequenced to confirm

the presence of the respective target gene cDNA in the final LR clone. Please refer to Figure 3.3 for vector maps of mcherry and gal4vp16 targeting cassettes.

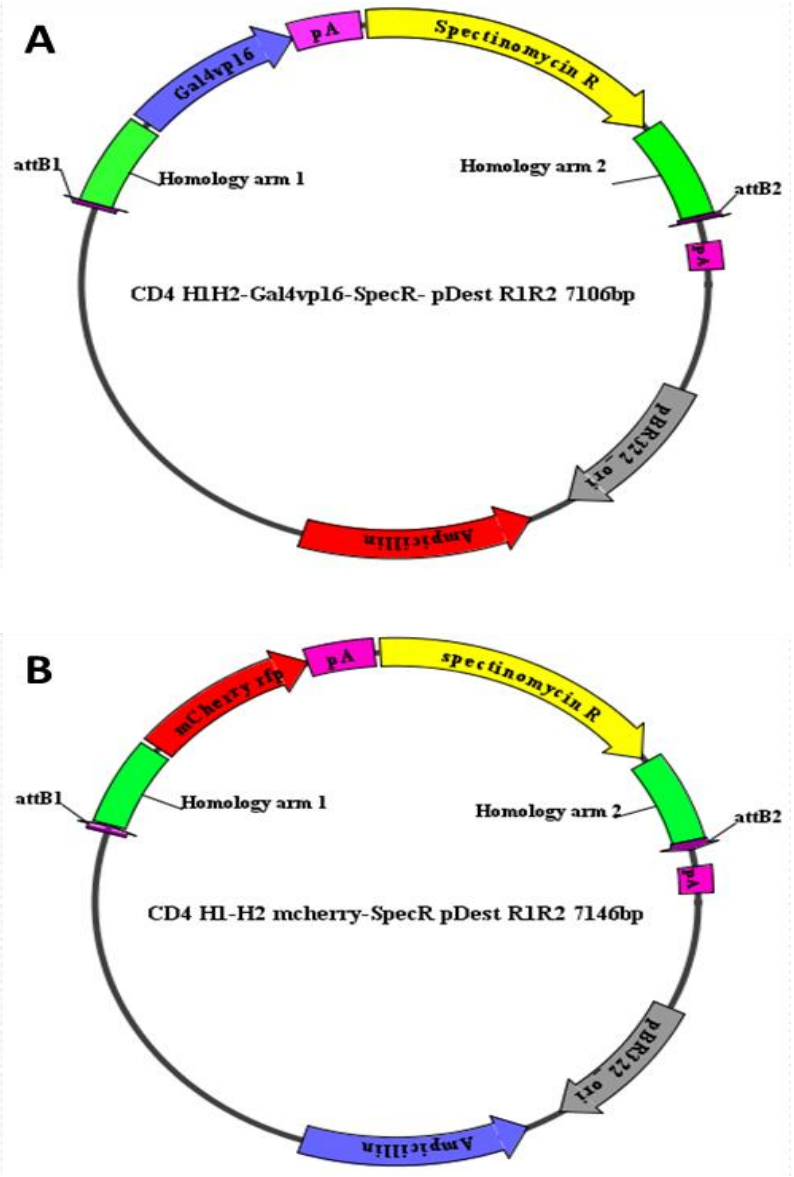

Figure 3.3: Vector maps of (A) gal4vp16 and (B) mcherry LR clones. Maps were generated using 'APE' software.

3.4 Target genes (mCherry and Gal4vp16) were successfully cloned in to CD4-1 BAC

Lineage specific regulation of an exogenous gene can be achieved by placing the target gene at the transcription initiation site of a lineage specific promoter in a vector. We wanted to express gal4vp16/mcherry specifically in CD4-1+ cells of zebrafish. As mentioned above, we assembled the two targeting cassettes (mCherry and Gal4vp16) using the multisite gateway cloning technique. Both the targeting cassettes were PCR amplified using a forward primer specific to homology arm-1 and a reverse primer specific to homology arm-2 and the products were subjected to dpnI digest (to remove parental LR plasmids, a possible source of contamination) before resolving on agarose gel. As expected we observed bands specific for mcherry (at around 3000 bp, figure 3.4 A) and gal4vp16 (at round 3000 bp, figure 3.4 A) targeting cassettes.

After gel purification, using the above targeting cassettes, we performed two independent BAC homologous recombination reactions to clone the mCherry/gal4vp16 in the CD4-1 BAC with integrated Tol2 arms transposons. Subsequently, the purified BAC DNAs were analyzed for integration of the respective targeting cassette in to the CD4-1 BAC by PCR (using a set of primers that are specific to CD4-1 BAC and different elements of targeting cassettes) and the products were resolved on agarose gel. As expected, we observed bands at around 1500 bp (contains homology arm-1 and mcherry, 1488 bp), 1500 bp (contains homology arm-1 and gal4vp16, 1457 bp), 1700 bp (contains spectinomycin and homology arm-2 of CD4-1:mcherry BAC, 1646 bp), 1700 bp (contains spectinomycin and homology arm-2 of CD4-1:gal4vp16 BAC, 1646

bp), 3000 bp (entire mCherry targeting cassette, 3134 bp) and 3000 bp (entire gal4vp16 targeting cassette, 3140 bp) (figure 3.4 B) confirming the appropriate integration of the mCherry/gal4vp16 cassette in to CD4-1 BAC, replacing the CD4-1 start codon with mCherry/gal4vp16 gene. Positive clones were partially sequenced to check for any possible mutations. The resultant sequence was mutation free showing close to 100% similarity with the expected sequence.

Finally, to check for any major unexpected deletions in the BAC, both CD4-1:mCherry and CD4-1:gal4 BACs were digested with SmaI and NheI enzymes and the products were resolved on agarose gel using pulse field gel electrophoresis (PFGE) (refer to section 2.11.3)(Figure 3.4 C-D). The digest pattern of the CD4-1:mcherry and CD4-1:gal4vp16 BACs was similar to the original CD4-1 BAC indicating that no significant rearrangements had occurred.

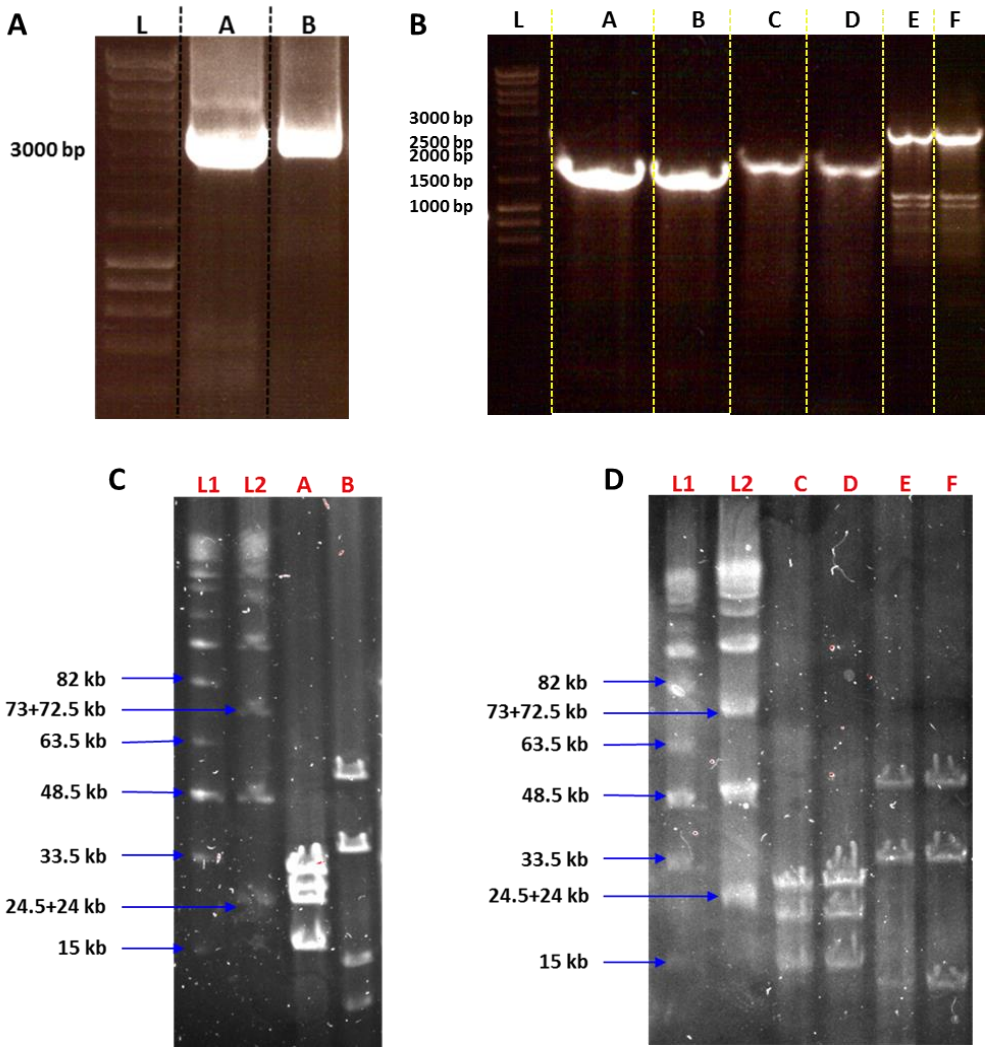

Figure 3.4: Validation of successful CD4-1 BAC recombineering. **(A)** PCR amplified products of Gal4vp16 (lane A) and mcherry (lane B) recombineering cassettes. **(B)** Validation of recombined BAC clones using PCR amplification; Lanes 'A' (homology arm-1+gal4vp16, 1457 bp), 'C' (spectinomycin+homology arm-2, 1646 bp) and 'E' (from homology arm-1 until homology arm-2, 3140 bp) corresponds to CD4:gal4vp16 BAC clone whereas lanes 'B' (homology arm-1+mcherry, 1488 bp), 'D' (Spectinomycin+homology arm-2, 1646 bp) and 'F' (from homology arm-1 until homology arm-2, 3134 bp) corresponds to CD4:mcherry BAC clone. All bands were of expected sizes thus validating the BAC clones. **(C-D)** PFGE patterns of NheI and SmaI digested CD4 BAC clones**.** Lanes 'C' and 'E' corresponds to NheI and SmaI digest of CD4:gal4vp16 BAC whereas lanes 'D' and 'F' corresponds to NheI and SmaI digest of CD4:mcherry BAC. The digest pattern of both the recombined CD4 BACs is broadly similar to that of original clone of CD4 BAC (A-NheI, B-SmaI), thus confirming the integrity of CD4:gal4vp16 and CD4:mcherry BACs is maintained. Lanes L1 and L2 corresponds to Mid-range-1 and Mid-range-2 PEG marker respectively.

3.5 Discussion

Traditionally, transgenic animal models are generated by injecting a plasmid containing cDNA (like fluorescent proteins) under the control of minimal promoter of the target gene (Suster et al. 2009). With some genes, including *cd4*, this approach may not result in true expression of target gene as they require other upstream and downstream regulatory elements apart from the regular promoter elements (Marodon *et al*. 2003). Apart from distinct regulatory elements, mouse and human *cd4* gene expression is also controlled by a silencer element located in the 1st intronic region, which ensures the silencing of *cd4* gene in activated CD8^{+} T cells (Marodon *et al*. 2003). The zebrafish *cd4-1* gene is reported to have similar regulatory elements and expected to be regulated by a complex promoter-enhancer-repressor mechanism (Yoon *et al*. 2015). However, like in mouse and humans, no in depth analysis of the zebrafish CD4-1 promoter has been reported and initial attempts to make a zebrafish reporter line with a minimal promoter (includes ~5kb of upstream region) were unsuccessful (Chris Secombes, University of Aberdeen, personal communication). Hence we decided to make our zebrafish CD4-1 reporter line using BAC transgenesis.

Bacterial Artificial Chromosomes (BACs) are widely used for generating various transgenic model vertebrates mainly because they provide a unique opportunity to express a cDNA under the control of native regulatory mechanisms of the target gene (Suster et al., 2009). Also, since BAC is a large piece of DNA, the transgene of interest can be better shielded from unwanted position effects resulting from random

integration of the transgene in to the host genome (Suster et al., 2009). To ensure an efficient and faithful lineage specific expression of the mcherry fluorescent protein in zebrafish CD4-1^{+} cells, we have selected a CD4-1 BAC clone (CH73-296E2) incorporating about 50 kb upstream region of the zebrafish *cd4-1* gene along with the 1st intron which potentially contains *cd4-1* silencer region (section 3.1). Once the selected CD4-1 BAC clone was obtained, prior to initiating the modification of the BAC, we verified the integrity of the delivered clone using restriction digestion and pulse field gel electrophoresis (PFGE). PFGE is a 2D electrophoresis technique which facilitates the separation of large sizes of DNA fragments on an agarose gel. As shown in figure 3.4 C, we found no apparent missing bits of DNA and total size all the DNA fragments was ~100kb as expected.

To generate a stable transgenic zebrafish, upon injection in to the embryos, the BAC DNA has to integrate with the zebrafish genome. Transposon mediated BAC transgenesis is one of the efficient ways to generate stable transgenic zebrafish (Suster L S et al., 2009). Tol2 is a medaka fish (*Oryzias latipes)* transposase that is active in a wide variety of vertebrates including zebrafish (Kawakami et al. 2007). Many laboratories including ours have used the Tol2 transposase system to generate various transgenic fish lines. It has been shown that 150 bp and 200 bp from the right and left ends of Tol2, respectively, are *cis*-sequences (transposons) essential for transposition and the insert between them is randomly integrated in to the host genome by a 'cut-and-paste' mechanism (Urasaki et al. 2006). It has been observed that Tol2 facilitates single copy integration of the transgene, thereby minimizing the chances of transgene

silencing affected by multiple copy number (Urasaki et al. 2006). Tol2 has been widely used to make zebrafish BAC transgenic lines and has been shown to be capable of carrying a cargo >160 kb (Suster L S et al. 2009). As our selected cd4-1 BAC is ~100kb, we believed that a Tol2 transposase system can efficiently facilitate its integration in to zebrafish genome. Accordingly, in the 1st round of BAC recombineering, we have cloned in the iTol2 cassette in to the CD4-1 BAC vector backbone using Red/ET BAC homologous recombineering kit.

Multisite gateway technology is a modular cloning technique that enables cloning of up to four fragments of DNA in a single cloning reaction. Employing this technique enabled us to efficiently build the two targeting constructs, with either mCherry or gal4vp16 cDNA sandwiched between the left and right CD4-1 homology arms (Homology arm-1 and homology arm-2 respectively). Subsequently, with the 2nd round of BAC homologous recombination, we cloned in the cDNA of mCherry fluorescent protein or gal4vp16 at the putative transcription initiation site of *cd4-1* gene thus potentially placing them under the native regulation elements of the *cd4-1* gene. Following the successful modification of the BAC, using restriction digestion and PFGE, we again verified the integrity of the BAC clone to check for any major deletions during the cloning process. As shown in figure 3.4 D, the restriction digestion pattern of the modified BAC was marginally dissimilar to that of the unmodified BAC. As both the products have been run at different time points, variables such as quality of the gel/run buffer, reduced activity of the restriction enzyme (NheI) used etc. could have affected the pattern of the bands appearing on the gel. Since the total size of the recombined

BAC was ~100kb as indicated by the SmaI digest (3.4 D, lane 'E' and 'F') we confirmed that the BAC was broadly intact.

Using homologous recombineering, we have now successfully modified the CD4-1 BAC enabling it to expresses either mCherry or gal4vp16 proteins specifically in the zebrafish CD4-1^{+} cells. Silencing of UAS elements in some cell types of adult zebrafish has been reported before. Our initial attempts to generate a gal4vp16-UAS:mCherry reporter line have also failed, as we could not detect any mCherry expressing cells in adult F_0 zebrafish. Hence, although we have generated BAC clones for the expression of both mCherry and gal4vp16, we only proceeded to generated *cd4-1:mCherry* reporter line. The next objective is to establish and validate a *cd4-1* zebrafish reporter line, which will be discussed in the next chapter of this thesis.

The following chapter, Chapter 4, is a paper I have published in the 'Journal of immunology' as a joint first author along with Christopher Dee. My contribution includes figure 4.1, figure 4.2, figure 4.3 (A-C, F), figure 4.4, figure 4.5 (I), figure 4.6, and the contribution of the co-authors includes figure 4.3 (D, E, G, H), figure 4.5 (A-H), figure 4.7 and figure 4.8. This article was published with open access under a creative commons agreement and I have obtained the permission from the co-authors to include it in my thesis.

Chapter 4. Generation and characterization of transgenic CD4 reporter zebrafish

Results

4.1 Generation of a transgenic CD4 reporter zebrafish

To facilitate visualisation and isolation of zebrafish $CD4^+$ cells, we decided to generate a fluorescent transgenic reporter line. As described in chapter 3, to utilise important transcriptional regulatory elements from the *cd4-1* locus, we used BAC recombineering to integrate mCherry fluorescent protein into the initiation codon of *cd4-1* located in exon 3 (Figure 4.1A). We then introduced the recombined BAC into the zebrafish genome by co-injecting it into zygotes together with Tol2 transposase mRNA. Expression of *cd4-1* mRNA was detectable at 4 days post fertilisation (dpf), but increased over days 5−6 of development (Figure 4.2). Consistent with this, breeding from a *Tg*(*cd4-1:mCherry)* founder resulted in progeny with robust red fluorescence apparent in the thymus by 5 dpf (Figure 4.1 B-E). Thereafter mCherry fluorescence persisted in the thymus into adulthood (Figure 4.1F) and a robust signal was still apparent in fish over 4 months. Breeding allowed us to combine the *Tg[cd4-1:mCherry]* line with the established pan-T cell reporter line, *lck:GFP* (Langenau et al. 2004). Double positive ($mCherry^+/GFP^+$) cells could be identified in the thymus of *cd4-1:mCherry;lck:GFP* transgenic animals (Figure 4.1C-E), which we presumed to be $CD4^+$ T cells.

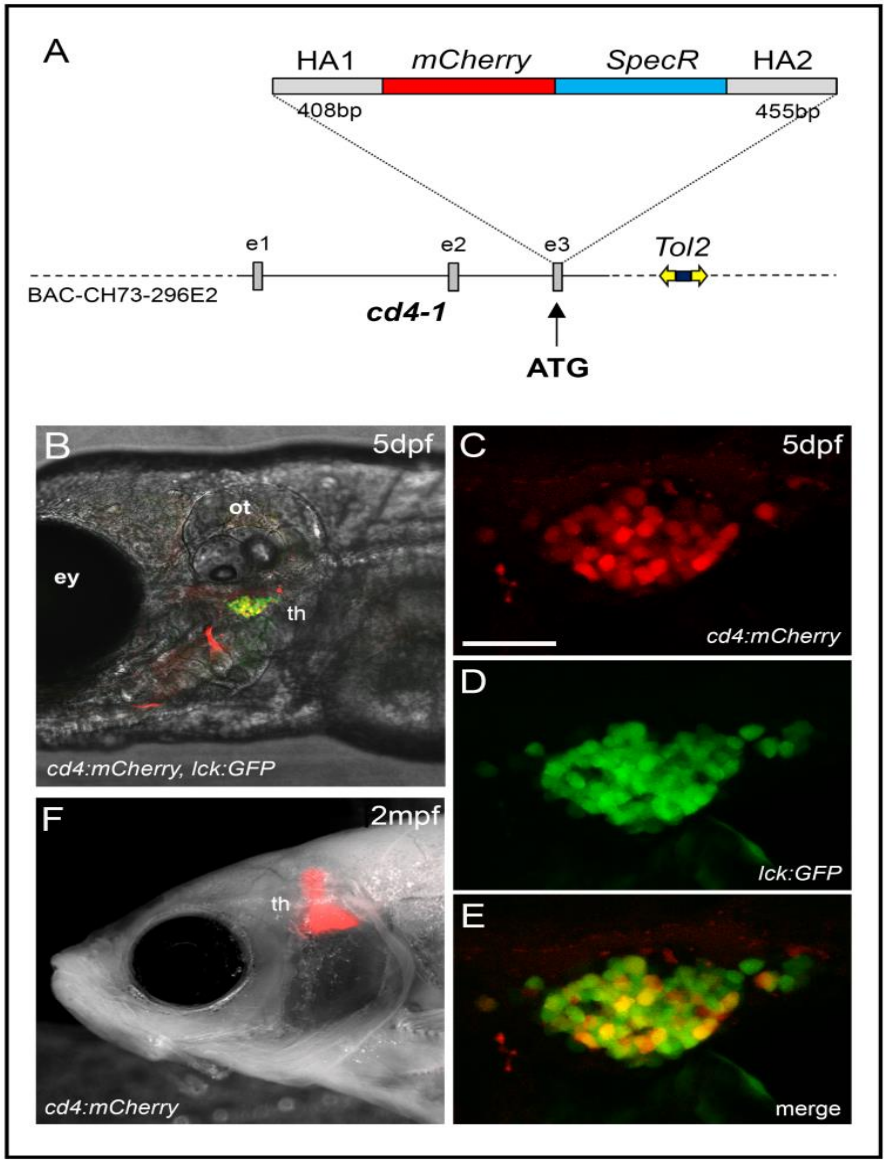

Figure 4.1: Generation of a *cd4-1* reporter line. (*A*) Schematic illustrating the construction of the transgene. A BAC containing the 5' region of the *cd4-1* gene was selected and modified by recombination to contain *Tol2* transposable elements with the kanamycin resistance gene (dark blue box) to allow selection. A cassette containing the *mCherry* coding sequence and the spectinomycin resistance gene (*SpecR*) flanked by *cd4-1* homology arms (HA1 and HA2) was then recombined into the *cd4-1* start codon (located in exon 3). **(*B*)** The *cd4:mCherry* reporter is expressed in the thymus by 5dpf and co-localises with the pan-T-cell reporter *lck:GFP.* **(*C-E*)** High magnification view of the thymus at 5dpf revealing $CD4^+$ ($mCherry^+$ GFP^+) and $CD4^-$ (GFP_+ only) T cells. **(*F*)** Reporter expression in the thymus of adult fish at 2mpf in the *casper* mutant background. Anterior is to the left. Scale bar is 10μm. Denoted features are eye (ey), otic vesicle (ot), thymus (th).

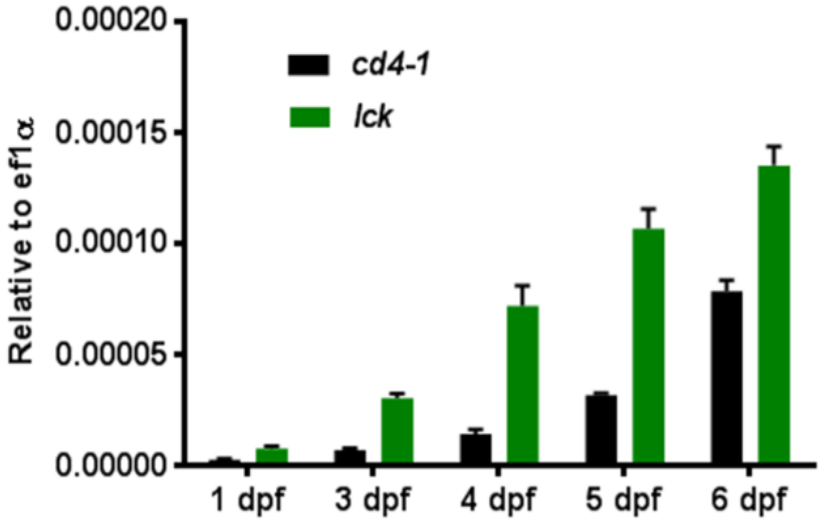

Figure 4.2: Expression of *cd4-1* mRNA during development. The *cd4-1* transcript is weak but detectable by Q-PCR at 4dpf and increases steadily at 5dpf and 6dpf. The expression pattern correlates with that of the *lck* gene, which is expressed in all T cells.

4.2 Morphology, expression characteristics and distribution of *cd4:mCherry*+ cells

To continue our characterisation of zebrafish CD4-1^{+} cells, we flow sorted cells from *Tg[cd4-1:mCherry;lck:GFP]* double transgenic zebrafish kidney and spleen using complexity and size to distinguish leukocyte populations (Traver et al. 2003). As expected, we found that mCherry^{+} cells comprised a small subset (5.34 ± 1.89%) of the lymphocyte fraction (Figure 4.3A). We also observed a mCherry^{+} population of cells within the monocyte/granulocyte gate (2.3 ± 1.18%), suggesting the existence of CD4-1^{+} mononuclear phagocytes (MNPs) (Figure 4.3A). Cytospin and Wright-Giemsa staining confirmed that mCherry^{+} cells isolated from the lymphocyte gate had characteristic lymphocyte morphology (Figure 4.3B), whereas mCherry^{+} cells isolated from the monocyte/granulocyte gate demonstrated heterogeneous morphologies typical of MNPs (Figure 4.3B). Gating the lymphocytes, we confirmed the existence of (GFP^{+}/mCherry^{+}) CD4-1^{+} T cells in addition to GFP^{+}-only T cells (Figure 4.3C). Flow cytometry revealed that CD4-1^{+} T cells comprised between 10 and 20% of T cells isolated from the kidney, gills and gut of adult zebrafish, but were significantly lower (5.55% ± 2.79) in the spleen (Figure 4.3D). Quantitative RT-PCR (Q-PCR) analysis revealed that both T cell populations expressed the T-cell markers *tcr alpha-chain* (*tcra*) and *lck*, but not the macrophage marker *mpeg1* (Figure 4.3E) consistent with their classification as T cells.

To further confirm their classification as T cells, we also examined *Tg*(*cd4-1:mCherry)* expression in the recombination activating gene 2 (*rag2*$^{-/-}$) mutant

background, which is known to cause a marked reduction of thymic and mature T cells (Tang et al. 2014). By 7 dpf the *rag2* mutant homozygous animals demonstrated loss of both *lck:GFP*$^{+}$ and *Tg*(*cd4-1:mCherry)*$^{+}$ T cell populations within in thymus (Figure 4.3F). Interestingly, we also noticed that a population of thymus associated CD4-1^{+} MNPs appeared to be retained in the *rag2* mutant larvae (Figure 4.3F, white arrows). We next examined gene expression in CD4-1^{+} and CD4-1^{-} T cell populations. We confirmed by QPCR that the *cd4-1* gene was expressed strongly in mCherry^{+} T cells, corroborating their identity as CD4-1^{+} T cells (Figure 4.3G). Furthermore, Q-PCR revealed increased expression of the TH (helper T cell) lineage committing transcription factor *Thpok* (*zbtb7b*) (Egawa and Littman 2008) in mCherry^{+} T cells, and greatly enriched expression of *cd4-2.1* and *cd4-2.2* (Figure 4.3H), indicating that the expression of *cd4* paralogues overlaps extensively in zebrafish. Conversely, *cd8*α expression was detected largely in the mCherry^{-} population, suggesting it is composed primarily of CD8^{+} T cells (Figure 4.3H). Expression of the *runx3* and *eomesb* transcription factors was enriched in CD4-1^{-} T cells relative to CD4-1^{+} T cells, consistent with their established roles in the development of mammalian CD8^{+} T cells (Cruz-Guilloty et al. 2009). Both CD4-1^{+} and CD4-1^{-} T cells expressed the *t-bet*/*tbx21* TF as is the case in mammals. These data confirm the *Tg[cd4-1:mCherry]* transgenic as an effective and accurate reporter of CD4-1^{+} T cells, and provide further evidence that the transcriptional machinery underlying CD4^{+} and CD8^{+} T cell maturation is conserved between mammals and teleost fish.

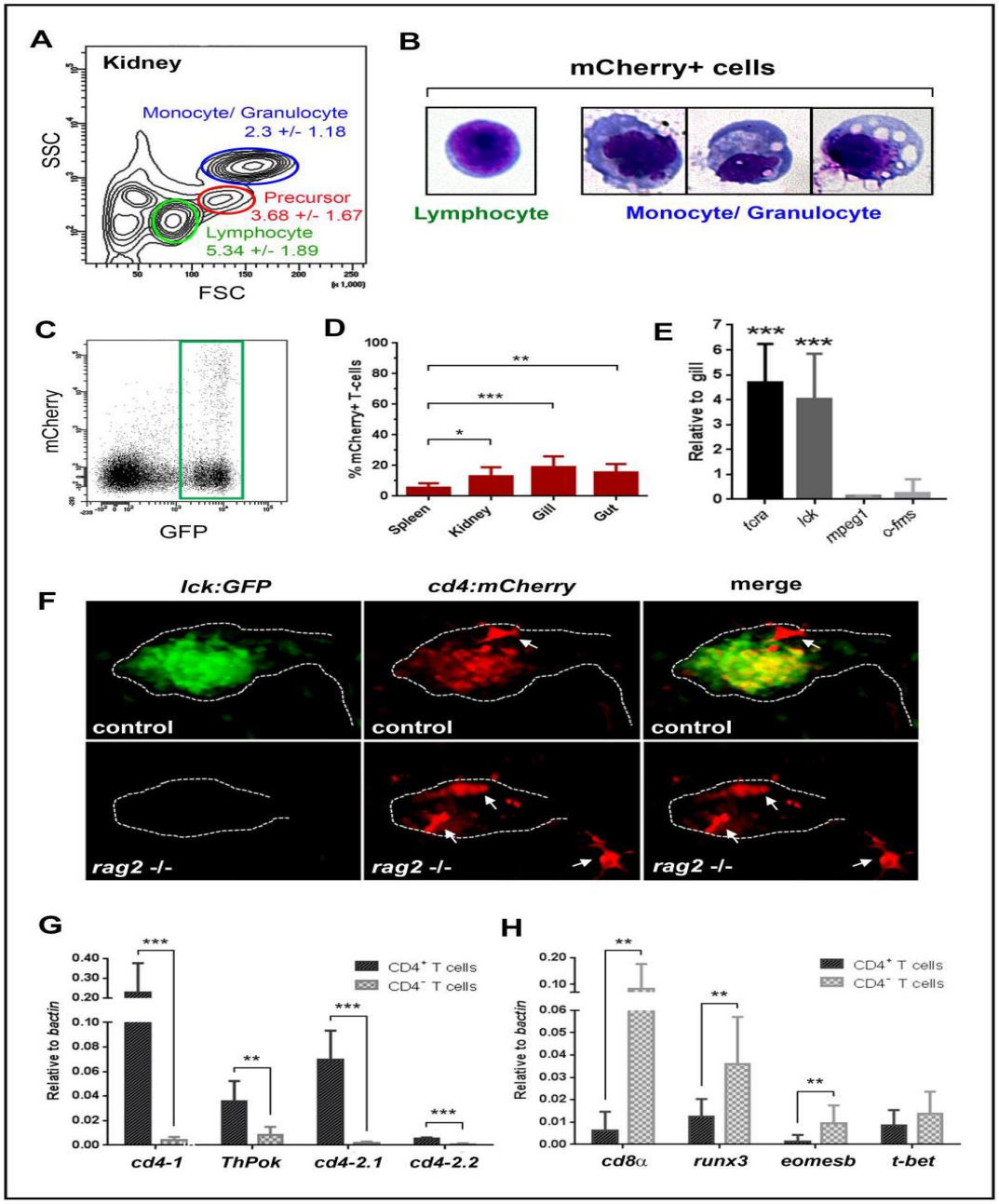

Figure 4.3: Distribution and gene expression in CD4^{+} T cells. (*A*) Forward and side scatter profile (FSC/SSC) indicating the percentage of mCherry+ cells present in each gate. **(*B*)** mCherry+ cells isolated from the lymphocyte (left panel) or monocyte/ granulocyte (right panel) gate when subjected to Wright-Geimsa stain. **(*C*)** Lymphocytes were gated for *lck:GFP+* cells. **(*D*)** Proportion of mCherry+ cells among GFP+ T cells in adult organs (*n*=8-11, *p*<0.05). **(*E*)** Q-PCR analysis shows that both populations isolated from the lymphocyte gate express *tcra* and *lck*, but not *mpeg*. **(F)** *rag2*$^{-/-}$ zebrafish (7dpf) demonstrate loss of both *lck:GFP*$^{+}$ and *Tg*(*cd4-1:mCherry)*$^{+}$ T cell populations within in thymus **(*G*)** Q-PCR analysis shows mCherry^{+} T cells express *cd4-1*, *ThPok*, *cd4-2.1* and *cd4-2.2* **(*H*)** mCherry^{-} T cells express *cd8a*, *runx3*, *eomesb* and *t-bet* (*n*=7, *p*<0.05). Error bars represent s.d.

4.3 Egress of zebrafish CD4-1$^+$ T cells and scrutiny by CD4-1$^+$ perithymic mononuclear phagocytes

In addition to facilitating studies of CD4-1$^+$ T cells, our initial observations indicate the intriguing possibility of an ancient evolutionary origin for CD4-1$^+$ MNPs. We first examined the developmental expression of *Tg[cd4-1:mCherry;lck:GFP]* double reporter, and noted that by 10 dpf, thymic egress by both CD4-1$^+$ and CD4-1$^-$ T cells could be readily observed (although CD4-1$^+$ MNPs appear in thymus as early as 7 dpf), with a steady stream of cells emanating from the caudal region of the thymus and entering the circulation, most notably migrating adjacent to the posterior region of the otic vesicle (Figure 4.4A-D). This region becomes densely populated by 20 dpf (Figure 4.5 A-G). Interestingly, we observed clear evidence of T cells resident in the periphery by 10 dpf, most notably in the integument (Figure 4.4A, yellow arrows). In addition, thymus resident MNPs (mCherry$^+$/GFP$^-$), are well established by 10 dpf intercalating between the densely arranged thymocytes (Figure 4.4E-G). At this stage we also observed the emergence of a population of "perithymic" macrophages which appeared to be located along the corridor of egress, apparently making regular contact with migrating T cells (Figure 4.4E-G, yellow arrows). In parallel, we also noted the emergence of a skin resident population of MNPs (Figure 4.4A, yellow arrowheads), which expands greatly in later development and has formed an extensive network of cells by adult stages (Figure 4.5 H-I).

The ability to visualise and distinguish CD4-1$^+$ T cell, CD4-1$^-$ T cell and MNP populations in the *Tg[cd4-1:mCherry;lck:GFP]* reporter provides an opportunity to

examine interactions between immune cells *in vivo*. We performed live time-lapse microscopy at the 10-14 dpf stage focussing on the disseminating stream of T cells and resident MNPs in the perithymic region (Figure 4.4 H-I). Live imaging revealed the dynamic nature of interactions between living leukocytes, with resident "sentry" like MNPs making frequent, intimate and dynamic physical contacts with migrating T cells. MNPs often form extended membrane synapses with both CD4-1^{+} and CD4-1^{-} T cells whilst in some cases forming tethers with neighbouring MNPs (Figure 4.4H). In addition, we observed that T cells were often detained by the long tether-like dendritic processes emanating from resident MNPs (Figure 4.4I). Interactions occurred over many minutes and we noted that MNPs frequently contained discrete beads of GFP^{+} cytoplasm.

Finally, to characterise the MNP population further, we combined *Tg[cd4-1:mCherry]* with the previously described *mhc2dab:GFP* reporter line which labels MNPs, including those of the skin (Wittamer et al. 2011). We observed two distinct populations of MNPs in the skin, a *cd4-1:mCherry* (mCherry^{+} GFP^{+}) expressing population, and a second group of MNPs which express only the *mhc2dab:GFP* reporter (mCherry^{-}GFP^{+}) which appear markedly less dendriform (Figure 4.6).

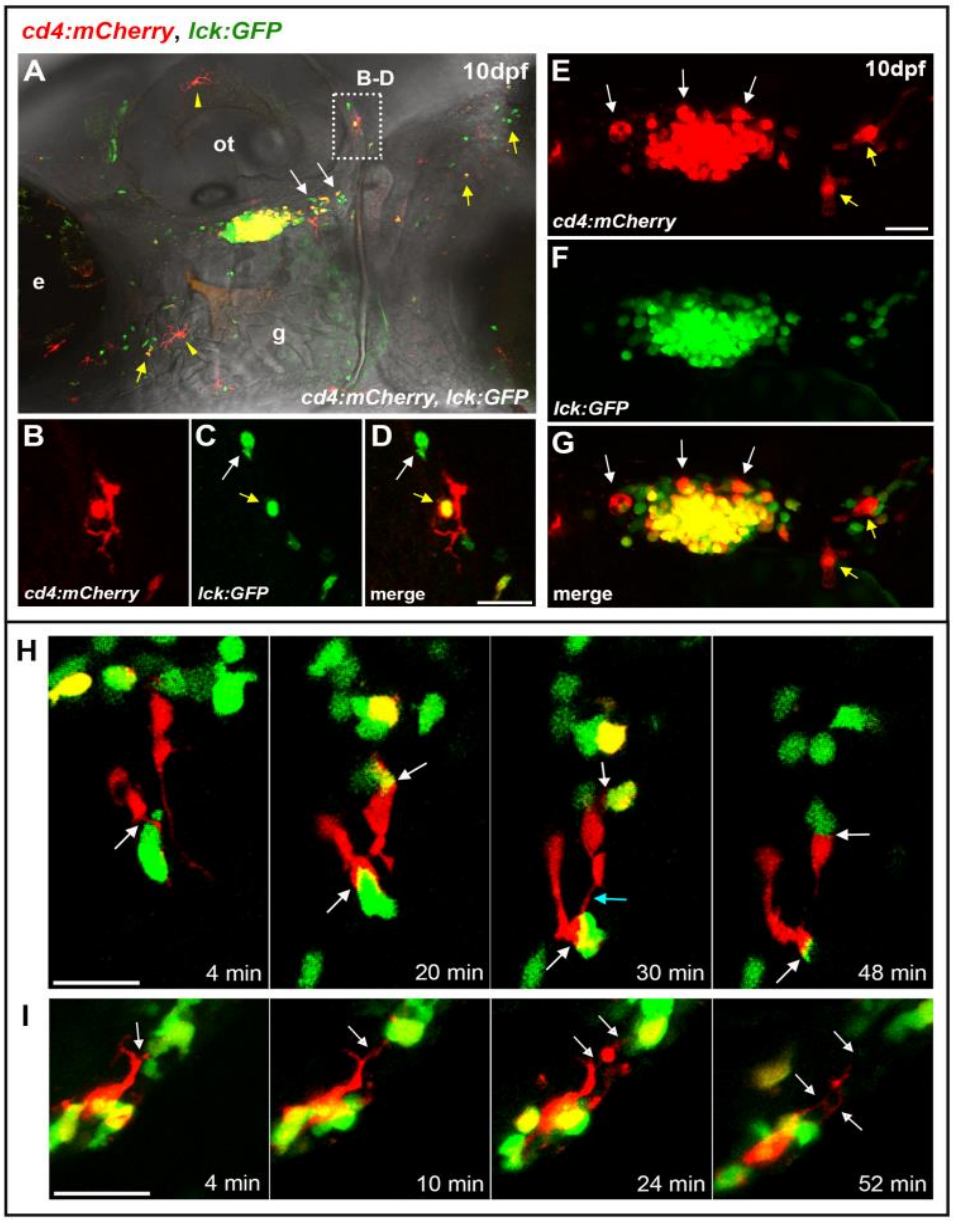

Figure 4.4: Developmental expression of *cd4:mCherry*. (*A*) Composite image of *cd4:mCherry* and *lck:GFP* expression at 10dpf. T cells can be seen migrating out of the thymus (white arrows). $CD4^+$ and $CD4^-$ T cells are visible in the integument (yellow arrows) as is a population of skin resident MNPs (yellow arrowheads). **(*B-D*)** High magnification image from the otic region in (*A*) showing a $CD4^-$ T cell (white arrow) and a $CD4^+$ T cell (yellow arrow) in close contact with a MNP (large red cell). **(*E-G*)** Intrathymic MNPs (white arrows) and perithymic MNPs (yellow arrows) can be identified by 10dpf. **(*H-I*)** Live time-lapse imaging of the perithymic region at 10-14 dpf. **(*H*)** Extended synapsing between $CD4^+$ MNPs and T cells (white arrows). MNPs are also seen to connect temporarily (blue arrow). **(*I*)** Cytoplasmic tethering (white arrows) occurs between an MNP and T cell. Scale bars equal 20μm. Denoted features are eye (e), otic vesicle (ot), gill (g).

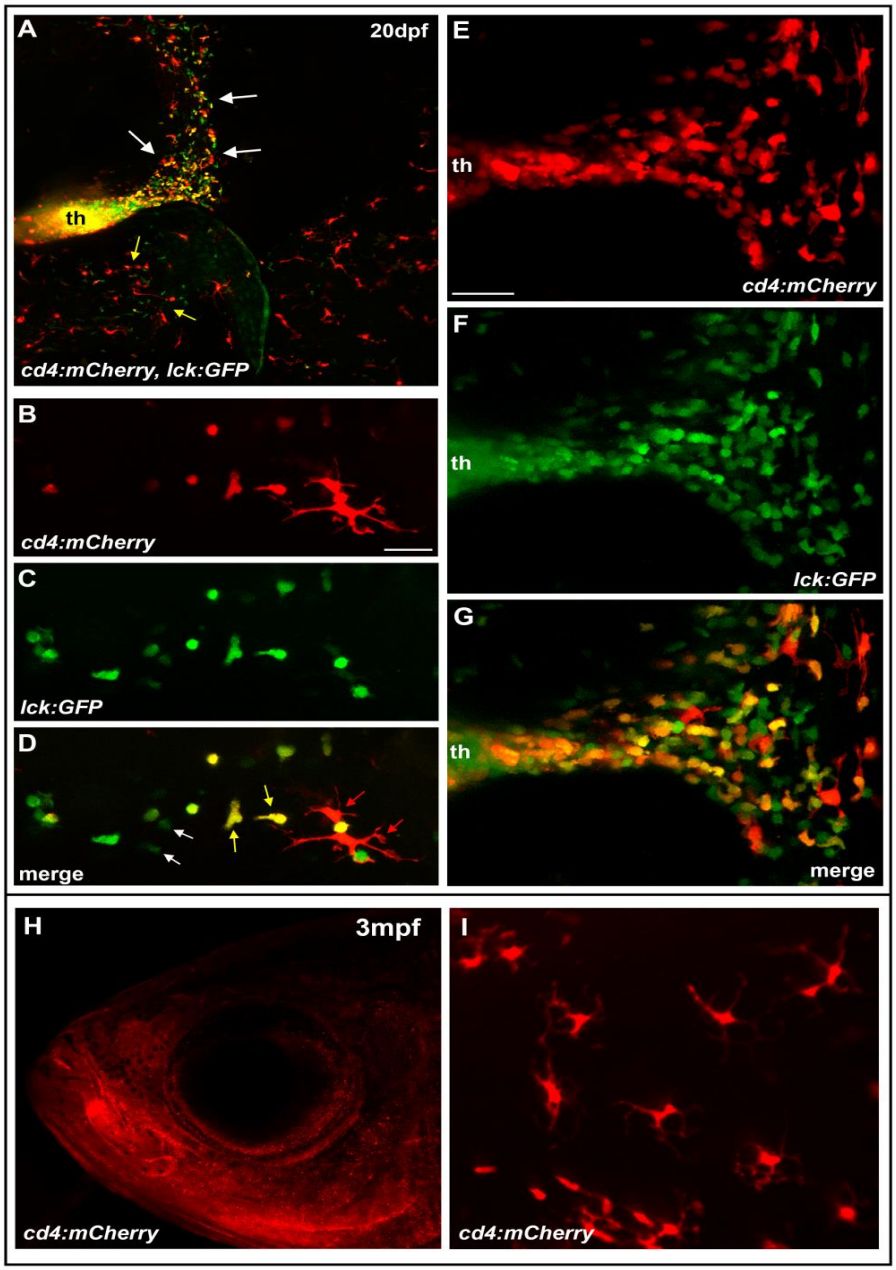

Figure 4.5: The developmental expression of *cd4:mCherry* at 20dpf. (*A*) Composite image of *cd4:mCherry* and *lck:GFP*. T cells can be seen migrating out of thymus in large numbers (white arrows). T cells and MNPs are also present in the integument (examples indicated by yellow arrows). **(*B-D*)** High magnification image from skin in the gill cover region showing examples of $CD4^+$ T cells (yellow arrows), $CD4^-$ T cells (white arrows) and MNPs (red arrows). **(*E-G*)** Higher magnification of the corridor of cells migration out of the thymus showing large numbers of T cells in addition to MNPs. **(*H*)** Extensive network of MNPs is visible throughout adulthood (representative image at 3 months post-fertilisation). **(*I*)** High magnification image showing the density and morphology of MNPs in the adult integument. th, thymus. Scale bars 20μm.

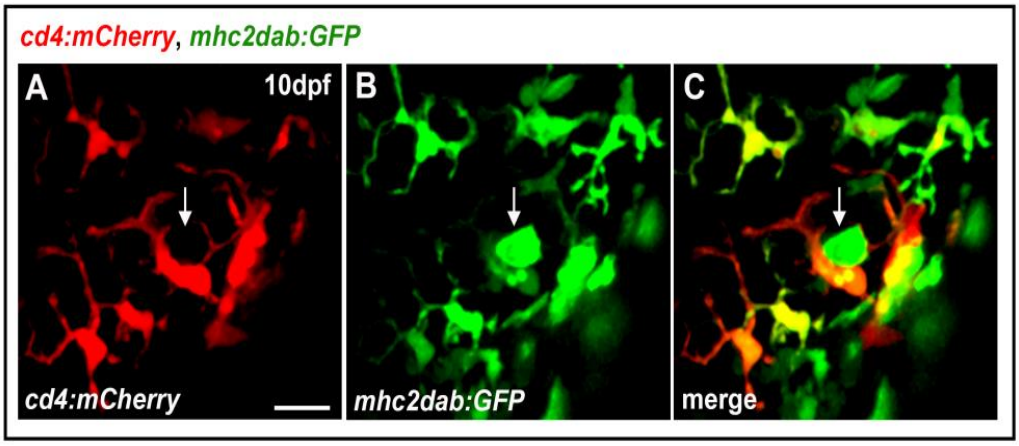

Figure 4.6: Morphology of skin resident CD4$^+$ and CD4$^-$ MNPs. (*A-C*) Images of *cd4:mCherry*; *mhc2dab:GFP* MNPs located in the skin of 10dpf zebrafish. The *cd4:mCherry*$^+$ **(*A,C*)** MNPs exhibit a noticeably more dendriform morphology than the *mhc2dab:GFP*$^+$ single positive cells (B,C, white arrows).

4.4 Differentiation of tissue resident CD4+ T cells indicates extensive subspecialisation – A conserved TH2-like phenotype in the gill mucosa

It is currently unclear whether TH subsets equivalent to TH1, TH2 and Treg cells are present in fish and the functional relationships of key signature cytokines has not been determined. Previous studies attempted to address this issue by challenging immune cells with pathogens or immunostimulants (Kono and Korenaga 2013; Mitra et al. 2010; Nunez Ortiz et al. 2014; Somamoto et al. 2014; Yamaguchi et al. 2013; Yamasaki et al. 2014; Yoon et al. 2015; Takizawa et al. 2016). However, we were interested by the observation that in the steady state certain tissues or organs maintain immune biased microenvironments, with significant implications for the administration of therapeutic agents. For example, the gill tissue has been shown in various fish species to constitutively express *Gata3* and *IL-4*-related cytokines, suggesting a TH2-biased microenvironment, although in all cases the source of this expression was unknown (Wang et al. 2010; Kumari, Bogwald, and Dalmo 2009; Takizawa et al. 2011; Li et al. 2007; Wang et al. 2016). The *Tg[cd4-1:mCherry]* reporter line provides a unique opportunity to explore the conservation and distinctiveness of fish TH cell differentiation within such an environment. Thus, to search for fish TH2 cells, we examined CD4-1^{+} T cells populations of the kidney and spleen, the gills and the gut.

We initially sought to confirm the presence of tissue resident CD4-1^{+} T cell populations in the gill and gut of adult zebrafish. Consistent with this, we detected CD4-1^{+} T cells studding the epithelium of the branchial filaments and occasionally in the lamellae epithelium (Figure 4.7A). Cryosectioning of the intestine revealed that

CD4-1$^+$ and CD4-1$^-$ T cells are abundant in the lamina propria of the gut mucosa, and dispersed among overlying epithelial cells (Figure 4.7B). We next isolated CD4-1$^+$ T cells from the kidney and spleen (KS), gills and gut and performed Q-PCR analysis. Compared to cells sourced from other tissues, CD4-1$^+$ T cells isolated from gills expressed significantly higher levels of the TH2 signature genes, *gata3* and *il-4/13b* (Figure 4.7C). By contrast, expression of the Th1 signature genes *t-bet* and *ifn*-γ remain low or significantly reduced (Figure 4.7D). Interestingly, we found that the expression of *il-4/13a* remains low in gill resident CD4-1$^+$ T cells (Figure 4.7C), supporting the notion that the IL-4/13 paralogues have distinctive roles in teleost fish (Wang et al. 2016). Previous studies in other fish species had noted constitutive expression of the *il-4/13a* paralogue (Takizawa et al. 2011; Wang et al. 2016). Consistent with this, in total gill tissue, we noted *il-4/13a* and *il-4/13b* were expressed at similar levels (Figure 4.8A). We therefore compared gill resident CD4-1$^+$ T cells to total gill tissue from the same animal (Figure 4.8B). CD4-1$^+$ T cells of the gill are greatly enriched for the expression of *il-4/13b*, and significantly depressed for the expression of *il-4/13a*, confirming that CD4-1$^+$ T cells are not the source of this cytokine. In addition, we found that CD4-1$^+$ cells isolated from the gut displayed a contrasting gene expression signature, with significant upregulation of the Treg signature genes *foxp3a* and *il-10* (Figure 4.7D). The presence of a CD4-1$^+$ *foxp3a*, *il-10* expressing population in the gut would appear to mirror the extensive and essential population of Treg cells found in the mammalian intestine (Bollrath and Powrie 2013).

Taken together, these data demonstrate three distinct polarised populations of CD4-1^{+} T cells with distinctive gene expression signatures. In particular, we are able to show that the gills represent a source of differentiated, *il-4/13b* -expressing CD4-1^{+} T cells and, to our knowledge, are the first *in-vivo* evidence for TH2-like cells in a teleost.

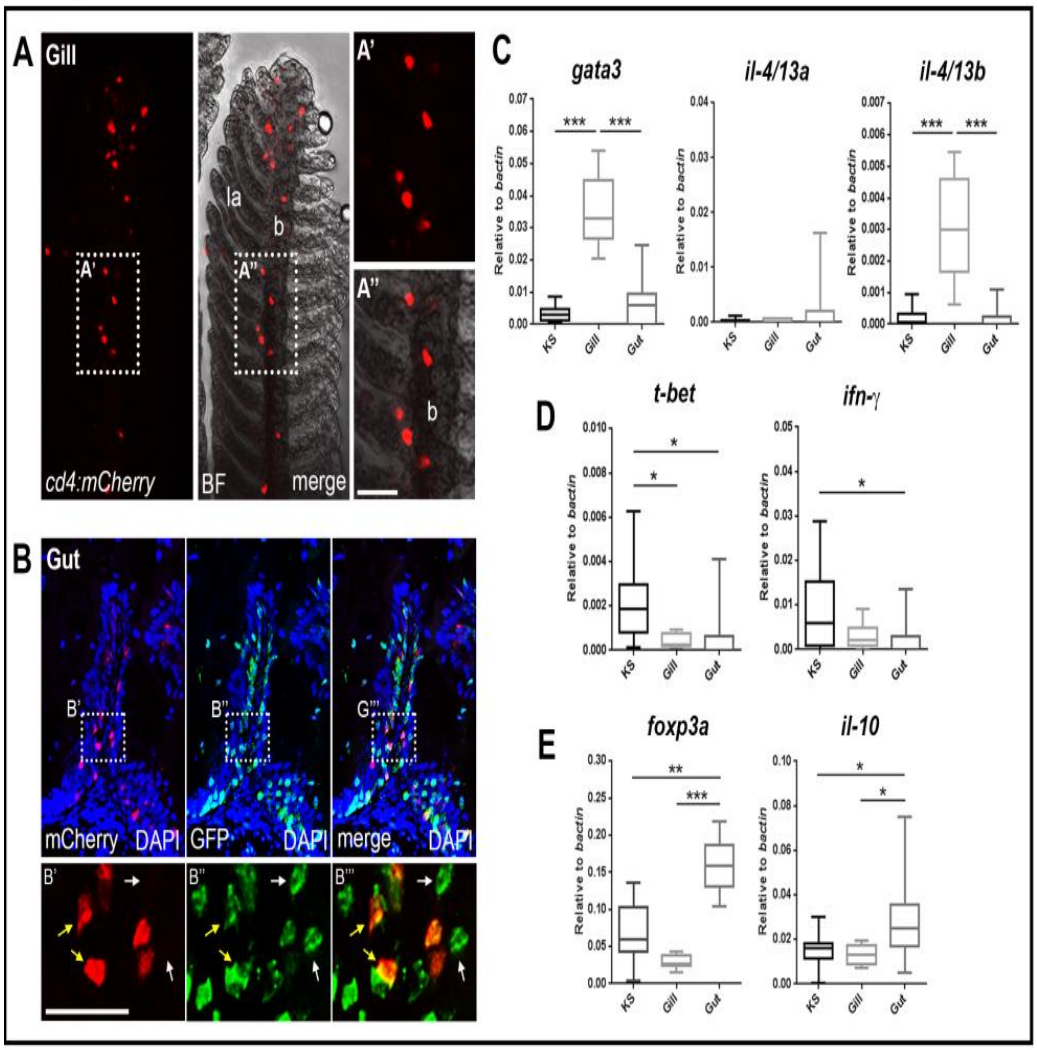

Figure 4.7: Differentiation of tissue resident CD4⁺ T cells. (*A*) Gill preparation confirming resident population of CD4⁺ cells (BF, bright field, la, lamella, b, branchial filament). **(*B*)** Cryosection and immunostain showing an intestinal villus populated by both CD4⁺ (yellow arrows) and CD4⁻ (white arrows) T cells. **(*C-E*)** Q-PCR analysis of CD4⁺ T cells isolated from kidney and spleen (KS), gill and gut. **(*C*)** Expression of *gata3* and *il-4/13b*, but not *il-4/13a* are significantly enhanced in CD4⁺ T cells of the gills **(*D*)** Expression of *t-bet* and *ifn-γ* is significantly lower or unaltered in CD4⁺ T cells of the gill or gut compared to KS. **(*E*)** CD4⁺ T cells of the gut show significantly enhanced expression of *foxp3a* and *il-10*. Error bars represent s.d, n=9-12, p<0.05. Scale bars are 20μm.

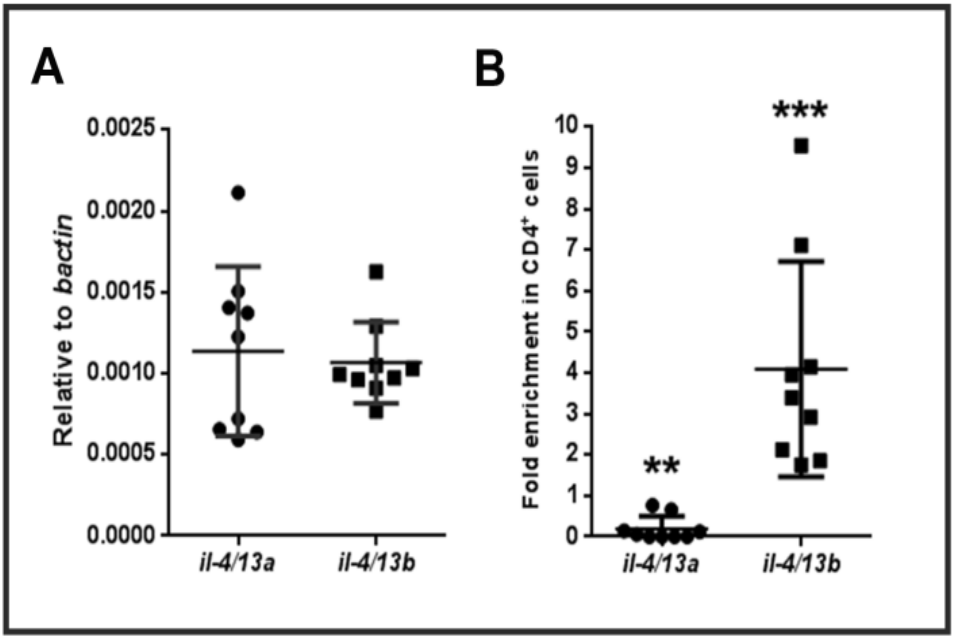

Figure 4.8: Expression of *il-4/13a* and *il-4/13b* in gill and resident CD4+ T cells. (*A*) Q-PCR analysis of whole zebrafish gills indicates that *il-4/13a* and *il-4/13b* are constitutively expressed at similar levels. **(*B*)** The expression of *il-4/13a* and *il-4/13b* in CD4+ T cells isolated from the gill. The expression of *il-4/13a* is significantly reduced in CD4+ T cells relative to the surrounding gill tissue, while *il-4/13b* expression is significantly enhanced. Error bars equal s.d, n=9, p<0.05.

4.5 Discussion

Adaptive immunity has been proposed as one of the key evolutionary innovations in the emergence of vertebrates (Boehm et al. 2012). In this chapter, exploiting the *Tg[cd4-1:mCherry]* transgenic reporter zebrafish we have begun to image and characterise the development of CD4-1^{+} leukocytes and present *in vivo* evidence for the differentiation and subspecialisation of CD4-1^{+} T cells. We also described specific populations of CD4-1^{+} MNPs suggesting that this cell type had already emerged in early vertebrates.

Our *Tg[cd4-1:mCherry]* zebrafish has mCherry expression pattern similar to the reported GFP expression pattern of *lck:GFP* fish (David et al. 2004). Both the reporter lines have fluorescent thymi (green for *lck:GFP*, red for *Tg[cd4-1:mCherry]*) with numerous fluorescent cells found also outside of the thymus (Figure 4A). All these observations are in agreement with the published findings that in vertebrates the thymus is an organ heavily populated with T cells undergoing maturation (Boehm et al. 2011).

Unlike *lck,* in mouse and humans, *cd4* is expressed not only in T cells but also in monocytes, macrophages, natural killer (NK) and dendritic cells (Bernard et al. 1984). Thus, a portion of mcherry positive cells observed in *Tg[cd4-1:mCherry]* fish may also include the above mentioned immune cells apart from T helper cells, which probably constitute the highest percentage of mcherry-labelled cells. To verify this hypothesis, we crossed *lck:GFP* and *Tg[cd4-1:mCherry]* fish to generate *Tg[lck:GFP; cd4-1:mCherry]*,

a double transgenic reporter zebrafish line with all of its T cells fluorescently labelled green, while CD4-1$^+$ T cells and other CD4-1$^+$ cells are fluorescently labelled red (Figure 4.1B-E). As hypothesized, we observed distinct populations of immune cells in the thymus of the zebrafish which included CD4-1$^+$ T cells (cells with both green and red fluorescence, may also include CD4-1 and CD8 double positive progenitor cells), CD4-1$^-$ T cells (only green fluorescence, possibly CD8$^+$ and other sub types), and other CD4-1$^+$ immune cells (only red fluorescence, possibly CD4$^+$ MNPs) (Figure 4.4 E-G).

It has so far remained unclear whether T_H subsets equivalent to the T_H1, T_H2 and T_{reg} cells of mammals are present in fish, however, a body of evidence has emerged in recent years which appears, at least broadly, to support the conservation of polarised type 1 and type 2 immune responses. Considerable effort has been made to identify homologues of relevant cytokines and transcription factors (Wang and Secombes 2013), while key effector cells such as CD8$^+$ cytotoxic T cells and natural killer (NK) cells (T_H1), mast cells and eosinophils (T_H2) have been identified in teleosts (Fischer, Koppang, and Nakanishi 2013; Somamoto, Koppang, and Fischer 2014; Sfacteria, Brines, and Blank 2015; Balla et al. 2010). Moreover, evidence has begun to emerge for polarisation of M1 and M2-like macrophages (Nguyen-Chi et al. 2015; Wiegertjes et al. 2016). However, the involvement of CD4-1$^+$ T cells, and the extent of their conservation has not yet been clarified. Recent studies employing antisera to CD4-1 in zebrafish and rainbow trout have shown that stimulation with antigen or infection results in the expression of relevant cytokines and transcription factors, but were unable to identify cell populations skewed towards a particular T_H phenotype

(Maisey et al. 2016; Yoon et al. 2015; Takizawa et al. 2016). In a search for differentiated zebrafish T_H cells, we speculated that the immune microenvironment of certain organs and tissues might be skewed towards a particular phenotype in the steady state. Organs such as the gills or intestine are constantly exposed to foreign antigens, including an extensive local microbiota, and must strike a tightly controlled balance between immunity and tolerance. It is well known that the mammalian gut contains an extensive population of T_{reg} cells, which are required to prevent autoimmunity (Bollrath and Powrie 2013). Previous studies had observed the constitutive expression of the putative T_H2 markers *Gata3* and *IL-4/13A* from the gill of teleost species, suggesting the maintenance of a type 2-like immune milieu. To look for T_H2-like cells we therefore examined gene expression in CD4-1^+ T cells from the gills and compared them to those isolated from the gut and kidney and spleen. We found that gill resident CD4-1^+ T cells were strongly enhanced for *gata3* and *il-4/13b* expression, indicating the presence of a novel population of teleost T_H2-like cells. In contrast, the CD4-1^+ T cells of the gut were enriched for *foxp3a* and *il-10*, suggesting they are skewed towards T_{reg}-like phenotype. In both cases the T_H1 associated genes *t-bet* and *ifnγ* were expressed only at low levels.

The observation that the T_H2-like population of the gills express *il-4/13b* and not *il-4/13a* may be highly significant in beginning to resolve the functional relationship of the teleost IL-4/13-related cytokines. It had previously been speculated that IL-4/13A might represent the functional orthologue of mammalian IL-4, based primarily on the observation of higher constitutive gene expression in certain lymphoid organs

and the presence of a Gata3 binding site in the prospective regulatory sequence (Ohtani et al. 2008; Zhu et al. 2012). However, a recent in depth study of IL-4/13 paralogues in trout indicated that while *IL-4/13A* is robustly expressed in various organs including the gill, the *IL-4/13B1* and *IL-4/13B2* (paralogues apparently derived from an additional genome duplication event specific to salmonids) genes are more responsive to viral or parasitic infection *in vivo* (Wang et al. 2016). Such observations are entirely consistent with our *in vivo* data which indicates that CD4-1$^+$ T cells are the source of *il-4/13b*, but not *il-4/13a* in the gills. Moreover, in carp a "T_H2-like" cell line clone has been reported to express *IL-4/13B*, but not *Il-4/13A* following PHA treatment (Yamaguchi et al. 2013). It will be interesting in future studies to explore the cellular source of *il-4/13a* expression in the gills, and whether this cytokine is required for the differentiation or recruitment of the *il-4/13b* expressing T cells. In any case, the identification of a T_H2-like population of cells within the ancient and specialised tissue of the gills poses interesting questions as to the evolutionary origin of vertebrate type 2 immunity. Further comparative studies of the gills in early vertebrate taxa might shed light on the origin of this type-2 immune niche.

In addition to T cells, the *Tg*(*cd4-1:mCherry)* reporter also identifies significant subpopulations of MNPs, including those associated with the thymus, and an extensive network of macrophage-like cells in the skin and gut. Taking advantage of the unique features of zebrafish, we showed that combination of the *Tg*(*cd4-1:mCherry)* reporter with the MNP reporters *c-fms:GFP* and *mhcIIdab:GFP* allows further visual resolution of distinct MNP subpopulations, providing a potential facility for the future

characterisation of MNPs in the adult fish. $CD4^+$ macrophages are prevalent in human biology, yet studies of the role of CD4 in MNPs are surprisingly limited. It has been proposed that CD4 acts as a co-receptor in macrophages, and some interesting work has suggested CD4 to be a key component of the mechanism of HIV infection (Zhen et al. 2014; Gibbings and Befus 2009). In mouse and rat, CD4 is expressed only by specific populations of MNPs, including those within the thymus (Esashi et al. 2004; Esashi et al. 2003). Our data suggest this population is conserved in zebrafish, and we have identified a novel population of perithymic MNPs which scrutinise T cells during thymic egress. Using live cell imaging, we were able to document dynamic interactions and extended cell contacts between CD4-1^+ T cells and MNPS in the perithymic region. The identification of CD4-1^+ MNPs in teleosts implies that these cells have an ancient evolutionary origin. The observations presented here are satisfyingly complimented by the recent discovery of CD4-1^+ macrophages in the spleen and kidney of rainbow trout (Takizawa et al. 2016). Interestingly, this study also suggested that CD4-1^+ macrophages may be among the most phagocytic of teleost MNPs. Comparative studies have the potential to highlight key features which have been missed in traditional models (Sunyer 2013). We suggest that the discovery that $CD4^+$ MNPs are present in lower vertebrates might justify further attention to the role of CD4 in innate immune cells.

Our understanding of adaptive immunity in teleosts lags far behind our state of knowledge for mammals. Nonetheless, in time this gap is likely to narrow rapidly as technologies allowing in depth molecular analysis of individual cells are brought to

bear. We propose that the zebrafish model has the potential to drive progress in the field of fish immunology. With the confidence of a validated *Tg*(*cd4-1:mCherry)* reporter, we now envisage to exploit the potential of zebrafish model to learn more about interactions between T lymphocytes and melanoma.

Chapter 5. Modulating tumour microenvironment to induce anti-tumour immune responses

Results

5.1 Zebrafish CD4$^+$ T cells can identify and respond to a developing melanoma lesion.

Having established that the zebrafish has CD4$^+$ T cells that can differentiate in to T_H2 and Treg like cells (probably also T_H1 like), we then wanted to explore whether the zebrafish immune system (in particular CD4$^+$ T cells) is challenged by the development of melanoma tumours. To facilitate this, we have generated Tg(mitfa:*V12RAS*::mitfa:venusgfp; cd4-1:mCherry) zebrafish by crossing the CD4-1: mCherry reporter line to *V12RAS* expressing zebrafish (Michailidu *et al*. 2009), an oncogenic *HRAS* driven autochthonous zebrafish melanoma model developed by our laboratory.

We initially performed cryosectioning of resulting tumours and identified lesions containing extensive populations of infiltrating CD4$^+$ cells (Figure 5.1 A) (in humans referred to as "brisk" tumours), in addition to lesions with little (Figure 5.1 B, B') or no (Figure 5.1 D) infiltrate. Interestingly, we also observed clustering of CD4$^+$ immune cells in the borders of some lesions which had very little to no CD4+ immune infiltrate (Figure 5.1 C, C'). We next isolated CD4$^+$ T cells from the tumours (tumour infiltrating lymphocytes, TILs) and compared gene expression to CD4$^+$ T cells isolated from spleens of wild-type siblings. Tumours represent a highly immunomodulatory tissue microenvironment, which while variable, are generally thought to maintain a

type-2 biased milieu favoring T_H2 or Treg phenotypes and the suppression of T_H1 differentiation and the recruitment of $CD8^+$ T cells (Whiteside *et al*. 2014, McCarter *et al*. 2005). Consistent with the literature, in a zebrafish model, $CD4^+$ TILs expressed significantly enhanced levels of *gata3* along with the alternative T_H2-associated cytokine, *il-4/13a* (Figure 5.1 E). In-line with this, there was no significant enrichment for the expression of the T_H1 markers t-bet or *ifn-γ*, nor indeed the Treg genes *foxp3a* or *il-10* (Figure 5.1 F). Taken together, our data suggests that zebrafish CD4-1^+ T cells can identify and respond to a developing melanoma lesion. Also, closely mimicking what is observed in melanoma patients, progressing zebrafish melanomas predominantly have T_H2 differentiated $CD4^+$ TILs.

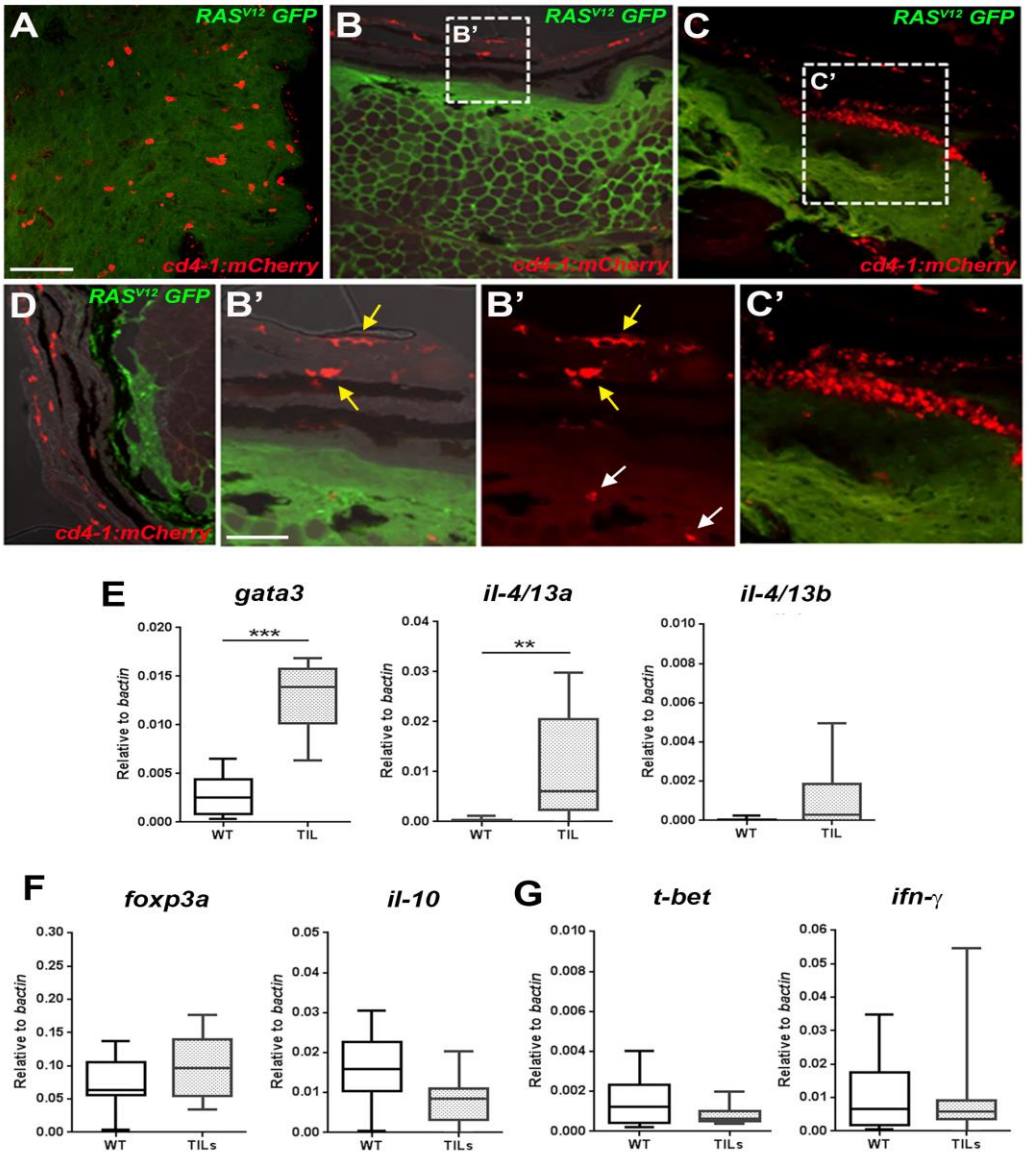

Figure 5.1. **Zebrafish CD4^{+} T cells respond to melanoma. (*A-D*)** Cryosection and immunostain of zebrafish tumours from animals carrying the *cd4:mCherry* and *mitfa:RAS^{V12}* (GFP labelled) transgenes. **(*A*)** Densely infiltrated tumour showing CD4^{+} cells (Red) and tumour cells (green) (scale bar 50um). **(*B*, *B'*)** Tumour with few infiltrating CD4^{+} cells shown (white arrows in *B'*). CD4^{+} MNPs can be seen in the overlying epidermis (yellow arrows in B'). **(*C*, *C'*)** Clustering of immune cells in adjacent skin. **(*D*)** A melanoma lesion with no detectable CD4^{+} infiltrate. **(*E-G*)** Q-PCR analysis showing gene expression in tumour infiltrating CD4^{+} T cells (TILs) compared to wild-type (WT) T cells. **(*E*)** CD4^{+} TILs significantly upregulate the expression of *gata3* and *il-4/13a* (zebrafish orthologue for il4), but not *il-4/13b*. **(*F-G*)** The expression of *foxp3a*, *il-10* **(*F*)** and *t-bet* or *ifn-γ* **(*G*)** is not significantly altered in CD4^{+} TILs. Error bars represent s.d, n=9-11, p<0.05.

5.2 A regressing zebrafish melanoma lesion is associated with 'Brisk' CD4+ TILs.

The optical translucency of zebrafish makes it an exciting model to study the complex tumour-immune cell interactions unlike any other existing cancer model system. Hence, exploiting this potential we wanted to study melanomas in an adult zebrafish using live imaging. Unfortunately melanoma is pigmented, which makes fluorescence imaging of melanoma in an adult zebrafish practically impossible. Knocking down tyrosinase, a vital catalytic enzyme required for pigment production in melanocytes, results in un-pigmented, optically translucent melanocytes without affecting the development and maturation of the melanocytes (Joe *et al*. 2013). So using CRISPR/Cas9 technology we have generated partial *tyr* knockout fish (Fo) in the Tg(mitfa:*V12RAS*::mitfa:venusgfp; cd4-1:mCherry) background. At 5dpi (days post injection), we observed marked reduction in the number of pigmented melanocytes in the knockout fish compared to the un-injected control (data not presented). As anticipated, in wide contrast to the control pigmented optically opaque tumours (figure 5.2 A), the adult tyr partial knock out fish developed un-pigmented, optically translucent tumours (figure 5.2B, indicated by red arrow) that are now conducive for live imaging.

Through live imaging of these tumours, we discovered that zebrafish melanoma lesions were not uniformly infiltrated by CD4-1^{+} immune cells, instead we observed regions of melanoma with 'Brisk' (Figure 5.3 A'-C', dense infiltration of immune cells, indicated by arrows in white) and 'non-Brisk' (Figure 5.3 A'-C', sparse infiltration of

immune cells, indicated by arrows in pink) infiltration of CD4-1^{+} immune cells. Furthermore, when we analyzed these tumours using confocal microscopy we observed that higher CD4-1^{+} immune cell infiltration was largely associated with tumour tissue with reduced GFP expression (potentially regressing) while the regions of tumour that were sparsely infiltrated showed no signs of potential regression (Figure 5.3 D-F).

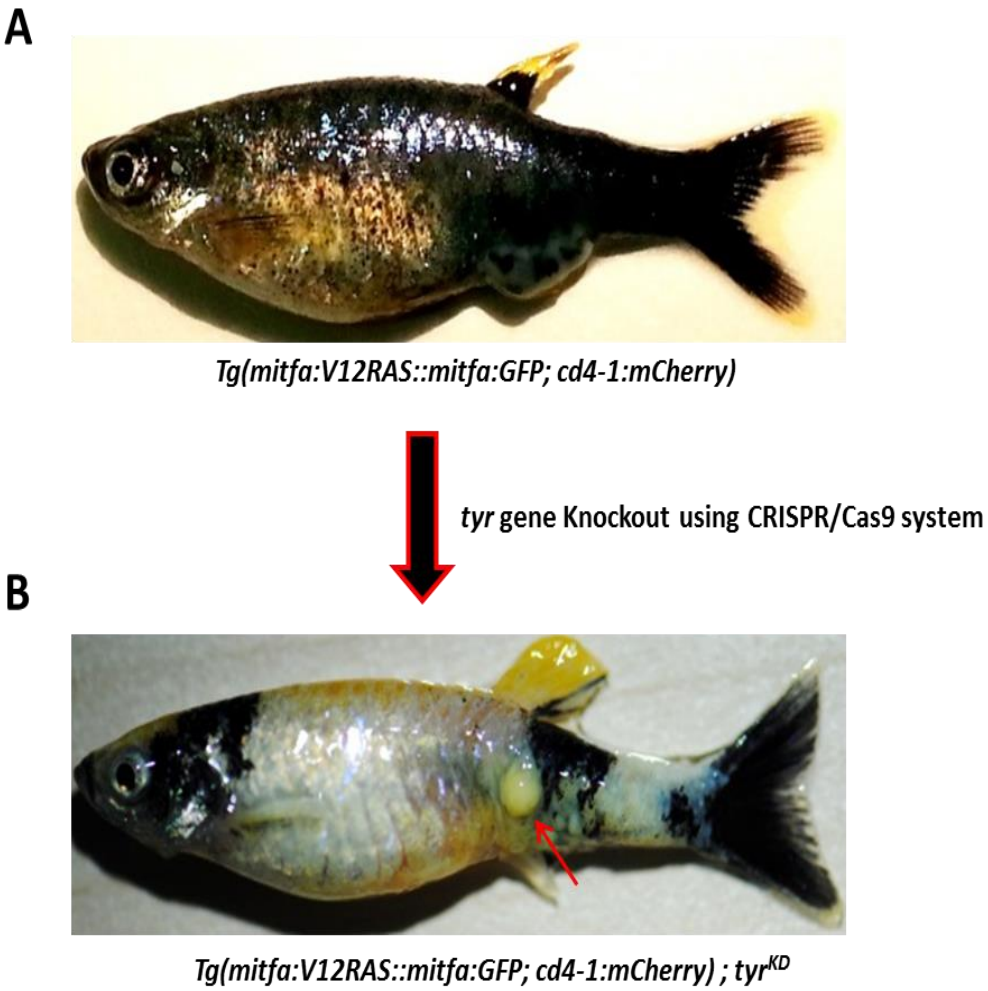

Figure 5.2. Tyrosinase (*tyr)* gene knockout results in optically translucent tumours in a zebrafish melanoma model. (A) Oncogenic *RAS* expressing adult zebrafish develops pigmented tumours that are non-conducive for florescence imaging. (B) Whereas the *tyr*$^{-/-}$ mutant zebrafish line now develops optically translucent tumours (Red arrow).

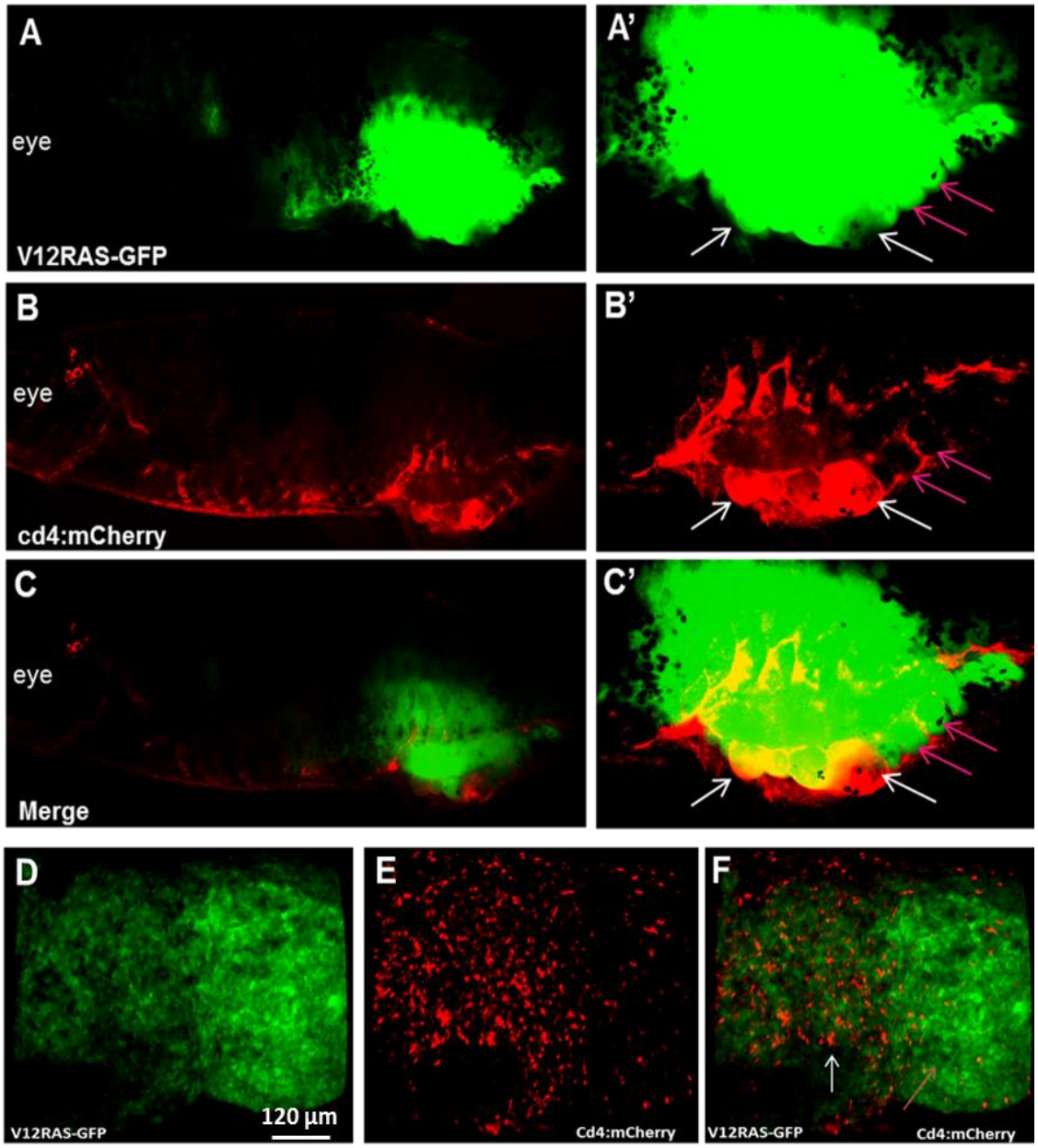

Figure 5.3. Varied infiltration of Zebrafish tumours by CD4-1+ immune cells. (A-C) Stereo fluorescence image of a V12RAS driven melanoma in *tyr*$^{-/-}$ mutant (Fo) zebrafish showing heterogeneous immune response by mCherry labelled CD4-1^{+} cells. (A'-C') We observed regions of melanoma with 'Brisk' (dense infiltration of immune cells, indicated by arrows in white) and 'non-Brisk' (sparse infiltration of immune cells, indicated by arrows in pink) infiltration of CD4-1^{+} immune cells. (D-F) Higher resolution confocal images of the same tumour clearly demonstrate that regressing tumour tissue is associated with significantly higher CD4-1^{+} immune cell infiltration (indicated by white arrows).

5.3 A longitudinal study of melanoma establishes immunoediting in a zebrafish melanoma model

A longitudinal study of tumours that captures the dynamics of tumour-immune cell interactions at the cellular level is crucial for understanding the mechanisms of successful and failed immunotherapies. Unfortunately, very little progress has been made in this direction mainly due to lack of appropriate model systems. As described in the previous section (5.2), through non-invasive imaging, our zebrafish model presents a unique opportunity to study the interactions of mCherry labeled CD4-1^{+} immune cells with GFP labelled melanoma cells. Using this model, we tracked tumours for over 7 weeks documenting various dynamic phases in tumour immunosurveillance. As shown in figure 5.4, on Day 0 we observed a blistering like region on the periphery of the tumour along with a significant accumulation of CD4-1^{+} immune cells, which over the period of first 26 days appeared to have consolidated on the periphery of the tumour. By 43 days we observed massive infiltration of the CD4-1^{+} TILs in to the tumour which interestingly disappeared by 52 days. Although the CD4-1^{+} immune infiltrate inside the tumour has considerably decreased by 52 days, the edges of the tumours were still briskly populated. Over the period of 52 days, the tumour was under active immune surveillance while progressively regressing in volume (as indicated by the expanse of GFP expression).

Interestingly, we also observed tumours that poorly responded to host immune control. As show in figure 5.5, on Day 0 we observed accumulation of CD4-1^{+} immune cells on the periphery of the tumour. Over the period of next 26 days, the immune cells

have consolidated around a regressing patch of the tumour (reduced GFP expression indicated with white arrow), resulting in a blistering like region (indicated with blue arrow). Unlike the tumour in figure 5.4, this melanoma lesion appeared to have gained resistance to host immune suppression as it continued to progress and grow in volume until the study was terminated around 52 days. Our data for the first time has demonstrated that immunoediting exists in a zebrafish melanoma model system thus making it a reliable model system to explore new immunotherapy strategies.

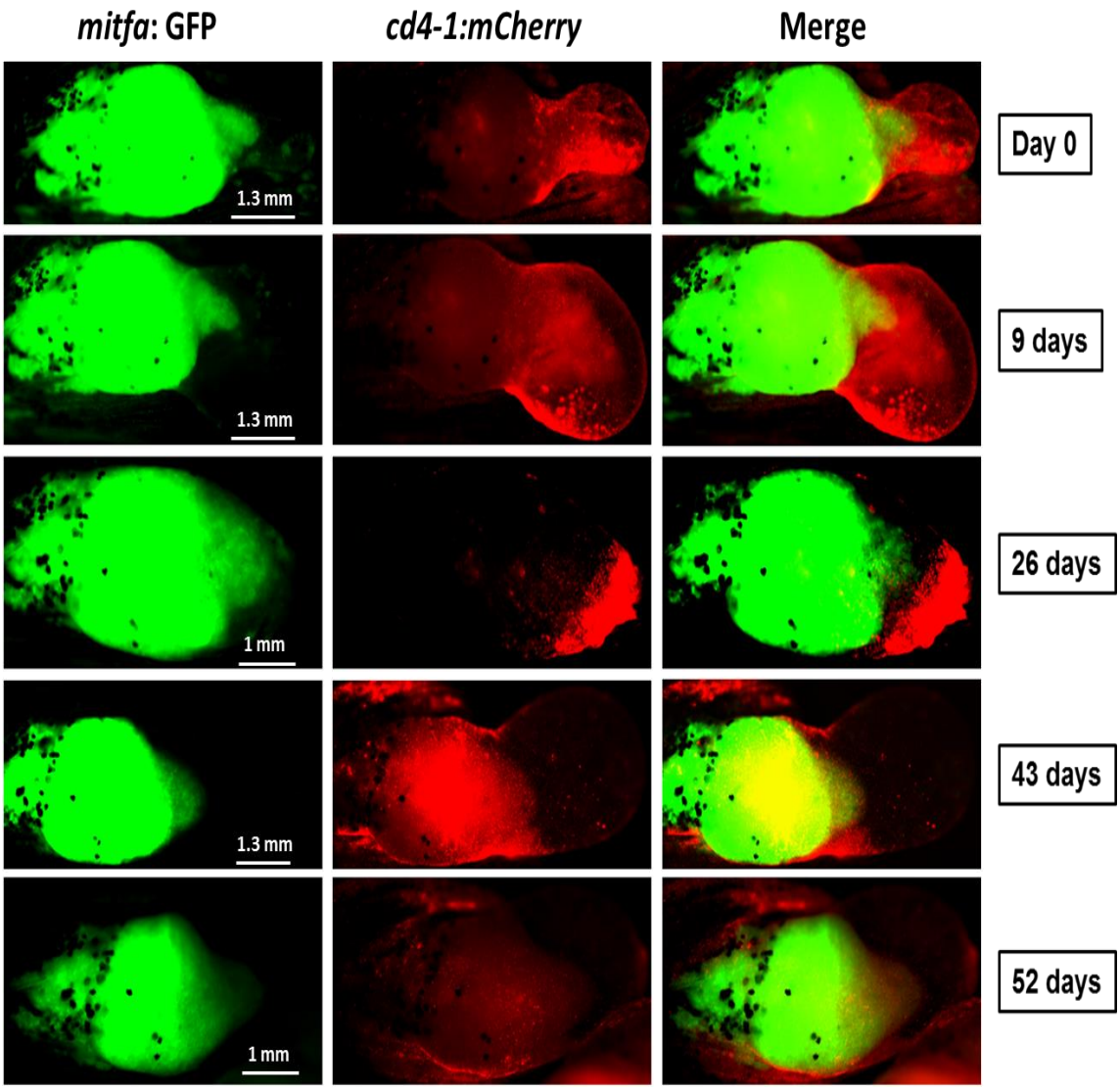

Figure 5.4. Tumour immunosurveillance exits in zebrafish. Using fluorescence microscopy, we have documented this spontaneously regressing V12RAS driven melanoma (GFP labelled) in a $tyr^{-/-}$ mutant (F_o) zebrafish over a period of 52 days. We observed a dynamic micro-environment where the mCherry labelled CD4-1^{+} TILs moved in and out of this regressing tumour, a potential hallmark of an effective immunosurveillance against melanoma.

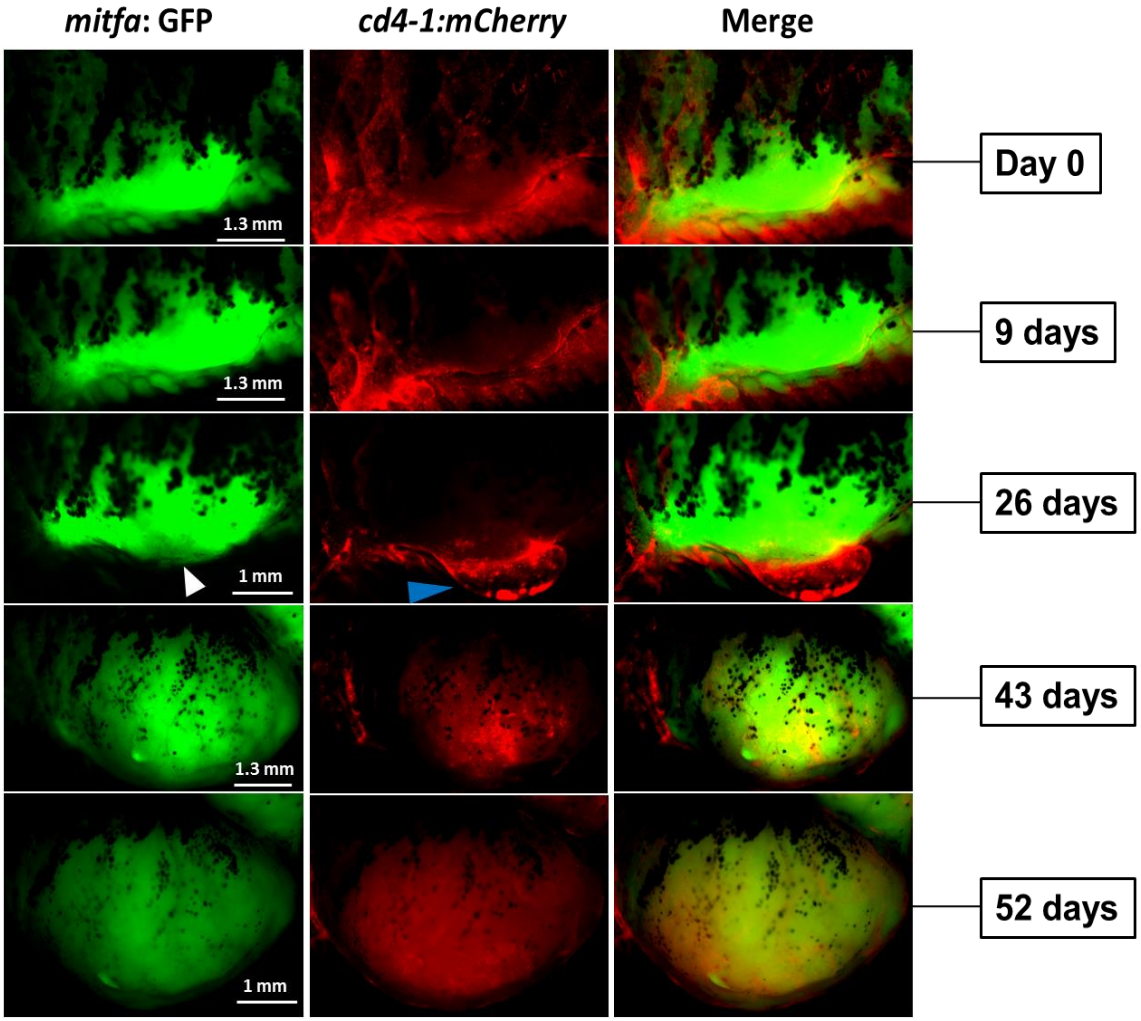

Figure 5.5. Tumours escaping immune suppression in zebrafish. Using fluorescence microscopy, we followed a developing V12RAS driven melanoma lesion (GFP labelled) in a *tyr*$^{-/-}$ mutant (F_0) zebrafish over a period of 52 days. Around day 26, we observed spontaneous tumour regression (white arrow) in the region associated with localised inflammation (blue arrow). Interestingly, the tumour subsequently escaped from the immune suppression and continued to grow until the end of this study.

5.4 A Tamoxifen inducible LSL/CreER^{T2} system for temporal regulation of target genes in tumour microenvironment

One of the primary aims of this project was to modify melanoma cells in order to express candidate genes (e.g. cytokines) and study their effect on tumour progression. The hypothesis we wanted to test was whether by skewing the cytokine profile in a tumour microenvironment to drive T_H1 helper T cell differentiation, we can induce an inflammatory immune response leading to tumour regression. To facilitate this, we have designed and built a Tamoxifen inducible CreER^{T2} recombinase based expression system for conditional induction of IFNγ in zebrafish melanoma cells. As illustrated in figure 5.6 A, using multisite gateway cloning technique, we assembled the ''mitfa:loxp-mCherry-loxp: IFNγ-P2A-venusGFP'' expression vector (minicoopR LSL) where the microphthalmia-associated transcription factor a (mitfa) promoter drives mCherry flanked by loxp sites (lox-stop-lox, LSL). In this configuration, acting as transcriptional stop, mCherry blocks the expression of the IFNγ-P2A-venusGFP fusion transcript (VenusGFP fused to IFNγ using P2A). This entire assembly was cloned in to minicoopR destination vector that has been previously published (Ceol *et al*. 2011).

The experimental design entailed co-injecting then minicoopR LSL expression vector with mitfa:NRAS^{Q61L} vector in to one-cell stage *Tg(ubi:creER^{T2})* casper (roy$^{-/-}$;nacre$^{-/-}$) embryos, that are totally devoid of melanocytes while ubiquitously expressing creER^{T2} recombinase (Mosimann *et al.* 2011). Because of the *mitfa* mini gene in its backbone, the minicoopR LSL vector will rescue melanocytes in the injected fish and the mitfa promoter will drive mCherry expression in those melanocytes. This system

also expresses oncogenic human NRAS ($NRAS^{Q61L}$) in those rescued melanocytes giving them the ability to transform in to melanoma (Figure 5.6 B). Upon treatment of injected fish with 4-Hydroxytamoxifen (4-OHT), the LSL cassette is excised following the activation and nuclear localization of Cre recombinase thus bringing IFNγ-P2A-venusGFP under the influence of mitfa promoter (Figure 5.6 C). The induction of IFNγ expression in tumours can be ascertained by visual confirmation of venusGFP expression. For this experiment we have used $NRAS^{Q61L}$ as both oncogenic HRAS (RAS^{V12}) and NRAS ($NRAS^{Q61L}$) have similar ability to induce melanoma lesions in zebrafish and the resulting tumours also share similar gene expression pattern (Hurlstone lab, unpublished data). Hence the tumour specific antigen profiles for both these melanomas will likely be similar and so will be the zebrafish immune responses.

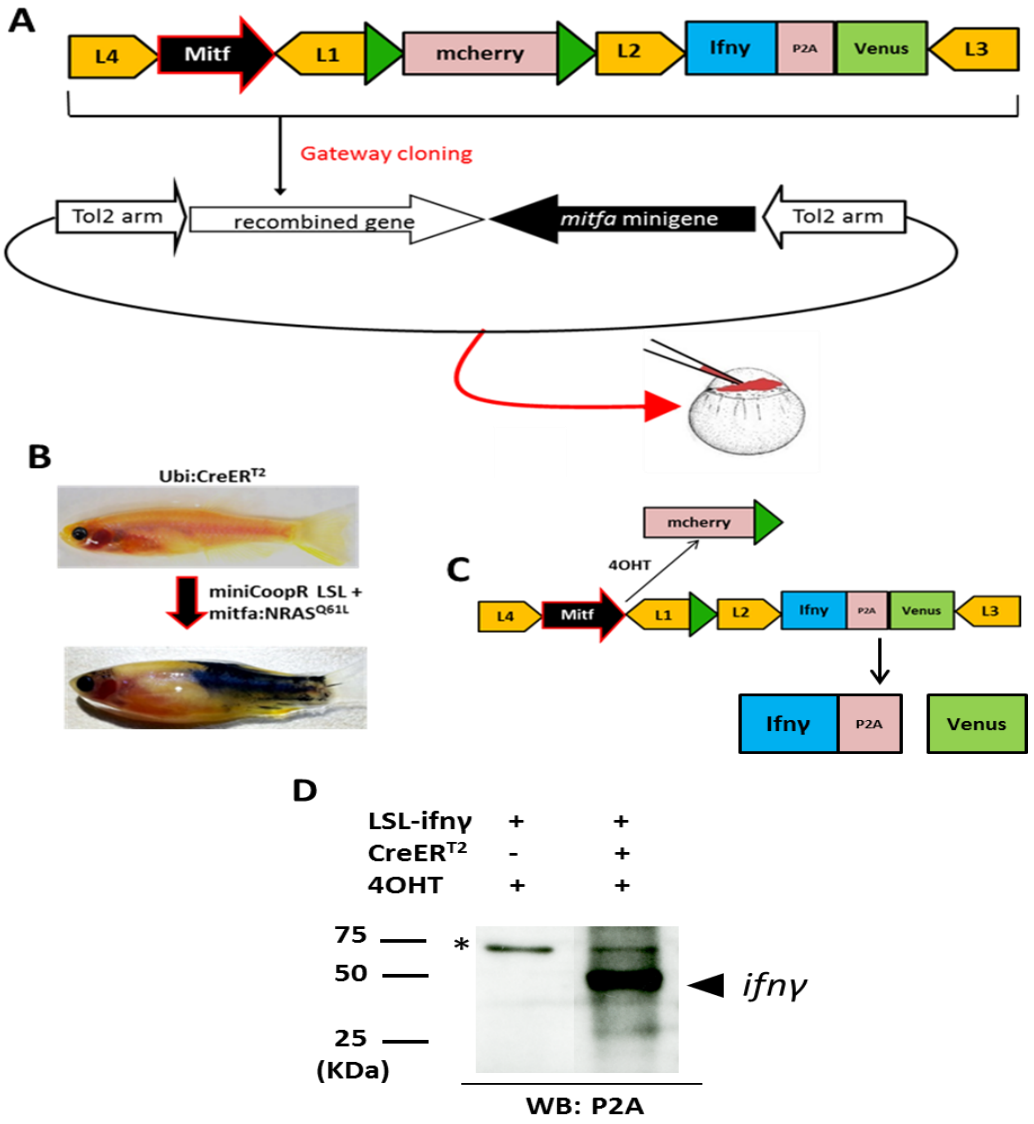

Figure 5.6. (A) Cloning strategy for Cre recombinase based self-excising system (miniCoopR LSL) for conditional induction of cytokine expression. **(B)** This system also rescues oncogenic RAS expressing melanocytes in a transgenic casper fish expressing CreER^{T2} under ubi promoter. **(C)** Upon treatment of injected fish with 10um 4-OHT (4-Hydroxytamoxifen), the lox-stop-lox (LSL) cassette is excised bringing the cDNA of the target cytokine (IFNγ) under the influence of the mitfa promoter. **(D)** Following 4OHT treatment, successful induction of IFNγ in the tumour microenvironment was ascertained through western blotting using an anti-P2A antibody that will specifically report forced IFNγ expression. Following 4OHT treatment, we observed induction of IFNγ in CreER^{T2} positive zebrafish but not in control CreER^{T2} negative zebrafish. * Non-specific band

5.5 Induced expression of IFNγ in the tumour microenvironment leads to tumour regression

Following the above described experimental set up, we have co-injected the *Tg(ubi:creER^{T2})* casper (roy$^{-/-}$;nacre$^{-/-}$) and casper (roy$^{-/-}$;nacre$^{-/-}$) embryos (controls, no induction of IFNγ due to lack cre recombinase) with minicoopR LSL and mitfa:NRAS^{Q61L} vectors. The embryos were later screened for rescue of melanocytes at 5 dpf and the positive larvae were subsequently segregated and regularly monitored for appearance of tumours. A majority of the injected fish, both *CreER^{T2+}* and control, developed tumours by round 6-8 weeks post injection (wpi) (Figure 5.7 A). We then treated these fish with 4-OHT, to initiate the induction of IFNγ expression in the melanoma cells (also in melanocytes). Following 4-OHT administration, by ~2 weeks post induction (WPI), we observed visible loss of pigmentation in IFNγ induced tumours which gradually increased over the study period (Figure 5.7 B), whereas no loss of pigmentation was observed in control tumours throughout the study period (data not shown). At 9 WPI, the study was terminated and tumours were histologically analysed. In tumours where IFNγ was induced, we observed that most of the tumour has regressed and the tumour tissue was now replaced with granulation tissue accompanied by a marked lymphocyte infiltration and patches of necrosis (Figure 5.7 D). As expected, 4-OHT treated control tumours showed no signs of tumour regression (Figure 5.7 C). Overall, 6 out of 9 tumours have regressed following IFNγ induction, while none of the control tumours have regressed (Figure 5.7 E).

While induced expression of IFNγ in the tumour microenvironment lead to regression of established tumours, we also observed new amelanotic resistant tumours developing in the vicinity of some of these regression tumours. For example, in figure 5.8, we see that following induction of IFNγ expression, the target tumour (marked with red arrow) started regressing by ~3 WPI and gradually the tumour was eliminated by ~9 WPI (The residual tissue is mostly fibrotic). But, we can also see a new amelanotic tumour (marked with black arrow) appearing in the vicinity of this regression tumour by ~6 WPI which rapidly grew in size by ~9 WPI. It is interesting to note that these resistant tumours develop in close proximity to regions with high IFNγ expression as indicated by VenusGFP. Taken together, our data demonstrates the dual role of IFNγ expression in the tumour microenvironment. While established tumours are eliminated in the presence of IFNγ, prolonged expression of IFNγ in the microenvironment can also lead to development of resistant amelanotic tumours.

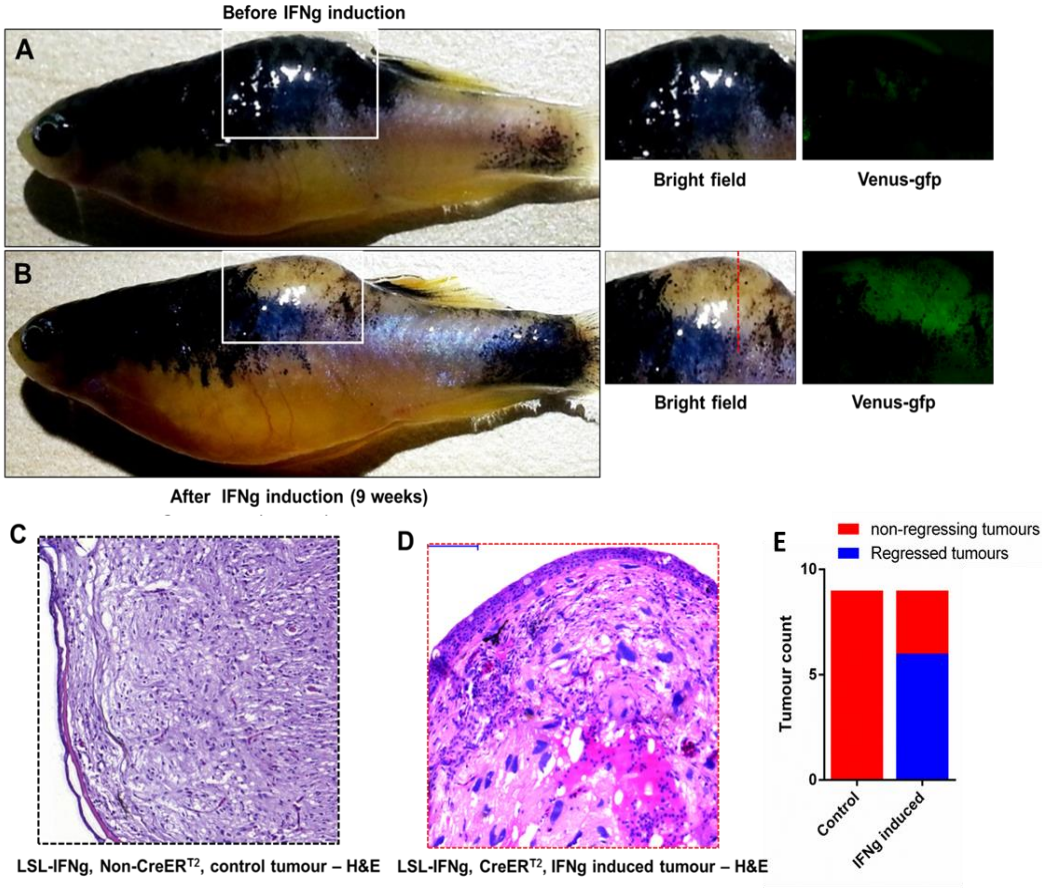

Figure 5.7. IFNγ induced tumour regression: Transgenic casper zebrafish expressing CreER^{T2} under ubi promoter is co-injected with miniCoopR LSL construct expressing IFNγ -P2A-venus and Human NRAS^{Q61L} under mitfa promoter. **(A)** Bright field image of the fish ~8 weeks post injection showing an established pigmented tumour captured before 4OHT treatment **(B)** Bright field image of the same fish 9 weeks post 4OHT treatment. Apparent Loss of pigmentation is observed in the boxed tumour region. **(C)** H&E stained paraffin section of a non-CreER^{T2} control tumour. **(D)** H&E stained paraffin section of the IFNγ induced tumour in panel 'B'. The tumour is now Hypocellular with patches of necrosis and inflammation. **(E)** Upon induction of IFNγ, 6 out of 9 tumours have regressed, while no sign of tumour regression was observed in control tumours.

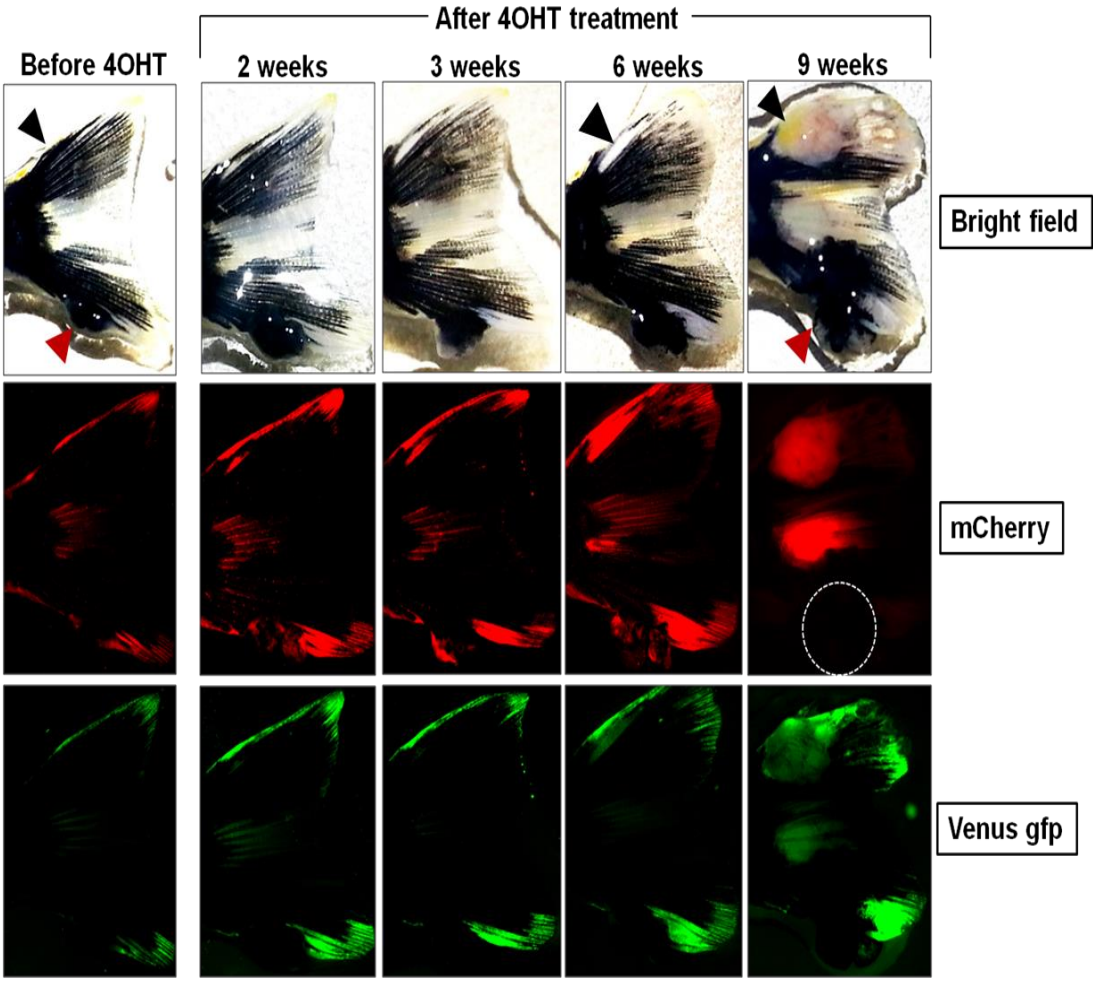

Figure 5.8. Amelanotic resistant tumours develop in the presence of IFNγ**:** Transgenic casper zebrafish expressing $CreER^{T2}$ under ubi promoter is co-injected with miniCoopR LSL construct expressing IFNγ -P2A-venus and Human $NRAS^{Q61L}$ under mitfa promoter. Bright field image of the fish captured ~8 weeks post injection showing an established pigmented tumour before 4OHT treatment, indicated by red arrow. The fish was then treated with 4OHT and imaged over regular intervals until 9 weeks post induction (wpi). By 9 wpi , the target tumour has completely regressed but interestingly a new amelanotic tumour, indicated by black arrow, appeared around 6 wpi in the vicinity of IFNγ expressing region.

5.6 Forced constitutive expression of soluble PDL1 (PDL1T) suppresses tumour formation in our zebrafish melanoma model

A major immune evasive strategy employed by tumour cells is to activate PD1-PDL1 mediated suppression of effector immune cells (Pardoll *et al.* 2012). We wanted to explore if zebrafish also have similar immune regulatory mechanism. To date, no PD1 like molecule has been reported in Zebrafish while a putative ligand-like molecule is annotated in the zebrafish genome (ENSDARG00000100899), but interestingly, PD1-PDL1 interaction sites appear to be conserved between human and zebrafish PDL1 (figure 5.9). When compared to human PDL1 (290 aa), zebrafish PDL1 (503 aa) is almost twice the length with a significantly longer endodomain (figure 5.10 A). In spite of being very diverse, structurally and sequence wise, human and Zebrafish PDL1 molecules share some key features. Firstly, both proteins share an 'IGv' domain in their ectodomain (figure 5.10 A), which is reported to be essential for PDL1 interactions with PD1 (Lin *et al.* 2007). Secondly, across species, in spite of massive dissimilarities in PDL1 sequence, PD1-PDL1 interaction sites are conserved (Lin *et al.* 2007).

In response to the pressure from the immune system, tumour cells are known to express more PDL1 on their membrane to activate PD1-PDL1 mediated killing of effector immune cells (Spranger *et al.* 2013). In our zebrafish melanoma model, preliminary analysis on primary tumours performed by a master student in our laboratory has indicated that melanoma tumours express significantly higher levels of PDL1 compared to surrounding non-malignant tissue (Hurlstone lab, unpublished data). Forced constitutive expression of a soluble form of human PD-L1 (sPD-L1) comprising

just the ecto-domain has been reported to effectively block the PD-1/PD-L1 signalling in an in-vitro experimental set-up (Pen et al. 2014). Hence, with an aim to further understand the role of PDL1 in tumour progression in our zebrafish melanoma model, we decided to mis-express soluble ectodomain of the Zebrafish PDL1 (PDL1T) specifically by the melanoma cells using the minicoopR system (figure 5.10 B). If zebrafish also has PD1-PDL1 mediated regulatory mechanism similar to mouse, once secreted in to the microenvironment, acting as a decoy, PDL1T will potentially compete with membrane bound endogenous PDL1 thus interfering with PD1-PDL1 signalling.

As illustrated in figure 5.10 B, we cloned PDL1T to be expressed under the control of the mitfa minimal promoter in a minicoopR vector so as to ensure its localised expression in the tumour micro-environment. The construct was co-injected with mitfa:NRAS^{Q61L} vector in to 2-cell stage embryos of casper zebrafish which were later screened for rescue of melanocytes at 5 dpf and the positive larvae were subsequently segregated and regularly monitored for appearance of tumours from 4 weeks post fertilization (wpf). *ccnd1* (an established oncogene known to accelerate tumour formation) and *eGFP* (a neutral cDNA choice) minicoopR constructs, a kind gift from Dr. Craig Ceol, were used as positive and negative controls respectively. At 24 wpf, when the study was terminated, 18 fish expressing eGFP (n=44) had tumours compared to 15 fish (n=81) that are expressing PDL1T. As expected, *ccnd1* expressing fish had the fastest tumour incidence and mortality with all 20 fish developing tumours by 12 wpf and were culled by 13 wpf. Compared to eGFP, forced constitutive expression of soluble PDL1 in the microenvironment significantly suppresses tumour

formation ($p<0.01$, Log-Rank test – tumour incidence). Figure 5.10 C is showing the Kaplan-Meier plot of tumour free survival for all three conditions (*ccnd1,* eGFP *and* PDL1T). Interestingly, we also observed that in PDL1T expressing fish most of the tumours (5 out of 6) appearing after ~16 wpf were amelanotic and had close resemblance to IFNγ induced resistant tumours (figure 5.11).

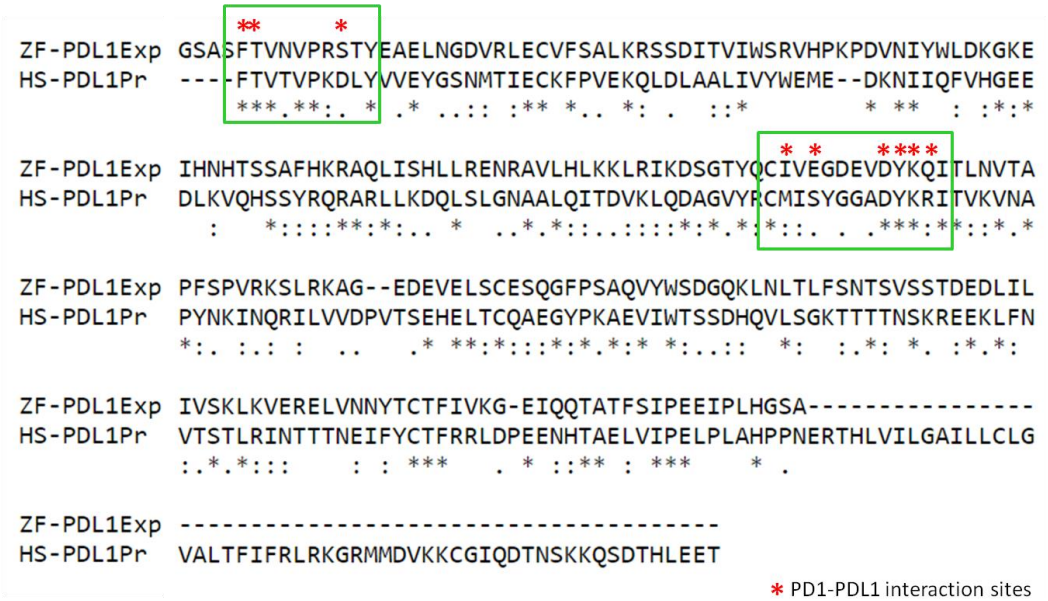

Figure 5.9. PD1-PDL1 interaction sites appear to be conserved between human and zebrafish PDL1. Ectodomain of zebrafish PDL1 protein was aligned with full lengh human PDL1 protein using Clastal omega tool on EMBL-EBI website. Although the overall protein conservation was poor with ~30% similarity, all the PD1-PDL1 interaction sites are conserved in zebrafish.

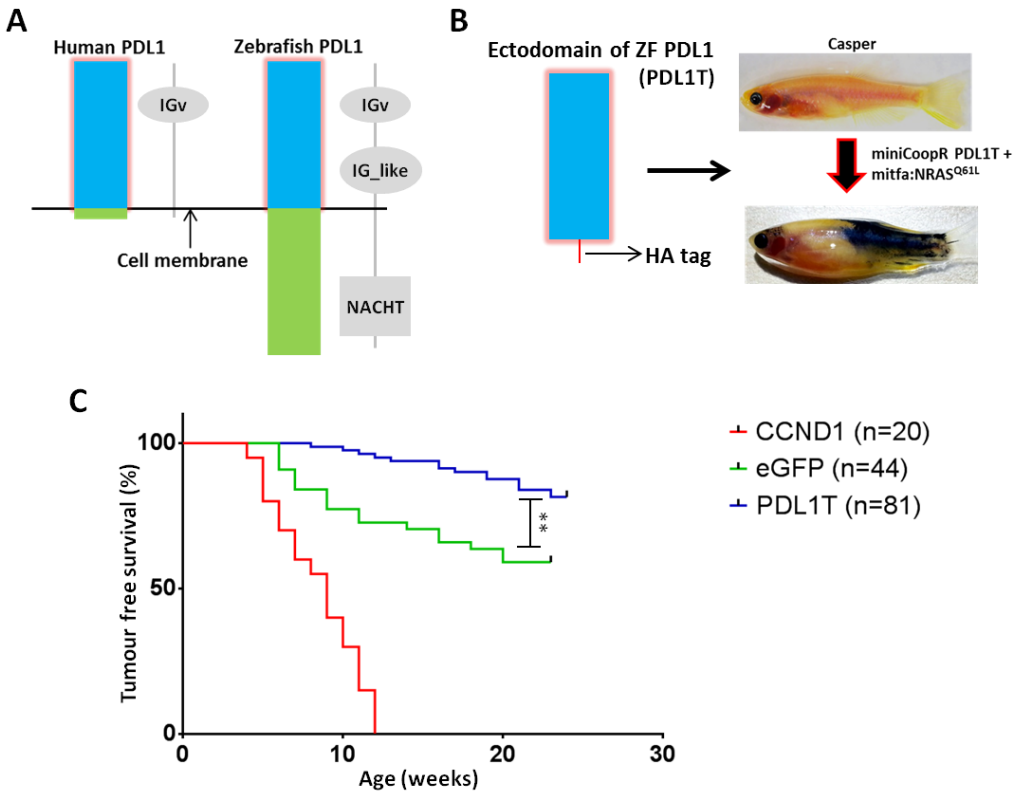

Figure 5.10. Forced constitutive expression of soluble PDL1 (PDL1T) significantly suppresses tumour formation in a zebrafish melanoma model. (A) Schematic representation of human and zebrafish PDL1 proteins (ZF PDL1). While the ZF PDL1 has bigger cytoplasmic domain compared to human PDL1, both the proteins share a crucial 'IGv' domain which is essential for PD1-PDL1 interactions. (B) we cloned the soluble ectodomain of the ZF PDL1 to expresses under mitfa minimal promoter so as to ensure its localised expression in the tumour micro-environment where it will potentially compete with membrane bound endogenous PDL1 thus interfering with PD1/PDL1 signalling. The construct was co-injected with a vector expressing oncogenic $NRAS^{Q61L}$ in to embryos of Casper zebrafish which will start developing tumours spontaneously from 4 weeks post injection. (C) Kaplan-Meier plot showing tumour free survival for fish expressing either CCND1 (accelerates tumour formation, positive control), eGFP (No effect on tumour formation, baseline) or PDL1T (test molecule). Compared to eGFP, forced constitutive expression of soluble PDL1 in the micro-environment significantly suppresses tumour formation ($p<0.01$).

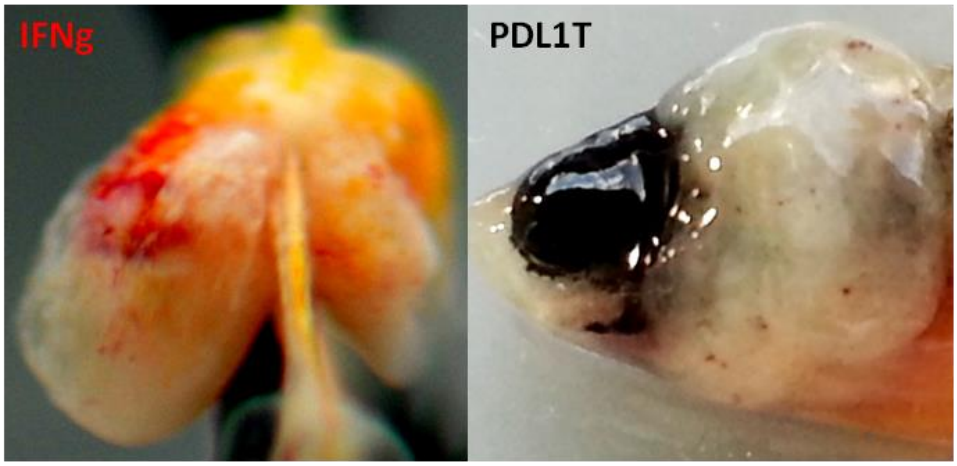

Figure 5.11. Forced expression of both IFNγ and PDL1T in the tumour micro-environment resulted in formation of amelanotic escape tumours. In our mitfa:NRAS^{Q61L} minicoopR model, tumours expressing either IFNγ or PDL1 ectodomain in the microenvironment developed aggressive amelanotic tumours after prolonged exposure (over 9 weeks).

5.7 Discussion

One of the primary aims of my PhD project was to establish whether zebrafish $CD4^+$ T cells react to melanoma development. In humans, developing tumours must evade eradication by hostile inflammatory effector cells and regularly enforce a type-2 biased milieu featuring infiltration by T_H2 cells or immunosuppressive T_{reg} cells (Whiteside *et al*. 2014, Mccarter *et al*. 2005). It has been observed that, in general, the presence of more T_H2 TILs results in poor prognosis in humans and mouse cancer models (Kohrt *et al*. 2005, Haabeth *et al*. 2011). In the presence of a T_H2-type tumour microenvironment, CD4+ TILs enhance cancer progression by stimulating tumour associated macrophages (TAMs) to secrete pro-angiogenic and pro-metastatic factors such as IL-4 (DeNardo *et al*. 2009, Haabeth *et al*. 2011). In recent years, zebrafish models of human cancer, including melanoma, have proven highly informative with extensive phenotypic conservation (Michailidou *et al*. 2009, Ceol *et al*. 2011). However, this is the first characterisation, to our knowledge, of the immunological phenotype of a zebrafish tumour model. We showed that progressing melanoma tumours are infiltrated by CD4-1^+ cells, and that these are enhanced for the expression of *gata3* and *il-4/13a* but not for t-bet and Ifnγ, indicating a T_H2 bias (Figure 5.1). In contrast to CD4-1^+ T_H2 cells in gills that expressed *il-4/13b,* tumour infiltrating T_H2 cells expressed *il-4/13a.* These results support the view that these cytokines have discrete functions in teleost immunity (Wang et al. 2016). The identification of a population of *il-4/13a* expressing T cells, in contrast to cells resident in the gill, raises the intriguing possibility of an alternative T_H2-like phenotype. Certainly, heterogeneity of T_H2 cells has been

observed in mammals, with reports of inflammatory and non-inflammatory T_H2 cells (Pulendran et al. 2012). The infiltration of developing zebrafish tumours by CD4-1^+ T cells implies a significant degree of functional conservation. However, the future challenge will be to explore the extent of functional homology between the cell populations described in this study and the equivalent cells of mammals, such as whether they respond to similar challenges and provide genuine helper or regulatory functions. The ongoing development of zebrafish models of infectious disease (Berg et al. 2016, Hammaren et al. 2014, Briolat et al. 2014, Achar et al. 2014 and Bojarczuk et al. 2016) and inflammatory disorders (Candel et al. 2014 and Brugman et al. 2009) coupled with novel genetic tools (such as immune-compromised fish) (Tang et al. 2016) presents an exciting opportunity to dissect these questions in detail.

On the other hand, the expression of *foxp3* and *il10* is not significantly enhanced in TILs (Figure 5.1F) indicating no apparent correlation of T_{regs} with progressing melanoma in zebrafish. However, we believe that this is not an accurate way of analysing our data as T_{regs} are very diverse across species and their role in tumour regulation is still an evolving and fiercely debated field of science (Whiteside *et al*. 2014). For example, the FOXP3 transcription factor is a reliable marker of murine T_{regs}, but its expression in human inducible (iT_{regs}), T_{regs} differentiated in the periphery, may be down regulated, while FOXP3 is expressed in some activated T cells which do not mediate suppression (Whiteside *et al*. 2012, deLeeuw *et al*. 2012). These inter-species differences interfere with extrapolation of our understanding about T_{regs} from humans and mouse models to zebrafish. Furthermore, there are intra-species

differences in the behavior of iT_{regs}. iT_{regs} can contribute to cancer progressing by suppressing anti-tumour immune responses (Gallimore *et al.* 2008), while they can also inhibit cancer progression by suppressing the cancer promoting inflammation (Erdman *et al*. 2005). All of these observations warrant for a more in-depth analysis of T_{reg} biology in zebrafish before we can understand their role in cancer regulation. Owing to the limitation of our *Tg(cd4-1:mCherry)* reporter to distinguish T_{regs} among CD4-1^{+} helper cells, we couldn't further investigate their behavior in a zebrafish tumour microenvironment.

In general, the zebrafish model system is highly conducive for live imaging. However, florescence imaging of melanoma in an adult zebrafish is practically impossible due to its pigmentation. Although the surrounding areas of the tumour were conducive for imaging the actual tumour mass was almost inaccessible for imaging even with a confocal microscope. This significantly affects our ability to accurately document the dynamics of immune responses to melanoma. Foreseeing this limitation at the very beginning of the project we started developing 'casper golden' zebrafish. Golden is a zebrafish strain which has polymorphic allele of *SLC24A5* gene that contributes to less intense pigmentation (Lamoson *et al.* 2005). Thus having golden phenotype makes the fish paler compared to wild type zebrafish (Lamason *et al*. 2005). So now when melanocytes are rescued (restoration of melanocytes through *mitfa* transgene expression) in 'casper golden' zebrafish, they will be faintly pigmented and when these cells eventually transform to form melanoma, the tumour mass will potentially be less pigmented facilitating an enhanced ability to image the tumour

mass. By crossing multiple generations of casper and golden lines, We tried to establish the 'casper golden' line but unfortunately these fish died after 10 dpf. Although we never firmly established the actual reason for their death, we observed that these fish had difficulty in feeding. We observed the 7-8 dpf larvae under the microscope and found no signs of food intake (data not show), so we believe that once the Yolk is depleted around 10 dpf the 'casper golden' fish were dying due to their inability to feed on alternative food source. In line with our animal license, we have terminated this experiment concluding that homozygous 'casper golden' zebrafish line is non-viable.

To overcome this challenge, using CRISPR/Cas9 technology, we have generated a *tyr*$^{-/-}$ mutant zebrafish line that develops un-pigmented melanocytes (Figure 5.2). In zebrafish, CRISPR/Cas9 system has been show to modify the target gene loci with high efficiencies both in somatic and germ cells (Jao *et al*. 2013). Consistent with the published data, injected TYR guide RNA in to Tg(mitfa:*V12RAS*::mitfa:venusgfp; cd4-1:mCherry) embryos resulted in more than 70 % animals with partial knock down (scored based on loss of pigmentation) and ~10% animals with almost complete knock down of *tyr* (data not shown). As anticipated, the melanoma tumours that spontaneously appeared in animals with near complete knock down of *tyr* were un-pigmented (Figure 5.2). Overcoming all the setbacks, we ultimately generated an *in-vivo* model system that can be used to study the dynamics of CD4-1^{+} T cell interactions with melanoma.

Helper T cells in tumour biopsies have been studied for decades to understand their potential impact on prognosis (Hadrup *et al*. 2013). Mainly using immune histochemistry (IHC), early data reported a simple correlation between 'brisk' infiltration of T cells in primary melanoma lesions and improved prognosis in patients (Clark 1991). Subsequent studies in later years have resulted in a standardized histological classification of melanoma lesions based on the density of TILs along with their correlating prognostic outcomes (Busam *et al*. 2001). The melanoma lesions were classified as either 'Brisk' (densely infiltrated), 'non-Brisk' (sparsely infiltrated) or 'Absent' (no infiltration), reflecting the heterogeneity in T cell responses against melanoma in mammals. Overall, lesions with 'Brisk' TILs show the best prognosis, while 'non-Brisk' tumours show better prognosis compared to lesions with no infiltrate (Busam *et al*. 2001). Interestingly, we observed that zebrafish melanomas also elicit similar heterogeneous responses by CD4-1+ cells. As shown in figure 5.3, in our zebrafish model we observed regions of melanoma with 'Brisk' (indicated by arrows in white) and 'non-Brisk' (indicated by arrows in pink) infiltration of CD4-1+ immune cells. In concurrence with prognostic prediction in patients, we discovered that regions with 'Brisk' CD4-1+ TILs overlap with regressing part of the tumour (loss of GFP fluoresce), while no signs of regression were observed in the regions with 'non-Brisk' infiltration of CD4-1+ TILs (Figure 5.3 D-F).

A longitudinal study of tumours that captures the dynamics of tumour-immune cell interactions is essential for developing more effective anti-tumour immunotherapies (Perentes *et al*. 2009). In vivo longitudinal studies involving tumour

cells have become increasingly feasible with the development of transgenic mouse models that expresses fluorescent proteins in the target cell types along with adoptive transfer protocols that facilitate infusion of fluorescently labeled cells (Boissonnas *et al*. 2007, Chiang *et al*. 2007, Breart *et al*. 2008). In particular, the development of intravital microscopy (IVM) has helped a great deal in understanding complex and important facets of cancer such as metastasis (Ellenbroek *et al*. 2014). Although the number of IVM tools that have become available has steadily increased, there are still technical (repeated anesthesia and surgery burden, limited imaging depth and field of view etc.) and financial (high maintenance costs for mice) limitations to these techniques (Ellenbroek *et al*. 2014). While complementing the existing mouse models, our *tyr* knock-out zebrafish line (Figure 5.2) provides a more simplistic and cost effective in-vivo model system with good biological representativeness. Using this model we have documented, through non-invasive imaging, the dynamics of mCherry labeled CD4-1+ immune cell interactions with GFP labeled melanoma cells, a first in a zebrafish model (Figure 5.4, Figure 5.5).

In a regressing melanoma, we observed distinct phases in immune system assisted killing of melanoma cells. As shown in Figure 5.4, firstly we see development of blistering on the periphery of the tumour, potentially resulting from immunogenic death of melanoma cells. Then by ~26 days we see CD4-1^{+} immune cells accumulating around the septic periphery where they are potentially being educated by the APCs on tumour antigens resulting in their activation. This is followed by massive infiltration of the tumour by CD4-1^{+} immune cells and likely also by other effector immune cell types

such as $CD8^+$ T cells, NK cells and dendritic cells. Lastly, by ~52 days when the study was terminated, we see that most of the $CD4\text{-}1^+$ immune infiltrate is now cleared from the tumour but more interestingly we also observe an apparent reduction in tumour volume from day 43, possibly indicating a targeted adaptive immunity mediated killing of melanoma cells. Our observations are inspiring and unprecedented, but due to glaring limitations of our current model system, for example, unable to follow and isolate T_H1, T_H2 and T_{regs} from these tumours, we can't draw many definitive conclusions at the moment. We are in the process of generating new reporter lines to address this imitation.

Tumours can acquire resistance to immune pressure. By activating multiple T cell inhibitory feedback mechanisms, checkpoint molecules such as LAG-3, TIM-3 and BTLA are reported to play a role in acquiring resistance (Pardoll 2012). In addition, a naturally occurring immune response may select for tumour cell subpopulations with loss of MHC class I expression, or other defects in the antigen processing machinery, thereby cloaking the tumour cell from the immune system (del Campo *et al*. 2014, Khong *et al*. 2004 and Restifo *et al*. 1996). A similar immune evasive effect may be achieved through selection of tumour sub-clones present within heterogeneous tumours lacking one or multiple antigens that are subject to strong Darwinian selection, a process called immunoediting (Dunn *et al*. 2002, Khong *et al*. 2002, and Matsushita *et al*. 2012). Most of the evidence for immunoediting has been obtained from mouse model systems. Here, we report that zebrafish melanoma can also naturally develop resistance and evade immune suppression. As shown in figure 5.5,

initially for ~26 days the tumour was under active immune surveillance as we see a region of blistering (indicated with blue arrow) associated with regressing patch of the tumour (loss of GFP expression indicated with white arrow). But, unlike the tumour in figure 5.4, this melanoma lesion appeared to have gained resistance to host immune suppression as it continued to progress and grow in volume until the study was terminated ~52 days. Taken together, our data has for the first time demonstrated that immunoediting of melanoma occurs in an autochthonous zebrafish model, thus making it a reliable *in-vivo* system to explore new immunotherapy strategies.

Having established that melanoma tumours are immunoedited in our autochthonous zebrafish model, we carried on to build an inducible in-vivo system that will enable us to modulate the tumour microenvironment through forced expression of candidate genes in melanoma cells. Initially, we started working on a heat -shock inducible Cre recombinase expression system using *hsp70* promoter. Soon, we decided not to pursue this strategy as we found *hsp70* promoter to be 'leaky', expressing target genes without being induced. Others have also reported the leakiness of *hsp70* promoter, albeit to varying degrees (Thummel *et al*. 2005, Feng *et al*. 2007, Le *et al*. 2007, Yoshikawa *et al*. 2008, Hans *et al*. 2009). Apart from the system being leaky, we also experienced difficulty in consistently inducing expressing of our candidate genes in melanocytes following heat shock (data not show). Owing to these technical difficulties we shelved this strategy and adopted a more robust tamoxifen inducible $CreER^{T2}$ recombinase system to express our candidate genes (Hans *et al*. 2009). $CreER^{T2}$ is generated by fusing Cre with mutated form of the modular ligand-sensing domain of

the Estrogen Receptor(ER), whereby the Cre recombinase activity is initiated by introduction of 4-OHT and not by endogenous estrogen (Feil *et al*. 1996). This gave the system a tighter control on target gene expression.

4-OHT is light and temperature sensitive, which meant we had to follow a few control measures to ensure consistency in our experiments. In spite of it being aliquoted and stored at -80 ^{o}c, we observed that efficiency of the drug gradually reduced overtime. Mindful of the potential batch effects of the drug, we always administered 4-OHT treatment to CreER^{T2} and controls zebrafish on the same day. Also, a fresh batch of 4-OHT was prepared every 6 months to ensure maximum efficiency. Exposure to light rapidly inactivates 4-OHT which meant that the fish had to be kept in the dark for the duration of the treatment. However, altering light cycles could potentially stress the zebrafish and introduce unwanted variables to the experiment. To circumvent this problem, we only administered the 4-OHT treatment overnight, during their natural dark cycle. Following initial trials using 5 dpf larvae, we found CreER^{T2} system to be a reliable system for expressing our candidate genes in melanoma cells (data not shown).

With the expression system chosen, we selected IFNγ as our first candidate gene and induced its expression in established zebrafish melanoma tumours. High IFNγ expression in the tumour microenvironment is often associated with better prognosis in cancer patients (Haabeth *et al*. 2011). In line with these observations, following IFNγ induction, 6 out of 9 tumours have shown signs of regression in our zebrafish model

(Figure 5.7 E). Furthermore, histological analysis revealed that these tumours are now hypocellular with patches of necrosis and inflammation, a strong indication of inflammation induced tumour regression (Figure 5.7 D). Here, using an autochthonous zebrafish melanoma model, we report that by forcing the expression of IFNγ specifically in the tumour microenvironment, thereby potentially enhancing T_H1 differentiation, we induced an inflammatory response leading to complete tumour regression.

However, in some zebrafish, new un-pigmented and potentially immuno-resistant tumours developed in the vicinity of these regressing (IFNγ responding) tumours (figure 5.8). It is interesting to note that all of the resistant tumours (n>12) we observed in this experiment had sustained expression of IFNγ in their microenvironment as indicated by VenusGFP expression. Melanoma cells express IFNγ receptor so can directly be regulated by IFNγ (Lollini *et al.* 1993, Bernabi *et al*. 2001). A series of in-vivo and in-vitro studies have shown that melanoma cells respond to IFNγ in a dose dependent manner (Zaidi *et al*. 2011, Son *et al*. 2014, Natarajan *et al*. 2014). Sustained high-level expression of IFNγ has been show to induce tumour suppression, while sustained low-level expression of IFNγ reportedly promotes tumour development and may also initiate new tumours (Son *et al*. 2014, Natarajan *et al*. 2014).

In our zebrafish model, as an unintended consequence of our design strategy, we believe to have created 2 distinct populations of cells expressing varied levels of IFNγ. Following 4-OHT treatment, IFNγ expression is induced both in melanoma cells

and melanocytes. However, in our zebrafish melanoma model, compared to normal melanocytes, *mitfa* expression is up-regulated in melanoma cells (Hurlstone lab, unpublished data). Since our IFNγ induction is controlled by the mitfa promoter, melanoma cells and melanocytes express IFNγ at varied levels. This potentially leads to a scenario where melanoma cells, by secreting 'high-levels' of IFNγ in the microenvironment, are inducing anti-tumour immune responses (Figure 5.7 D). On the other hand, sustained 'low-level' expression of IFNγ by the melanocytes could be driving new amelanotic resistant tumours (Figure 5.8).

In parallel, we have also observed that forced secretion of the ectopic domain of zebrafish PDL1 homologue suppresses tumour formation but again late escapee tumours were unpigmented. Intrigued by the possibility of these tumours being escape immune resistant tumours, we decided to perform RNA sequencing of the amelanotic tumours induced by IFNγ or PDL1T forced expression along with control pigmented tumours. We have extracted total RNA from 24 individual tumour samples (IFNγ: 7, PDL1T: 9, control: 8), however only 4 samples from each group were sent for sequencing. RNA sequencing was performed at Epicore, in collaboration with Dr. Yariv Houvras, Cornell University, New York. Since data analysis is still on-going, we will not be discussing our RNA sequencing results in this thesis.

6 Summary Discussion

The concept that the immune system can identify and eliminate establishing tumours has been around for more than 100 years, but due to lack of appropriate in-vivo model systems, the hypothesis remained largely un-tested for decades. Conducting experiments on patients being difficult and at times impractical, mouse model systems drove the field of cancer immunotherapy, with most of the immune-biology concepts evolving from this model. Led by the pioneering work of Prof. Robert schreiber and colleagues, it was only in the last 20 years the concepts of immunosurveillance and immunoediting have been firmly established with the help of sophisticated mouse models. While mammalian model systems undoubtedly advanced the field of cancer immunotherapy, they also have limitations when it comes to high throughput screening of immunotherapy strategies and longitudinal studies using non-invasive imaging along with high cost of maintenance per animal. Zebrafish has the potential to be the alternative model system that can help the field overcome the above mentioned shortcomings while nicely complementing the mammalian model systems. In recent years, zebrafish models of human cancer, including melanoma, have proven to be highly informative in understanding molecular regulation of cancers (Michailidou *et al.* 2009, Jones et al. 2009, Ceol, Houvras et al. 2011). However, very little is known about the immunological phenotype of a zebrafish tumour. In this thesis, our work has focused on establishing zebrafish as a viable model system to study $CD4^+$ T cell mediated immune responses against melanoma as well as an in-vivo model system compatible for testing multiple immunotherapy strategies.

Scarcity of highly specific monoclonal antibodies against many zebrafish proteins has always plagued the development of zebrafish model system. Its effect was more prominent on studies involving zebrafish immune system. At the start of this project, contrary to the situation in humans and mouse model, where a collection of high end, ultra-specific antibodies facilitate identification of even niche immune populations, zebrafish model even lacked antibodies to isolate $CD4^+$ T cells. So, to facilitate visualisation and isolation of zebrafish $CD4^+$ cells, we generated a zebrafish CD4-1 reporter line (*Tg[cd4-1:mCherry])* using BAC transgenesis. This resource enabled us to specifically isolate and characterise various CD4-1^+ immune populations in zebrafish.

It has so far remained unclear whether T_H subsets equivalent to the T_H1, T_H2 and T_{reg} cells of mammals are present in zebrafish. Exploiting the *Tg[cd4-1:mCherry]* transgenic reporter zebrafish we begun to image and characterise the development of CD4-1^+ leukocytes and gathered *in-vivo* evidence for the differentiation and sub-specialisation of CD4-1^+ T cells. We report that gill resident CD4-1^+ T cells are strongly enhanced for *gata3* and *il-4/13b* expression, indicating the presence of a novel population of teleost T_H2-like cells. In contrast, the CD4-1^+ T cells of the gut are enriched for *foxp3a* and *il-10*, suggesting they are skewed towards T_{reg}-like phenotype. We also described specific populations of CD4-1^+ MNPs, thymic, peri-thymic and skin resident, suggesting that this cell type had already emerged in early vertebrates.

One of the primary aims of this PhD project was to establish whether zebrafish $CD4^+$ T cells react to melanoma development. In this report we presented data from three different experiments exploring this objective. Firstly, we show that zebrafish $CD4^+$ TILs expressed significantly higher levels of *gata3* and *il-4/13a,* indicating that, similar to mouse tumours, progressing zebrafish melanomas predominantly have T_H2 differentiated $CD4^+$ TILs. Secondly, in line with reported data from melanoma patients, zebrafish melanomas elicit heterogeneous responses by CD4-1^+ cells. Through live imaging, we observed regions of 'Brisk' and 'non-Brisk' infiltration of CD4-1^+ immune cells in zebrafish melanoma. In concurrence with prognostic prediction in patients, we showed that regions with 'Brisk' CD4-1^+ TILs are associated with seemingly regressing tumour, while no signs of regression were observed in the regions with 'non-Brisk' infiltration of CD4-1^+ TILs. Finally, our longitudinal studies revealed a more dynamic tumour micro-environment where the CD4-1^+ immune cells moved in and out of regressing melanoma tumours, which we hypothesise as a potential hallmark of an effective immunosurveillance against melanoma. Taken together, our data has for the first time demonstrated that immunoediting of melanoma occurs in an autochthonous zebrafish model, thus making it a reliable *in-vivo* system to explore new immunotherapy strategies.

The final aim of this project was to develop a zebrafish based *in-vivo* model system that can be used to test the efficacy of multiple immune-regulatory (IR) molecules to modulate the tumour micro-environment and enhance anti-tumour immune responses. We have built and optimised a Tamoxifen inducible $CreER^{T2}$

system, which can be used to specifically induce the expression of selected IR molecules such as cytokines and chemokines by the zebrafish melanocytes. Using this system we have induced the expression of IFNγ in the tumour microenvironment to potentially drive T_H1 helper T cell differentiation and induce an inflammatory immune response against a developing melanoma lesion. We report that forced expression of IFNγ in the tumour microenvironment has resulted in enhanced tumour regressing in our autochthonous zebrafish melanoma model.

In the field of cancer immunotherapy, IFNγ has currently taken the centre stage with regards to acquired adaptive resistance to anti-PD1/PDL1 therapy. In patients who respond to anti-PD1/PDL1 therapy, enhanced expression of IFNγ plays a critical role in effective tumour suppression (She et al. 2016). IFNγ secreted in to the tumour micro-environment apart from activating the T_H1 helper T cell differentiation, has also been reported to increase the expression of class II MHC complex on tumour cells (Ikeda et al. 2002). This subsequently enhances the presentation of tumour antigens to the host immune system thereby further enhancing the immune system mediated tumour suppression. However, according the current clinical data, in some of the patients who have responded to the anti-PDL1 therapy, relapsing tumours are now resistant to anti-PDL1 therapy (Zaretsky et al. 2016). It is reported that some of these relapsing tumours have loss of function mutations in *Jak2* thereby losing the ability to respond to the IFNγ signalling, apparently a potential mechanism of adaptive resistance to IFNγ induced tumour suppression (Zaretsky et al. 2016). Contrary to these findings, another latest publication has demonstrated that IFNγ induced transcriptional changes drive the

adaptive resistance to anti-PD/PDL1 therapy in melanoma cell lines (Joseph et al. 2016). They have reported that the chronic exposure of melanoma cells to IFNγ can enable STAT1 mediated epigenomic and transcriptomic changes that promote PDL1-independent adaptive resistance to immune suppression (Joseph et al. 2016). In line with this study, in our autochthonous zebrafish melanoma model, we report that while established tumours are eliminated in the presence of IFNγ, prolonged expression of IFNγ in the microenvironment has led to the development of amelanotic resistant tumours. We believe that the mRNA sequencing of the resistant tumours (IFNγ or PDL1 expressing) could reveal unique but also shared signatures of acquired adaptive resistance in response to prolonged exposure to IFNγ, which can be exploited to ultimately predict responses to immunotherapy in patients.

References

Bernabei, P., Coccia, E.M., Rigamonti, L., Bosticardo, M., Forni, G., Pestka, S., Krause, C.D., Battistini, A. & Novelli, F. 2001. Interferon-gamma receptor 2 expression as the deciding factor in human T, B, and myeloid cell proliferation or death. *J Leukoc Biol,* 70(6):950-960.

Boissonnas, A., Fetler, L., Zeelenberg, I.S., Hugues, S. & Amigorena, S. 2007. In vivo imaging of cytotoxic T cell infiltration and elimination of a solid tumor. *J Exp Med,* 204(2):345-356.

Breart, B., Lemaître, F., Celli, S. & Bousso, P. 2008. Two-photon imaging of intratumoral CD8+ T cell cytotoxic activity during adoptive T cell therapy in mice. *J Clin Invest,* 118(4):1390-1397.

Busam, K.J., Antonescu, C.R., Marghoob, A.A., Nehal, K.S., Sachs, D.L., Shia, J. & Berwick, M. 2001. Histologic classification of tumor-infiltrating lymphocytes in primary cutaneous malignant melanoma. A study of interobserver agreement. *Am J Clin Pathol,* 115(6):856-860.

Ceol, C.J., Houvras, Y., Jane-Valbuena, J., Bilodeau, S., Orlando, D.A., Battisti, V., Fritsch, L., Lin, W.M., Hollmann, T.J., Ferré, F., Bourque, C., Burke, C.J., Turner, L., Uong, A., Johnson, L.A., Beroukhim, R., Mermel, C.H., Loda, M., Ait-Si-Ali, S., Garraway, L.A., Young, R.A. & Zon, L.I. 2011. The histone methyltransferase SETDB1 is recurrently amplified in melanoma and accelerates its onset. *Nature,* 471(7339):513-517.

Chiang, E.Y., Hidalgo, A., Chang, J. & Frenette, P.S. 2007. Imaging receptor microdomains on leukocyte subsets in live mice. *Nat Methods,* 4(3):219-222.

Clark, W.H. 1991. Tumour progression and the nature of cancer. *Br J Cancer,* 64(4):631-644.

Danial, N.N. & Korsmeyer, S.J. 2004. Cell death: critical control points. *Cell,* 116(2):205-219.

del Campo, A.B., Kyte, J.A., Carretero, J., Zinchencko, S., Méndez, R., González-Aseguinolaza, G., Ruiz-Cabello, F., Aamdal, S., Gaudernack, G., Garrido, F. & Aptsiauri, N. 2014. Immune escape of cancer cells with beta2-microglobulin loss over the course of metastatic melanoma. *Int J Cancer,* 134(1):102-113.

deLeeuw, R.J., Kost, S.E., Kakal, J.A. & Nelson, B.H. 2012. The prognostic value of FoxP3+ tumor-infiltrating lymphocytes in cancer: a critical review of the literature. *Clin Cancer Res,* 18(11):3022-3029.

DeNardo, D.G., Barreto, J.B., Andreu, P., Vasquez, L., Tawfik, D., Kolhatkar, N. &

Coussens, L.M. 2009. CD4(+) T cells regulate pulmonary metastasis of mammary carcinomas by enhancing protumor properties of macrophages. *Cancer Cell,* 16(2):91-102.

Diefenbach, A., Jensen, E.R., Jamieson, A.M. & Raulet, D.H. 2001. Rae1 and H60 ligands of the NKG2D receptor stimulate tumour immunity. *Nature,* 413(6852):165-171.

Dunn, G.P., Old, L.J. & Schreiber, R.D. 2004. The three Es of cancer immunoediting. *Annu Rev Immunol,* 22:329-360.

Ellenbroek, S.I. & van Rheenen, J. 2014. Imaging hallmarks of cancer in living mice. *Nat Rev Cancer,* 14(6):406-418.

Erdman, S.E., Sohn, J.J., Rao, V.P., Nambiar, P.R., Ge, Z., Fox, J.G. & Schauer, D.B. 2005. CD4+CD25+ regulatory lymphocytes induce regression of intestinal tumors in ApcMin/+ mice. *Cancer Res,* 65(10):3998-4004.

Feil, R., Brocard, J., Mascrez, B., LeMeur, M., Metzger, D. & Chambon, P. 1996. Ligand-activated site-specific recombination in mice. *Proc Natl Acad Sci U S A,* 93(20):10887-10890.

Feng, H., Langenau, D.M., Madge, J.A., Quinkertz, A., Gutierrez, A., Neuberg, D.S., Kanki, J.P. & Look, A.T. 2007. Heat-shock induction of T-cell lymphoma/leukaemia in conditional Cre/lox-regulated transgenic zebrafish. *Br J Haematol,* 138(2):169-175.

Gajewski, T.F., Schreiber, H. & Fu, Y.X. 2013. Innate and adaptive immune cells in the tumor microenvironment. *Nat Immunol,* 14(10):1014-1022.

Gallimore, A.M. & Simon, A.K. 2008. Positive and negative influences of regulatory T cells on tumour immunity. *Oncogene,* 27(45):5886-5893.

Girardi, M., Oppenheim, D.E., Steele, C.R., Lewis, J.M., Glusac, E., Filler, R., Hobby, P., Sutton, B., Tigelaar, R.E. & Hayday, A.C. 2001. Regulation of cutaneous malignancy by gammadelta T cells. *Science,* 294(5542):605-609.

Haabeth, O.A., Lorvik, K.B., Hammarström, C., Donaldson, I.M., Haraldsen, G., Bogen, B. & Corthay, A. 2011. Inflammation driven by tumour-specific Th1 cells protects against B-cell cancer. *Nat Commun,* 2:240.

Hadrup, S., Donia, M. & Thor Straten, P. 2013. Effector CD4 and CD8 T cells and their role in the tumor microenvironment. *Cancer Microenviron,* 6(2):123-133.

Hans, S., Kaslin, J., Freudenreich, D. & Brand, M. 2009. Temporally-controlled site-specific recombination in zebrafish. *PLoS One,* 4(2):e4640.

Humbert, P., Russell, S. & Richardson, H. 2003. Dlg, Scribble and Lgl in cell polarity, cell

proliferation and cancer. *Bioessays,* 25(6):542-553.

Janes, S.M. & Watt, F.M. 2006. New roles for integrins in squamous-cell carcinoma. *Nat Rev Cancer,* 6(3):175-183.

Jao, L.E., Wente, S.R. & Chen, W. 2013. Efficient multiplex biallelic zebrafish genome editing using a CRISPR nuclease system. *Proc Natl Acad Sci U S A,* 110(34):13904-13909.

Kawakami, K. 2007. Tol2: a versatile gene transfer vector in vertebrates. *Genome Biol,* 8 Suppl 1:S7.

Khong, H.T., Wang, Q.J. & Rosenberg, S.A. 2004. Identification of multiple antigens recognized by tumor-infiltrating lymphocytes from a single patient: tumor escape by antigen loss and loss of MHC expression. *J Immunother,* 27(3):184-190.

Kohrt, H.E., Nouri, N., Nowels, K., Johnson, D., Holmes, S. & Lee, P.P. 2005. Profile of immune cells in axillary lymph nodes predicts disease-free survival in breast cancer. *PLoS Med,* 2(9):e284.

Lamason, R.L., Mohideen, M.A., Mest, J.R., Wong, A.C., Norton, H.L., Aros, M.C., Jurynec, M.J., Mao, X., Humphreville, V.R., Humbert, J.E., Sinha, S., Moore, J.L., Jagadeeswaran, P., Zhao, W., Ning, G., Makalowska, I., McKeigue, P.M., O'donnell, D., Kittles, R., Parra, E.J., Mangini, N.J., Grunwald, D.J., Shriver, M.D., Canfield, V.A. & Cheng, K.C. 2005. SLC24A5, a putative cation exchanger, affects pigmentation in zebrafish and humans. *Science,* 310(5755):1782-1786.

Le, X., Langenau, D.M., Keefe, M.D., Kutok, J.L., Neuberg, D.S. & Zon, L.I. 2007. Heat shock-inducible Cre/Lox approaches to induce diverse types of tumors and hyperplasia in transgenic zebrafish. *Proc Natl Acad Sci U S A,* 104(22):9410-9415.

Lin, D.Y., Tanaka, Y., Iwasaki, M., Gittis, A.G., Su, H.P., Mikami, B., Okazaki, T., Honjo, T., Minato, N. & Garboczi, D.N. 2008. The PD-1/PD-L1 complex resembles the antigen-binding Fv domains of antibodies and T cell receptors. *Proc Natl Acad Sci U S A,* 105(8):3011-3016.

Lollini, P.L., Bosco, M.C., Cavallo, F., De Giovanni, C., Giovarelli, M., Landuzzi, L., Musiani, P., Modesti, A., Nicoletti, G. & Palmieri, G. 1993. Inhibition of tumor growth and enhancement of metastasis after transfection of the gamma-interferon gene. *Int J Cancer,* 55(2):320-329.

Marodon, G., Mouly, E., Blair, E.J., Frisen, C., Lemoine, F.M. & Klatzmann, D. 2003. Specific transgene expression in human and mouse CD4+ cells using lentiviral vectors with regulatory sequences from the CD4 gene. *Blood,* 101(9):3416-3423.

Matsushita, H., Vesely, M.D., Koboldt, D.C., Rickert, C.G., Uppaluri, R., Magrini, V.J., Arthur, C.D., White, J.M., Chen, Y.S., Shea, L.K., Hundal, J., Wendl, M.C., Demeter, R.,

Wylie, T., Allison, J.P., Smyth, M.J., Old, L.J., Mardis, E.R. & Schreiber, R.D. 2012. Cancer exome analysis reveals a T-cell-dependent mechanism of cancer immunoediting. *Nature,* 482(7385):400-404.

Matzinger, P. 1994. Tolerance, danger, and the extended family. *Annu Rev Immunol,* 12:991-1045.

McCarter, M., Clarke, J., Richter, D. & Wilson, C. 2005. Melanoma skews dendritic cells to facilitate a T helper 2 profile. *Surgery,* 138(2):321-328.

Michailidou, C., Jones, M., Walker, P., Kamarashev, J., Kelly, A. & Hurlstone, A.F. 2009. Dissecting the roles of Raf- and PI3K-signalling pathways in melanoma formation and progression in a zebrafish model. *Dis Model Mech,* 2(7-8):399-411.

Mosimann, C., Kaufman, C.K., Li, P., Pugach, E.K., Tamplin, O.J. & Zon, L.I. 2011. Ubiquitous transgene expression and Cre-based recombination driven by the ubiquitin promoter in zebrafish. *Development,* 138(1):169-177.

Nakano, I., Fukuda, Y., Katano, Y., Toyoda, H., Hayashi, K., Hayakawa, T., Kumada, T. & Nakano, S. 2001. Interferon responsiveness in patients infected with hepatitis C virus 1b differs depending on viral subtype. *Gut,* 49(2):263-267.

Natarajan, V.T., Ganju, P., Singh, A., Vijayan, V., Kirty, K., Yadav, S., Puntambekar, S., Bajaj, S., Dani, P.P., Kar, H.K., Gadgil, C.J., Natarajan, K., Rani, R. & Gokhale, R.S. 2014. IFN-γ signaling maintains skin pigmentation homeostasis through regulation of melanosome maturation. *Proc Natl Acad Sci U S A,* 111(6):2301-2306.

Pardoll, D.M. 2012. The blockade of immune checkpoints in cancer immunotherapy. *Nat Rev Cancer,* 12(4):252-264.

Perentes, J.Y., Duda, D.G. & Jain, R.K. 2009. Visualizing anti-tumor immune responses in vivo. *Dis Model Mech,* 2(3-4):107-110.

Peter, M.E. & Krammer, P.H. 2003. The CD95(APO-1/Fas) DISC and beyond. *Cell Death Differ,* 10(1):26-35.

Restifo, N.P., Marincola, F.M., Kawakami, Y., Taubenberger, J., Yannelli, J.R. & Rosenberg, S.A. 1996. Loss of functional beta 2-microglobulin in metastatic melanomas from five patients receiving immunotherapy. *J Natl Cancer Inst,* 88(2):100-108.

Sato, E., Olson, S.H., Ahn, J., Bundy, B., Nishikawa, H., Qian, F., Jungbluth, A.A., Frosina, D., Gnjatic, S., Ambrosone, C., Kepner, J., Odunsi, T., Ritter, G., Lele, S., Chen, Y.T., Ohtani, H., Old, L.J. & Odunsi, K. 2005. Intraepithelial CD8+ tumor-infiltrating lymphocytes and a high CD8+/regulatory T cell ratio are associated with favorable prognosis in ovarian cancer. *Proc Natl Acad Sci U S A,* 102(51):18538-18543.

Serrano, M., Lin, A.W., McCurrach, M.E., Beach, D. & Lowe, S.W. 1997. Oncogenic ras provokes premature cell senescence associated with accumulation of p53 and p16INK4a. *Cell,* 88(5):593-602.

Shang, B., Liu, Y. & Jiang, S.J. 2015. Prognostic value of tumor-infiltrating FoxP3+ regulatory T cells in cancers: a systematic review and meta-analysis. *Sci Rep,* 5:15179.

Smyth, M.J., Crowe, N.Y. & Godfrey, D.I. 2001. NK cells and NKT cells collaborate in host protection from methylcholanthrene-induced fibrosarcoma. *Int Immunol,* 13(4):459-463.

Son, J., Kim, M., Jou, I., Park, K.C. & Kang, H.Y. 2014. IFN-γ inhibits basal and α-MSH-induced melanogenesis. *Pigment Cell Melanoma Res,* 27(2):201-208.

Spranger, S., Spaapen, R.M., Zha, Y., Williams, J., Meng, Y., Ha, T.T. & Gajewski, T.F. 2013. Up-regulation of PD-L1, IDO, and T(regs) in the melanoma tumor microenvironment is driven by CD8(+) T cells. *Sci Transl Med,* 5(200):200ra116.

Suster, M.L., Kikuta, H., Urasaki, A., Asakawa, K. & Kawakami, K. 2009. Transgenesis in zebrafish with the tol2 transposon system. *Methods Mol Biol,* 561:41-63.

Thummel, R., Burket, C.T., Brewer, J.L., Sarras, M.P., Li, L., Perry, M., McDermott, J.P., Sauer, B., Hyde, D.R. & Godwin, A.R. 2005. Cre-mediated site-specific recombination in zebrafish embryos. *Dev Dyn,* 233(4):1366-1377.

Urasaki, A., Morvan, G. & Kawakami, K. 2006. Functional dissection of the Tol2 transposable element identified the minimal cis-sequence and a highly repetitive sequence in the subterminal region essential for transposition. *Genetics,* 174(2):639-649.

Vanaudenaerde, B.M., Verleden, S.E., Vos, R., De Vleeschauwer, S.I., Willems-Widyastuti, A., Geenens, R., Van Raemdonck, D.E., Dupont, L.J., Verbeken, E.K. & Meyts, I. 2011. Innate and adaptive interleukin-17-producing lymphocytes in chronic inflammatory lung disorders. *Am J Respir Crit Care Med,* 183(8):977-986.

Whiteside, T.L. 2012. What are regulatory T cells (Treg) regulating in cancer and why? *Semin Cancer Biol,* 22(4):327-334.

Whiteside, T.L. 2014. Regulatory T cell subsets in human cancer: are they regulating for or against tumor progression? *Cancer Immunol Immunother,* 63(1):67-72.

Xue, W., Zender, L., Miething, C., Dickins, R.A., Hernando, E., Krizhanovsky, V., Cordon-Cardo, C. & Lowe, S.W. 2007. Senescence and tumour clearance is triggered by p53 restoration in murine liver carcinomas. *Nature,* 445(7128):656-660.

Yoshikawa, S., Kawakami, K. & Zhao, X.C. 2008. G2R Cre reporter transgenic zebrafish.

Dev Dyn, 237(9):2460-2465.

Zaidi, M.R., Davis, S., Noonan, F.P., Graff-Cherry, C., Hawley, T.S., Walker, R.L., Feigenbaum, L., Fuchs, E., Lyakh, L., Young, H.A., Hornyak, T.J., Arnheiter, H., Trinchieri, G., Meltzer, P.S., De Fabo, E.C. & Merlino, G. 2011. Interferon-γ links ultraviolet radiation to melanomagenesis in mice. *Nature,* 469(7331):548-553.

Zitvogel, L., Tesniere, A. & Kroemer, G. 2006. Cancer despite immunosurveillance: immunoselection and immunosubversion. *Nat Rev Immunol,* 6(10):715-727.

Bernabei, P., Coccia, E.M., Rigamonti, L., Bosticardo, M., Forni, G., Pestka, S., Krause, C.D., Battistini, A. & Novelli, F. 2001. Interferon-gamma receptor 2 expression as the deciding factor in human T, B, and myeloid cell proliferation or death. *J Leukoc Biol,* 70(6):950-960.

Boissonnas, A., Fetler, L., Zeelenberg, I.S., Hugues, S. & Amigorena, S. 2007. In vivo imaging of cytotoxic T cell infiltration and elimination of a solid tumor. *J Exp Med,* 204(2):345-356.

Breart, B., Lemaître, F., Celli, S. & Bousso, P. 2008. Two-photon imaging of intratumoral CD8+ T cell cytotoxic activity during adoptive T cell therapy in mice. *J Clin Invest,* 118(4):1390-1397.

Busam, K.J., Antonescu, C.R., Marghoob, A.A., Nehal, K.S., Sachs, D.L., Shia, J. & Berwick, M. 2001. Histologic classification of tumor-infiltrating lymphocytes in primary cutaneous malignant melanoma. A study of interobserver agreement. *Am J Clin Pathol,* 115(6):856-860.

Ceol, C.J., Houvras, Y., Jane-Valbuena, J., Bilodeau, S., Orlando, D.A., Battisti, V., Fritsch, L., Lin, W.M., Hollmann, T.J., Ferré, F., Bourque, C., Burke, C.J., Turner, L., Uong, A., Johnson, L.A., Beroukhim, R., Mermel, C.H., Loda, M., Ait-Si-Ali, S., Garraway, L.A., Young, R.A. & Zon, L.I. 2011. The histone methyltransferase SETDB1 is recurrently amplified in melanoma and accelerates its onset. *Nature,* 471(7339):513-517.

Chiang, E.Y., Hidalgo, A., Chang, J. & Frenette, P.S. 2007. Imaging receptor microdomains on leukocyte subsets in live mice. *Nat Methods,* 4(3):219-222.

Clark, W.H. 1991. Tumour progression and the nature of cancer. *Br J Cancer,* 64(4):631-644.

Danial, N.N. & Korsmeyer, S.J. 2004. Cell death: critical control points. *Cell,* 116(2):205-219.

del Campo, A.B., Kyte, J.A., Carretero, J., Zinchencko, S., Méndez, R., González-Aseguinolaza, G., Ruiz-Cabello, F., Aamdal, S., Gaudernack, G., Garrido, F. & Aptsiauri, N. 2014. Immune escape of cancer cells with beta2-microglobulin loss over the course

of metastatic melanoma. *Int J Cancer,* 134(1):102-113.

deLeeuw, R.J., Kost, S.E., Kakal, J.A. & Nelson, B.H. 2012. The prognostic value of FoxP3+ tumor-infiltrating lymphocytes in cancer: a critical review of the literature. *Clin Cancer Res,* 18(11):3022-3029.

DeNardo, D.G., Barreto, J.B., Andreu, P., Vasquez, L., Tawfik, D., Kolhatkar, N. & Coussens, L.M. 2009. CD4(+) T cells regulate pulmonary metastasis of mammary carcinomas by enhancing protumor properties of macrophages. *Cancer Cell,* 16(2):91-102.

Diefenbach, A., Jensen, E.R., Jamieson, A.M. & Raulet, D.H. 2001. Rae1 and H60 ligands of the NKG2D receptor stimulate tumour immunity. *Nature,* 413(6852):165-171.

Dunn, G.P., Old, L.J. & Schreiber, R.D. 2004. The three Es of cancer immunoediting. *Annu Rev Immunol,* 22:329-360.

Ellenbroek, S.I. & van Rheenen, J. 2014. Imaging hallmarks of cancer in living mice. *Nat Rev Cancer,* 14(6):406-418.

Erdman, S.E., Sohn, J.J., Rao, V.P., Nambiar, P.R., Ge, Z., Fox, J.G. & Schauer, D.B. 2005. CD4+CD25+ regulatory lymphocytes induce regression of intestinal tumors in ApcMin/+ mice. *Cancer Res,* 65(10):3998-4004.

Feil, R., Brocard, J., Mascrez, B., LeMeur, M., Metzger, D. & Chambon, P. 1996. Ligand-activated site-specific recombination in mice. *Proc Natl Acad Sci U S A,* 93(20):10887-10890.

Feng, H., Langenau, D.M., Madge, J.A., Quinkertz, A., Gutierrez, A., Neuberg, D.S., Kanki, J.P. & Look, A.T. 2007. Heat-shock induction of T-cell lymphoma/leukaemia in conditional Cre/lox-regulated transgenic zebrafish. *Br J Haematol,* 138(2):169-175.

Gajewski, T.F., Schreiber, H. & Fu, Y.X. 2013. Innate and adaptive immune cells in the tumor microenvironment. *Nat Immunol,* 14(10):1014-1022.

Gallimore, A.M. & Simon, A.K. 2008. Positive and negative influences of regulatory T cells on tumour immunity. *Oncogene,* 27(45):5886-5893.

Girardi, M., Oppenheim, D.E., Steele, C.R., Lewis, J.M., Glusac, E., Filler, R., Hobby, P., Sutton, B., Tigelaar, R.E. & Hayday, A.C. 2001. Regulation of cutaneous malignancy by gammadelta T cells. *Science,* 294(5542):605-609.

Haabeth, O.A., Lorvik, K.B., Hammarström, C., Donaldson, I.M., Haraldsen, G., Bogen, B. & Corthay, A. 2011. Inflammation driven by tumour-specific Th1 cells protects against B-cell cancer. *Nat Commun,* 2:240.

Hadrup, S., Donia, M. & Thor Straten, P. 2013. Effector CD4 and CD8 T cells and their role in the tumor microenvironment. *Cancer Microenviron,* 6(2):123-133.

Hans, S., Kaslin, J., Freudenreich, D. & Brand, M. 2009. Temporally-controlled site-specific recombination in zebrafish. *PLoS One,* 4(2):e4640.

Humbert, P., Russell, S. & Richardson, H. 2003. Dlg, Scribble and Lgl in cell polarity, cell proliferation and cancer. *Bioessays,* 25(6):542-553.

Janes, S.M. & Watt, F.M. 2006. New roles for integrins in squamous-cell carcinoma. *Nat Rev Cancer,* 6(3):175-183.

Jao, L.E., Wente, S.R. & Chen, W. 2013. Efficient multiplex biallelic zebrafish genome editing using a CRISPR nuclease system. *Proc Natl Acad Sci U S A,* 110(34):13904-13909.

Kawakami, K. 2007. Tol2: a versatile gene transfer vector in vertebrates. *Genome Biol,* 8 Suppl 1:S7.

Khong, H.T., Wang, Q.J. & Rosenberg, S.A. 2004. Identification of multiple antigens recognized by tumor-infiltrating lymphocytes from a single patient: tumor escape by antigen loss and loss of MHC expression. *J Immunother,* 27(3):184-190.

Kohrt, H.E., Nouri, N., Nowels, K., Johnson, D., Holmes, S. & Lee, P.P. 2005. Profile of immune cells in axillary lymph nodes predicts disease-free survival in breast cancer. *PLoS Med,* 2(9):e284.

Lamason, R.L., Mohideen, M.A., Mest, J.R., Wong, A.C., Norton, H.L., Aros, M.C., Jurynec, M.J., Mao, X., Humphreville, V.R., Humbert, J.E., Sinha, S., Moore, J.L., Jagadeeswaran, P., Zhao, W., Ning, G., Makalowska, I., McKeigue, P.M., O'donnell, D., Kittles, R., Parra, E.J., Mangini, N.J., Grunwald, D.J., Shriver, M.D., Canfield, V.A. & Cheng, K.C. 2005. SLC24A5, a putative cation exchanger, affects pigmentation in zebrafish and humans. *Science,* 310(5755):1782-1786.

Le, X., Langenau, D.M., Keefe, M.D., Kutok, J.L., Neuberg, D.S. & Zon, L.I. 2007. Heat shock-inducible Cre/Lox approaches to induce diverse types of tumors and hyperplasia in transgenic zebrafish. *Proc Natl Acad Sci U S A,* 104(22):9410-9415.

Lin, D.Y., Tanaka, Y., Iwasaki, M., Gittis, A.G., Su, H.P., Mikami, B., Okazaki, T., Honjo, T., Minato, N. & Garboczi, D.N. 2008. The PD-1/PD-L1 complex resembles the antigen-binding Fv domains of antibodies and T cell receptors. *Proc Natl Acad Sci U S A,* 105(8):3011-3016.

Lollini, P.L., Bosco, M.C., Cavallo, F., De Giovanni, C., Giovarelli, M., Landuzzi, L., Musiani, P., Modesti, A., Nicoletti, G. & Palmieri, G. 1993. Inhibition of tumor growth and enhancement of metastasis after transfection of the gamma-interferon gene. *Int J Cancer,* 55(2):320-329.

Marodon, G., Mouly, E., Blair, E.J., Frisen, C., Lemoine, F.M. & Klatzmann, D. 2003. Specific transgene expression in human and mouse CD4+ cells using lentiviral vectors with regulatory sequences from the CD4 gene. *Blood,* 101(9):3416-3423.

Matsushita, H., Vesely, M.D., Koboldt, D.C., Rickert, C.G., Uppaluri, R., Magrini, V.J., Arthur, C.D., White, J.M., Chen, Y.S., Shea, L.K., Hundal, J., Wendl, M.C., Demeter, R., Wylie, T., Allison, J.P., Smyth, M.J., Old, L.J., Mardis, E.R. & Schreiber, R.D. 2012. Cancer exome analysis reveals a T-cell-dependent mechanism of cancer immunoediting. *Nature,* 482(7385):400-404.

Matzinger, P. 1994. Tolerance, danger, and the extended family. *Annu Rev Immunol,* 12:991-1045.

McCarter, M., Clarke, J., Richter, D. & Wilson, C. 2005. Melanoma skews dendritic cells to facilitate a T helper 2 profile. *Surgery,* 138(2):321-328.

Michailidou, C., Jones, M., Walker, P., Kamarashev, J., Kelly, A. & Hurlstone, A.F. 2009. Dissecting the roles of Raf- and PI3K-signalling pathways in melanoma formation and progression in a zebrafish model. *Dis Model Mech,* 2(7-8):399-411.

Mosimann, C., Kaufman, C.K., Li, P., Pugach, E.K., Tamplin, O.J. & Zon, L.I. 2011. Ubiquitous transgene expression and Cre-based recombination driven by the ubiquitin promoter in zebrafish. *Development,* 138(1):169-177.

Nakano, I., Fukuda, Y., Katano, Y., Toyoda, H., Hayashi, K., Hayakawa, T., Kumada, T. & Nakano, S. 2001. Interferon responsiveness in patients infected with hepatitis C virus 1b differs depending on viral subtype. *Gut,* 49(2):263-267.

Natarajan, V.T., Ganju, P., Singh, A., Vijayan, V., Kirty, K., Yadav, S., Puntambekar, S., Bajaj, S., Dani, P.P., Kar, H.K., Gadgil, C.J., Natarajan, K., Rani, R. & Gokhale, R.S. 2014. IFN-γ signaling maintains skin pigmentation homeostasis through regulation of melanosome maturation. *Proc Natl Acad Sci U S A,* 111(6):2301-2306.

Pardoll, D.M. 2012. The blockade of immune checkpoints in cancer immunotherapy. *Nat Rev Cancer,* 12(4):252-264.

Perentes, J.Y., Duda, D.G. & Jain, R.K. 2009. Visualizing anti-tumor immune responses in vivo. *Dis Model Mech,* 2(3-4):107-110.

Peter, M.E. & Krammer, P.H. 2003. The CD95(APO-1/Fas) DISC and beyond. *Cell Death Differ,* 10(1):26-35.

Restifo, N.P., Marincola, F.M., Kawakami, Y., Taubenberger, J., Yannelli, J.R. & Rosenberg, S.A. 1996. Loss of functional beta 2-microglobulin in metastatic melanomas from five patients receiving immunotherapy. *J Natl Cancer Inst,* 88(2):100-108.

Sato, E., Olson, S.H., Ahn, J., Bundy, B., Nishikawa, H., Qian, F., Jungbluth, A.A., Frosina, D., Gnjatic, S., Ambrosone, C., Kepner, J., Odunsi, T., Ritter, G., Lele, S., Chen, Y.T., Ohtani, H., Old, L.J. & Odunsi, K. 2005. Intraepithelial CD8+ tumor-infiltrating lymphocytes and a high CD8+/regulatory T cell ratio are associated with favorable prognosis in ovarian cancer. *Proc Natl Acad Sci U S A,* 102(51):18538-18543.

Serrano, M., Lin, A.W., McCurrach, M.E., Beach, D. & Lowe, S.W. 1997. Oncogenic ras provokes premature cell senescence associated with accumulation of p53 and p16INK4a. *Cell,* 88(5):593-602.

Shang, B., Liu, Y. & Jiang, S.J. 2015. Prognostic value of tumor-infiltrating FoxP3+ regulatory T cells in cancers: a systematic review and meta-analysis. *Sci Rep,* 5:15179.

Smyth, M.J., Crowe, N.Y. & Godfrey, D.I. 2001. NK cells and NKT cells collaborate in host protection from methylcholanthrene-induced fibrosarcoma. *Int Immunol,* 13(4):459-463.

Son, J., Kim, M., Jou, I., Park, K.C. & Kang, H.Y. 2014. IFN-γ inhibits basal and α-MSH-induced melanogenesis. *Pigment Cell Melanoma Res,* 27(2):201-208.

Spranger, S., Spaapen, R.M., Zha, Y., Williams, J., Meng, Y., Ha, T.T. & Gajewski, T.F. 2013. Up-regulation of PD-L1, IDO, and T(regs) in the melanoma tumor microenvironment is driven by CD8(+) T cells. *Sci Transl Med,* 5(200):200ra116.

Suster, M.L., Kikuta, H., Urasaki, A., Asakawa, K. & Kawakami, K. 2009. Transgenesis in zebrafish with the tol2 transposon system. *Methods Mol Biol,* 561:41-63.

Thummel, R., Burket, C.T., Brewer, J.L., Sarras, M.P., Li, L., Perry, M., McDermott, J.P., Sauer, B., Hyde, D.R. & Godwin, A.R. 2005. Cre-mediated site-specific recombination in zebrafish embryos. *Dev Dyn,* 233(4):1366-1377.

Urasaki, A., Morvan, G. & Kawakami, K. 2006. Functional dissection of the Tol2 transposable element identified the minimal cis-sequence and a highly repetitive sequence in the subterminal region essential for transposition. *Genetics,* 174(2):639-649.

Vanaudenaerde, B.M., Verleden, S.E., Vos, R., De Vleeschauwer, S.I., Willems-Widyastuti, A., Geenens, R., Van Raemdonck, D.E., Dupont, L.J., Verbeken, E.K. & Meyts, I. 2011. Innate and adaptive interleukin-17-producing lymphocytes in chronic inflammatory lung disorders. *Am J Respir Crit Care Med,* 183(8):977-986.

Whiteside, T.L. 2012. What are regulatory T cells (Treg) regulating in cancer and why? *Semin Cancer Biol,* 22(4):327-334.

Whiteside, T.L. 2014. Regulatory T cell subsets in human cancer: are they regulating for or against tumor progression? *Cancer Immunol Immunother,* 63(1):67-72.

Xue, W., Zender, L., Miething, C., Dickins, R.A., Hernando, E., Krizhanovsky, V., Cordon-Cardo, C. & Lowe, S.W. 2007. Senescence and tumour clearance is triggered by p53 restoration in murine liver carcinomas. *Nature,* 445(7128):656-660.

Yoshikawa, S., Kawakami, K. & Zhao, X.C. 2008. G2R Cre reporter transgenic zebrafish. *Dev Dyn,* 237(9):2460-2465.

Zaidi, M.R., Davis, S., Noonan, F.P., Graff-Cherry, C., Hawley, T.S., Walker, R.L., Feigenbaum, L., Fuchs, E., Lyakh, L., Young, H.A., Hornyak, T.J., Arnheiter, H., Trinchieri, G., Meltzer, P.S., De Fabo, E.C. & Merlino, G. 2011. Interferon-γ links ultraviolet radiation to melanomagenesis in mice. *Nature,* 469(7331):548-553.

Zitvogel, L., Tesniere, A. & Kroemer, G. 2006. Cancer despite immunosurveillance: immunoselection and immunosubversion. *Nat Rev Immunol,* 6(10):715-727.

Teng, M.W., Galon, J., Fridman, W.H. and Smyth, M.J., 2015. From mice to humans: developments in cancer immunoediting. The Journal of clinical investigation, 125(9), pp.3338-3346.